Lawrence Livermore National Laboratory

Building Protection Against External Ionizing Fallout Radiation

Michael B. Dillon
Steven G. Homann

December 2016

This work was sponsored by the U.S. Department of Defense.

LLNL-TR-714297

Lawrence Livermore National Laboratory is operated by Lawrence Livermore National Security, LLC, for the U.S. Department of Energy, National Nuclear Security Administration under Contract DE-AC52-07NA27344.

Auspices and Disclaimer

This work was performed under the auspices of the U.S. Department of Energy by Lawrence Livermore National Laboratory under Contract DE-AC52-07NA27344. The U.S. Department of Homeland Security sponsored this work.

Acknowledgements

The authors also gratefully acknowledge the funding support from Todd Hann at the Department of Defense, Defense Threat Reduction Agency for the current effort. We also appreciate the helpful discussion and assistance of: Todd Hann and Emmary Webb at the Defense Threat Reduction Agency; Andy Li, Tyler Dant, and Kevin Kramer at Applied Research Associates; Amy Rose at the Oak Ridge National Laboratory; Sue Wright at Leidos; Gus Potter at the Sandia National Laboratories; Timothy Boe at the Environmental Protection Agency; John Nasstrom, Brenda Pobanz, David Myers, Paul Miller, Barry Kirkendall, and Kathy Dean at the Lawrence Livermore National Laboratory; and Charles Dillon. The authors also thank the prior efforts of Brooke Buddemeier at Lawrence Livermore National Laboratory and Steve Meheras at the Pacific Northwest National Laboratory in identifying and obtaining many of the underlying documents used.

The authors also acknowledge previous funding support for the early development of the PFscreen model from the Department of Homeland Security Federal Emergency Management Agency Response Division (Donald Daigler - CBNRE Branch; Donald Lumpkins – Planning Coordination and Assistance Branch) and the Department of Homeland Security Science and Technology (Patricia Underwood – Integrated Terrorism Risk and Assessment). Additional individuals who supported previous versions of the PFscreen model include Brooke Buddemeier and Priya Doshi at the Lawrence Livermore National Laboratory.

The authors are indebted to numerous prior investigators who supported the US Fallout Shelter System with a vast and comprehensive array of theoretical, experimental, and modeling research. Without these contributions, this work would not be possible.

Finally, the authors deeply appreciate the endless hours Jave Kane (Lawrence Livermore National Laboratory) spent meticulously digitating and quality assuring the data points needed for verification.

Everything should be as simple as possible, but not simpler…

attributed to Albert Einstein

EXECUTIVE SUMMARY

A nuclear explosion has the potential to injure or kill tens to hundreds of thousands of people through exposure to fallout (external gamma) radiation. Existing buildings can protect their occupants (reducing external radiation exposures) by placing material and distance between fallout particles and indoor individuals. This protection is not well captured in current fallout risk assessment models and so the US Department of Defense is implementing the Regional Shelter Analysis methodology to improve the ability of the Hazard Prediction and Assessment Capability (HPAC) model to account for building protection.

This HPAC improvement effort requires accurate estimates of building protection for common building construction types worldwide. Building protection against outdoor radiation sources has been studied for seven decades within the context of (a) nuclear fallout protection and the (b) remediation of nuclear power plant accidents and other cases of wide-spread radiological contamination. The building types and corresponding protection factor estimates currently in use are primarily based on work performed during (a) the early cold war and (b) the remediation of the Chernobyl and Fukushima nuclear power plant accidents. While these prior building protection estimates describe some building types well, they do not cover the range of worldwide building construction. This is problematic as reasonable variations in building protection can significantly alter the number of people adversely affected by nuclear fallout.

This report supports the HPAC improvement effort by identifying a set of building attributes (next page) that, when collectively specified, are sufficient to calculate reasonably accurate, i.e., within a factor of 2, fallout shelter quality estimates for many individual buildings. The set of building attributes were determined by first identifying the key physics controlling building protection from fallout radiation and then assessing which building attributes are relevant to the identified physics. This approach was evaluated by developing a screening model (PFscreen) based on the identified physics and comparing the screening model results against the set of existing independent experimental, theoretical, and modeled building protection estimates. In the interests of transparency, we have developed a benchmark dataset containing (a) most of the relevant primary experimental data published by prior generations of fallout protection scientists as well as (b) the screening model results.

Key Building Attributes for Assessing Protection from Fallout Radiation

General Building Attributes

- Existence of a basement
- Building footprint (length and width)

Story-Specific Attributes (these can vary by story)

- Story height (room height)
- Height of story floor above ground
- Exterior wall density
- Interior density (includes both room contents and internal walls)
- Ceiling-floor density (includes both ceiling and floor density)
- Roof density
- Apertures (windows and/or doors)
    - Aperture start height above floor (e.g., window sill height)
    - Aperture stop height above floor (e.g., top of window)
    - Aperture fraction of exterior wall area
    - Aperture density

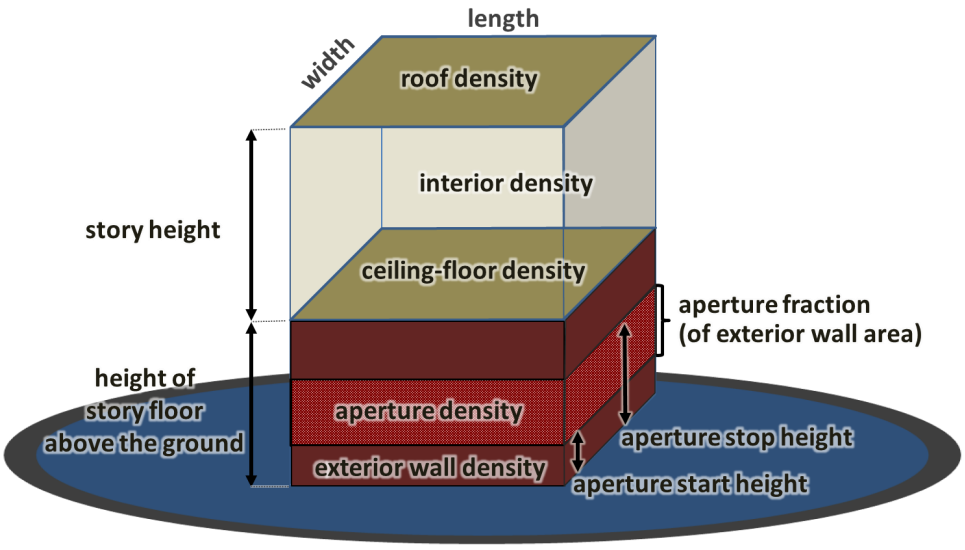

Figure. Illustration of key building attributes for fallout building protection. Basements are also important, but are not shown in this figure.

TABLE OF CONTENTS

INTRODUCTION

A nuclear explosion has the potential to injure or kill tens to hundreds of thousands of people through exposure to fallout (external gamma) radiation.[1] **Sheltering in existing buildings can significantly reduce fallout radiation** exposure by placing material and distance between fallout particles and exposed individuals [1].

Building protection against outdoor fallout radiation has been studied for seven decades within the context of nuclear fallout protection and the remediation of nuclear power plant accidents, see [3] and references therein. Current practice uses a relatively small set of building types with single (or a small range) of building protection factors [1]–[8], e.g., *Figure 1*. These building types and corresponding protection factor estimates are primarily based on foundational work performed during the early cold war. This work was performed to support the US National Fallout Shelter System which provided the US civilian population some protection against the effects of a large, thermonuclear attack [9].

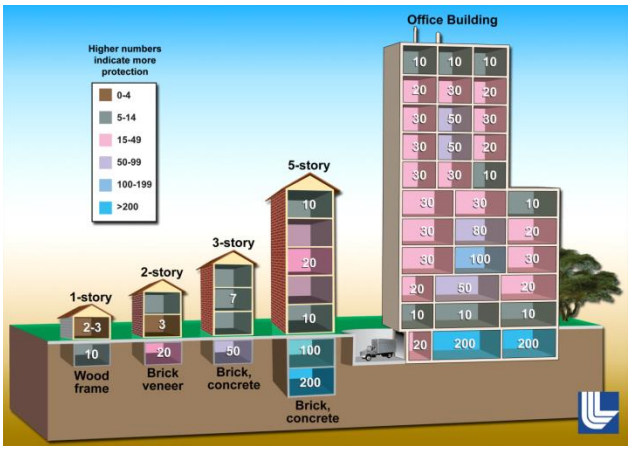

Figure 1. Example of fallout (external gamma) building protection estimates as a function of building type and location [1], [3]–[7].

These prior building protection estimates are relevant to some important building types, but they do not cover the range of worldwide building construction. For example, no prior study has examined glass curtain wall buildings commonly used for offices and residences. Furthermore, current practice does not capture the full range of protection known to be present within many buildings. This is problematic as (a) building protection can vary many orders of magnitude within a single building [3] and (b) variations in building protection can significantly alter casualty estimates relative to traditional casualty estimation based on using a single "typical" building protection value [10]. Finally, current practice provides limited to no

[1] (1) For some scenarios, hazardous levels of fallout radiation can extend well beyond the regions directly affected by the nuclear explosion (prompt effects) [1], [2]. (2) This report does not consider other nuclear effects including, but not limited to, prompt radiation injuries and blast effects.

information on other key parameters such as the geographic distribution of the variety of existing building types and the population posture (degree to which they are populated at any given time).

The Regional Shelter Analysis methodology [10] has been developed, in part, to address these needs. The Regional Shelter Analysis allows the consideration of (a) multiple building types, (b) variations of building protection within a given building type, (c) local, regional, and country specific estimates, (d) population posture (e.g., unwarned vs. minimally warned), and (e) the time of day (e.g., night vs. day). Regional Shelter Analysis building protection estimates can be combined with fallout predictions or measurements to (a) provide a more accurate assessment of population exposures and injuries and (b) evaluate the effectiveness of various casualty mitigation strategies, see *Figure 2*.

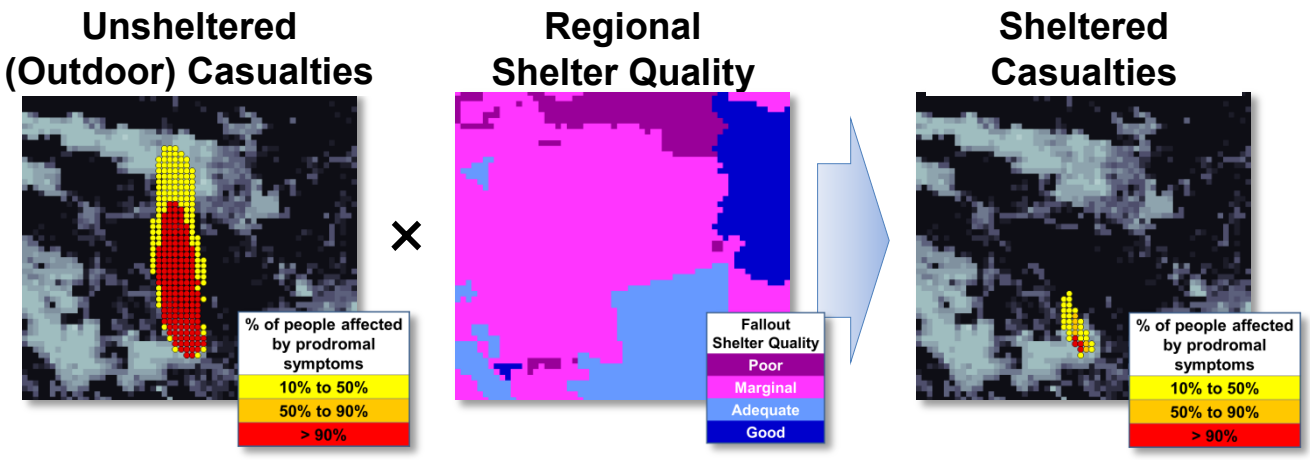

Figure 2. Example of a regional shelter analysis (center panel) and associated unsheltered (outdoor) and sheltered casualties due to fallout radiation (left and right panels, respectively).

The Regional Shelter Analysis results depend, in part, upon the accuracy of the building protection estimates. Local, regional, and worldwide databases of modern building construction exist; however, it is unclear how to defensibly map the building features specified in these databases to building fallout protection distributions [10]. This gap needs to be addressed prior to the operational use of a Regional Shelter Analysis.

The US Department of Defense is implementing the Regional Shelter Analysis methodology to improve the ability of the Hazard Prediction and Assessment Capability (HPAC) model to account for the protective effects of the built environment against fallout radiation.[2] Collaborators are (a) developing a worldwide database of building construction and (b) performing high-fidelity building protection modeling. This report supports these efforts by providing military and civilian planners a set of building attributes that control individual building fallout protection.

Specifically, this report:

1) **Identifies a set of key building attributes that are sufficient to reasonably characterize fallout shelter quality for individual buildings and assesses the degree to which these attributes can characterize fallout shelter quality, and**

2) **Enhances the reader's understanding of fallout shelter physics and key building attributes by describing the physics most relevant to assessing building protection from externally deposited radioactive material (see *Appendix A*).**

This report aims to accomplish the above tasks in a concise, efficient manner. As such, the reader should be aware that it does not provide a definitive summary of all relevant radiation physics, nuclear fallout, building protection considerations, or building construction practices.

This report also describes the PFscreen model which calculates the distribution of building protection within an individual building based on the identified radiation physics and building attributes. The comparisons between (a) PFscreen and (b) independent experimental, theoretical, and modeled building protection results assesses the degree to which the identified physics and building attributes are capable of adequately characterizing building protection. When higher accuracy estimates are required, we recommend using more detailed building descriptions and modern Monte Carlo radiation transport codes. In the interests of transparency, this report, and its supplemental material [12], describes a new benchmark

[2] This report does not consider the full suite of potential injuries, e.g., thermal burns, blast effects, prompt radiation, ingestion, and internal (inhalation and ingestion) and external fallout radiation exposure due to the passing airborne cloud and resuspended material. Other efforts are addressing these items for use in an expanded Regional Shelter Analysis capability. Furthermore, this effort is primarily focused on exposures within the first few hours after a nuclear explosion. Finally, this effort does not discuss when to seek shelter, e.g., [11] and ref therein.

dataset containing (a) most of the relevant primary experimental data published by prior generations of fallout protection scientists as well as the (b) screening model results.

Due to wide range of potential audiences, this report has been divided into several, partially overlapping, sections. The main document provides general science readers an overview of the study purpose and results. *Appendix A* provides analysts an overview of the physics and key building attributes needed to assess building protection against nuclear fallout. In this appendix, the text in footnotes and blue boxes provide readers with additional information such as elaboration on a particular topic or a brief summary of how the PFscreen model implements a particular topic. *Appendix B* provides analysts with a more detailed discussion of how the PFscreen model results compare with prior studies of building protection. *Appendices C and D* provide the technical expert a (a) theoretical basis for calculating radiation dose from surface contamination and (b) description of the PFscreen model, respectively. As a general resource, we recommend interested readers consult *Spencer et al.* [9] for a comprehensive treatment of the scientific aspects of the US National Fallout Shelter System.

BUILDING ATTRIBUTES

KEY FALLOUT BUILDING ATTRIBUTES

***Figure 3* shows the key fallout building attributes required to reasonably characterize the degree to which buildings protect occupants from fallout radiation.**

General Building Attributes

- Existence of a basement
- Building footprint (length and width)

Story-Specific Attributes (these can vary by story)

- Story height (room height)
- Height of story floor above ground
- Exterior wall density
- Interior density (includes both room contents and internal walls)
- Ceiling-floor density (includes both ceiling and floor density)
- Roof density
- Apertures (windows and/or doors)
    - Aperture start height above floor (e.g., window sill height)
    - Aperture stop height above floor (e.g., top of window)
    - Aperture fraction of exterior wall area
    - Aperture density

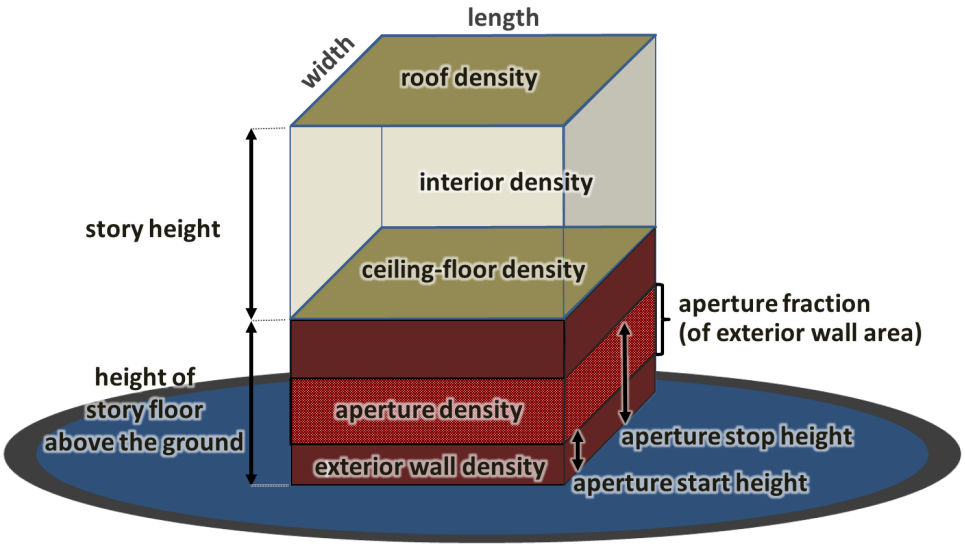

Figure 3. Illustration of key building attributes for fallout building protection. Basements are also important, but are not shown in this figure.

DETERMINING BUILDING ATTRIBUTES FROM ARCHITECTURAL FEATURES

Architectural features of buildings are characterized using a variety of different description methods (taxonomies). Established taxonomies are in use for (a) hazards planning including natural hazards, such as earthquakes, e.g., [13]–[15], and man-made hazards, such as explosions and/or airborne clouds of toxic materials, e.g., [16] and (b) property tax assessment, e.g., [17].

Oak Ridge National Laboratory is characterizing the global distribution of building construction using the Global Earthquake Model (GEM) taxonomy. The GEM taxonomy describes the seismically relevant building features in a comprehensive, uniform manner that is accessible to a wide range of users [15]. However, the GEM building properties relevant to fallout protection are described in qualitative, architectural terms and require mapping to quantitative values required for use in fallout protection calculations. For example, a "wood-frame wall with a stucco exterior" is estimated to have an exterior wall density of 21 psf (lbs per sq ft).[3] A separate report documents this mapping process and its underlying assumptions in detail [18]. For context, *Table 1* (adapted from Table 1 in [18]) provides an overview of the method to determine fallout building attribute numerical values from architectural features.

Applied Research Associates will be generating the building protection estimates required for fallout assessment.

Table 1. Mapping between select fallout building attributes and architectural features.[4]

Fallout building attribute	Architectural features
Exterior wall density	Dead load of the building exterior + Dead load of the building frame in exterior wall (if any) + Dead load of the internal wall affixed to the exterior wall (if any)
Interior density	Live load of the building contents + Dead load of the interior walls and partition + Dead load of the building frame associated with interior walls (if any)
Roof density	Live load of the roof + Dead load of the roof + Dead load of top floor ceiling + Dead load of the building frame in roof (if any)
Ceiling-floor density	Dead load of the floor (including joists) + Dead load of the ceiling attached to the floor + Dead load of the building frame in floor (if any)

[3] Assuming a (a) 10 psf exterior stucco dead load, (b) 9 psf building frame dead load (2" x 4" spaced 16" on center and 3/8" wood sheathing), and (c) 2 psf interior wall dead load (1/2" drywall).

[4] Dead load refers to the weight of materials, such as walls, that are intrinsically part of the building. Live load refers to weight of the building contents, such as furniture, that can be readily moved.

FALLOUT BUILDING ATTRIBUTE VERIFICATION

To evaluate our overall approach, we developed the PFscreen model, see *Appendix D* for a detailed description. Specifically, comparisons between (a) PFscreen model results and (b) independent experimental, theoretical, and modeled building protection estimates assess the degree to which the currently identified physics and building attributes are capable of determining building protection. The detailed comparison results are provided in *Appendices A* and *B*. The comparisons performed to date represent much, but not all, of the previously identified data listed in [3] – see [12] for more detail. We note that there are several key building types for which no prior, independent study has been performed – leaving open the possibility that additional building attributes may be required in these instances.

***Figure 4*, which summarizes the more detailed comparisons discussed in *Appendix B*, demonstrates that our overall approach agrees with most prior experimental, modeled, and theoretical building protection estimates within a factor of 2.**

In this figure,

- The prior study protection factor is plotted on the horizontal (x) axis and the PFscreen model protection factor is plotted on the vertical (y) axis.
- Each symbol indicates a comparison between a PFscreen result and previously reported protection factor at a single location and time within a building.
- The number of data points (n) plotted is provided in the upper left corner.
- For visualization purposes, we provide lines that indicate perfect agreement (1:1, black solid line), factor of 2 agreement (1:2 and 2:1, blue dashed lines), and factor of 10 agreement (1:10 and 10:1, magenta dotted lines).
- The top panel shows the comparison with data based on Co-60 and Cs-137 contamination (surrogates for 1 h and 1 d old fallout, respectively) and includes basements, lightweight metal sheds, single family homes, and large, concrete structures.
    - The cluster of comparisons at PFscreen protection factor ~ 100 to 300 that extend beyond the blue factor of 2 agreement lines are associated with measurements taken in partially buried basements.

- The bottom panel shows the comparison with data based on 1 h to 3 d old fallout contamination measured in a lightweight metal shed that included a basement.
    - The instruments used to measure much of the below ground data (protection factor > 10) are known to overestimate the protection factor.
    - In the 1 h to 3 d fallout source panel, the cluster of comparisons at PFscreen protection factor ~ 4 (fallout protection factor ~ 4 to 30) are ground-level (~ 0 m agl) measurements. PFscreen assumes these measurements are above the ground and so exposed to direct radiation. Based on the protection factor values, it is likely that these measurements were only partially (or not at all) exposed to direct radiation, potentially due to a short (0.1 m high) concrete foundation that extends above the ground. These measurements are included for completeness, but provide a less reliable verification of the PFscreen model results.
    - The PFscreen model results shown on the 1 h to 3 d fallout source panel assume the roof contamination is 10% of the ground contamination – consistent with measured contamination levels.

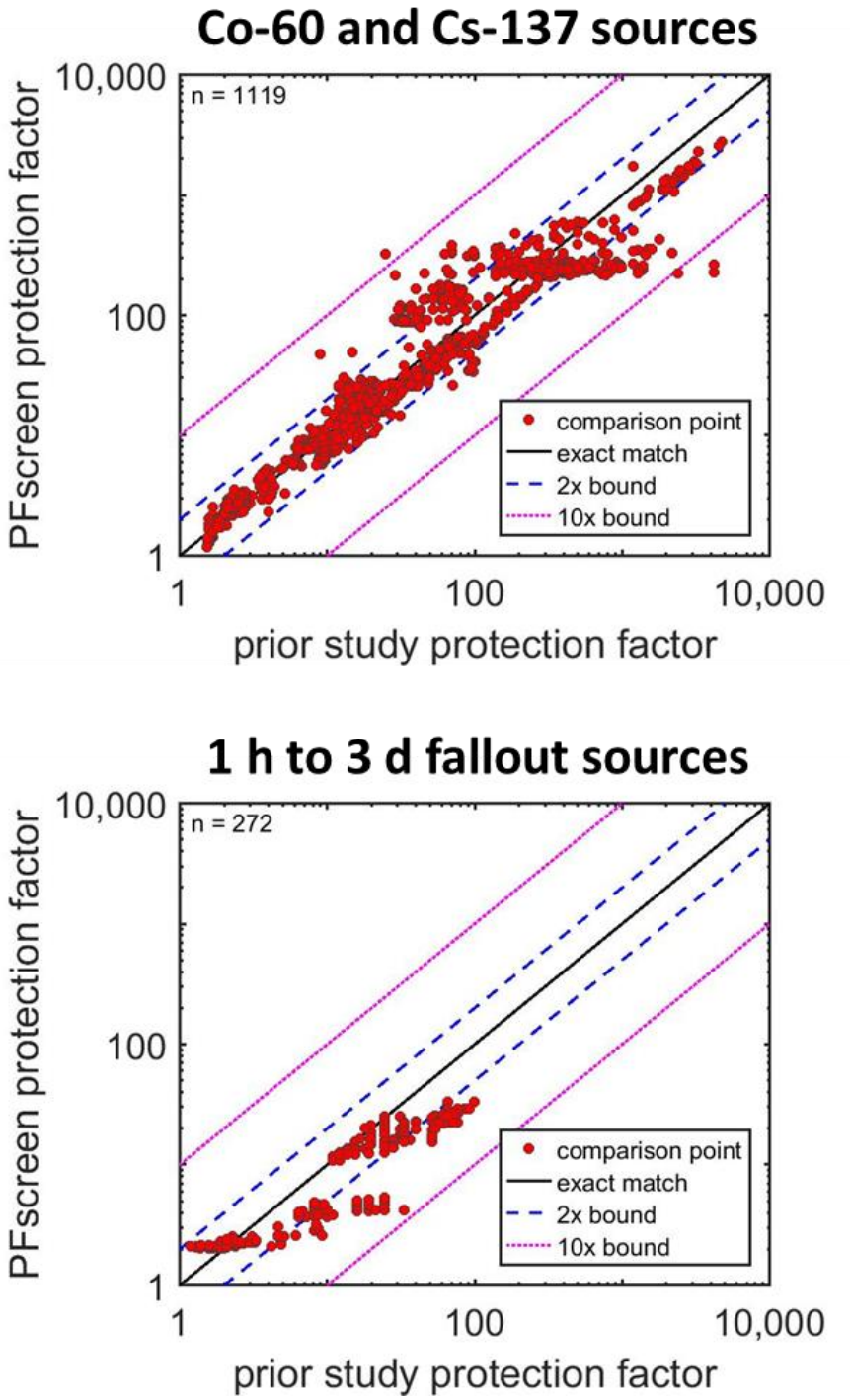

Figure 4. Comparison between PFscreen and prior study building protection estimates. Each red dot indicates a comparison between PFscreen model result and a prior study estimate for a single location. (top panel) Comparisons based on Co-60 and Cs-137 sources (surrogates for 1 h and 1 d old fallout, respectively) for a variety of buildings. (bottom panel) Comparisons based on 1 h to 3 d old fallout sources in a lightweight metal shed that had a basement.

DISCUSSION AND CONCLUSIONS

Exposure to radiation from nuclear fallout particles has the potential to cause mass casualties and fatalities. The built environment can protect building occupants by placing material and distance between fallout particles and indoor occupants - reducing indoor radiation exposures. The current distribution and degree of building protection is not well captured by current models and so the US Department of Defense is implementing the Regional Shelter Analysis methodology to improve the ability of the Hazard Prediction and Assessment Capability (HPAC) model to account for building protection.

This report supports the HPAC improvement effort by identifying a set of key building attributes that are sufficient to characterize fallout shelter quality for individual, isolated buildings. Using these building attributes, the protection that many buildings provide their occupants against nuclear fallout can be determined within a factor of 2 for individual locations – particularly for above ground exposures. The verification performed is unusual, in part due to the use of extensive comparisons against the experimental and theoretical data developed by prior generations of fallout protection scientists (prior to this effort, there was no standardized, benchmark dataset of fallout protection verification/validation data). The supplemental material [12] provides the data used in a standardized format to (a) provide transparency for this effort and (b) facilitate other researcher's efforts to advance this field. While this study examined a wide range of building types, there are several key building types for which no prior, independent study has been performed – leaving open the possibility of additional building attributes.

Comparison with the prior study results demonstrates that the inclusion of additional building attributes may be desirable for some building types. If the corresponding building data are available, the use of these attributes could improve the building protection accuracy. Specifically, the available data indicates that below ground prediction accuracy could be improved if partial basements (non-uniform ground level) were considered in more detail. While the current method accurately predicts the average basement protection, the protection measured in several large footprint, partial basements varied widely (factor of 10) about the average value. Beyond this, fallout particles can, but do not necessarily, slide (or are washed) off

some roofs – resulting in significant (factor of 10) differences in the relative contamination of the roof and surrounding ground. This difference has the potential to bias (typically underestimate) the building protection predictions (the amount of bias depending on the specific building being considered). Finally, this study scope was limited to examining the building fallout protection for the important case of isolated buildings. It is well known than the local environment, e.g., terrain, nearby buildings, etc., can enhance or reduce the building protection.

REFERENCES

[1] National Security Staff Interagency Policy Coordination Subcommittee for Preparedness and Response to Radiological and Nuclear Threats, "Planning Guidance for Response to a Nuclear Detonation, 2nd Edition," Executive Office of the President, Washington DC, Jun. 2010.

[2] B. R. Buddemeier and M. B. Dillon, "Key Response Planning Factors for the Aftermath of Nuclear Terrorism," Lawrence Livermore National Laboratory, Livermore, CA, LLNL-TR-410067, Aug. 2009.

[3] M. B. Dillon, J. Kane, J. Nasstrom, S. Homann, and B. Pobanz, "Summary of Building Protection Factor Studies for External Exposure to Ionizing Radiation," Lawrence Livermore National Laboratory, Livermore, CA, LLNL-TR-684121, Feb. 2016.

[4] US Environmental Protection Agency, "PAG Manual: Protective Action Guides and Planning Guidance for Radiological Incidents," US Environmental Protection Agency, Washington DC, EPA-400/R-16/001, Nov. 2016.

[5] Federal Radiological Monitoring and Assessment Center, "FRMAC Assessment Manual: Volume 1, Overview and Methods," Albuquerque, NM and Livermore, CA, SAND2015-2884 R, Apr. 2015.

[6] Defense Civil Preparedness Agency, "DCPA Attach Environment Manual, Chapter 6 - What the Planner Needs to Know About Fallout," US Department of Defense, CPG 2-1A6, Jun. 1973.

[7] K. P. Ferlic, "Fallout: Its characteristics and management," Armed Forces Radiobiology Research Institute, Bethesda, MD, AFRRI Technical Report TR83-5, Dec. 1983.

[8] A. Rose, "Global Protection Type 2012 Disclaimer." Oak Ridge National Laboratory, Jul-2013.

[9] L. V. Spencer, A. B. Chilton, and C. Eisenhauser, "Structure Shielding Against Fallout Gamma Rays From Nuclear Detonations," US Department of Commerce, Washington DC, National Bureau of Standards Special Publication 570, Sep. 1980.

[10] M. B. Dillon, D. Dennison, J. Kane, H. Walker, and P. Miller, "Regional Shelter Analysis Methodology," Lawrence Livermore National Laboratory, Livermore, CA, LLNL-TR-675990, Aug. 2015.

[11] M. B. Dillon, "Determining optimal fallout shelter times following a nuclear detonation," *Proc. R. Soc. Math. Phys. Eng. Sci.*, vol. 470, no. 2163, pp. 20130693–20130693, Jan. 2014.

[12] M. B. Dillon and J. Kane, "Supplemental Material for Building Protection Against External Ionizing Fallout Radiation," Lawrence Livermore National Laboratory, Livermore, CA, LLNL-TR-727361, Mar. 2017.

[13] US Department of Homeland Security, Federal Emergency Management Agency, Emergency Preparedness and Response Directorate, "Multi-hazard Loss Estimation Methodology, Earthquake Model, Hazus-MH 4 Technical Manual," US Department of Homeland Security, Federal Emergency Management Agency, Washington DC, Aug. 2009.

[14] "PAGER - Prompt Assessment of Global Earthquakes for Response," 26-Jul-2015. [Online]. Available: http://earthquake.usgs.gov/earthquakes/pager/. [Accessed: 26-Jul-2015].

[15] Brzev, Svetlana *et al.*, "GEM Building Taxonomy Version 2.0," GEM Foundation, Pavia, Italy, GEM Technical Report 2013-02 V1.0.0, 2013.

[16] M. Ettouney, P. Schneider, R. F. Walker, and M. Chipley, "Integrated Rapid Visual Screening of Buildings," Department of Homeland Security, Science and Technology, BIPS 04, Sep. 2011.

[17] "PLUTO Data Dictionary (16v1)," NY Dept of City Planning, New York, NY, Mar. 2016.

[18] M. B. Dillon and S. R. Kane, "Mapping Architectural Features to Key Fallout Building Attributes," Lawrence Livermore National Laboratory, Livermore, CA, LLNL-TR-728739, Mar. 2017.

[19] Z. G. Burson, "Experimental Evaluation of the Fallout-Radiation Protection Provided by Structures in the Control Point Area of the Nevada Test Site," US Atomic Energy Commission, Washington DC, CEX-69.5, Oct. 1970.

[20] A. J. Breslin, P. Loysen, and M. S. Weinstein, "Protection Against Fallout Radiation in a Simple Structure," Civil Effects Test Group, Project 32.1, Washington DC, WT-1462, Aug. 1963.

[21] M. Little, "Risks associated with ionizing radiation," *Br. Med. Bull.*, vol. 68, no. 1, pp. 259–275, Dec. 2003.

[22] T. C. Pellmar and D. R. Oldson, "Critical Review of Selected Components of RIPD (Radiation-Induced Performance Decrement)," Applied Research Associates, Arlington, VA, DTRA-TR-12-047, Dec. 2012.

[23] K. F. Eckerman, A. B. Wolbarst, and A. C. B. Richardson, "Federal Guidance Report 11 - Limiting Values of Radionuclide Intake and Air Concentration and Dose Conversion Factors for Inhalation, Submersion, and Ingestion," Office of Radiation and Indoor Air, U.S. Environmental Protection Agency, Washington DC, EPA-520/1-88-020, corrected in 1989 1988.

[24] K. F. Eckerman and J. C. Ryman, "Federal Guidance Report 12 - External Exposure to Radionuclides in Air, Water, and Soil," Office of Radiation and Indoor Air, U.S. Environmental Protection Agency, Washington DC, EPA-402-R-93-081, Sep. 1993.

[25] K. Eckerman, J. Harrison, H.-G. Menzel, and C. H. Clement, "ICRP Publication 119: Compendium of Dose Coefficients based on ICRP Publication 60," *Ann. ICRP*, vol. 42, no. 4, pp. e1–e130, Aug. 2013.

[26] H. Beck and G. de Planque, "The Radiation Field in Air Due to Distributed Gamma-Ray Sources in the Ground," U.S. Atomic Energy Commission, HASL-195, May 1968.

[27] L. V. Spencer, "Structure Shielding Against Fallout Radiation From Nuclear Weapons," US Department of Commerce, Washington DC, National Bureau of Standards Monograph 42, Jun. 1962.

[28] M. Zaehringer and G. Pfister, "Representativeness and comparability of dose rate measurements: description of site-specific uncertainties and data bias," *Kerntechnik*, vol. 63, no. 4, pp. 178–184, Aug. 1998.

[29] Z. G. Burson and R. L. French, "Simulating Energy and Angle Distributions Above Infinite Plane Cobalt-60 Sources," *Health Phys.*, vol. 18, no. 5, pp. 507–521, 1970.

[30] C. M. Huddleston, Q. G. Klingler, Z. G. Burson, and R. M. Kinkaid, "Ground Roughness Effects on the Energy and Angular Distribution of Gamma Radiation from Fallout," *Health Phys.*, vol. 11, no. 6, pp. 537–548, 1965.

[31] Z. G. Burson, "Experimental Radiation Measurements in Conventional Structures: Part II Comparison of Measurements in Above-Ground and Below-Ground Structures from Simulated and Actual Fallout Radiation," US Atomic Energy Commission, Washington DC, CEX-59.7B Part II, Feb. 1963.

[32] M. J. Schumchyk, M. A. Schmoke, W. O. Egerland, and E. L. Schulman, "Scattered Radiation (Shyshine) Contribution to an Open Basement Located in a Simulated Fallout Field," Nuclear Defense Laboratory, Edgewood, MD, NDL-TR-68, Dec. 1966.

[33] R. Spring and C. H. McDonnell, "An Experimental Evaluation of Roof Reduction Factors within a Multi-story Structure," Office of Civil Defense, PSDC-TR-16, Supplement No. 1, Apr. 1967.

[34] J. F. Batter Jr., A. L. Kaplan, and E. T. Clarke, "An Experimental Evaluation of the Radiation Protection Afforded by a Large Modern Concrete Office Building," US Atomic Energy Commission, Washington DC, CEX-59.1, Jan. 1960.

[35] Z. Burson and A. E. Profio, "Structure Shielding in Reactor Accidents," *Health Phys.*, vol. 33, no. 4, pp. 287–299, Oct. 1977.

[36] C. McDonnell and J. Velletri, "Radiation Distribution within a Multistory Structure," Office of Civil Defense, TR-24, Feb. 1967.

[37] R. Meckbach, P. Jacob, and H. G. Paretzke, "Shielding of gamma radiation by typical European houses," *Nucl. Instrum. Methods Phys. Res. Sect. Accel. Spectrometers Detect. Assoc. Equip.*, vol. 255, no. 1–2, pp. 160–164, Mar. 1987.

[38] H. Borella, Z. Burson, and J. Jacovitch, "Evaluation of the Fallout Protection Afforded by the Brookhaven National Laboratory Medical Research Center," US Atomic Energy Commission, Washington DC, CEX-60.1, Oct. 1961.

[39] Z. Kis, K. Eged, G. Voigt, R. Meckbach, and H. Müller, "Modeling of an Industrial Environment: External Dose Calculations based on Monte Carlo Simulations of Photon Transport," *Health Phys.*, vol. 86, no. 2, pp. 161–173, Feb. 2004.

[40] J. A. Stoddard, "Civic Improvement Program: Volume II - Fallout Protection Factor Analysis Capabilities," Science Applications International Corporation, San Diego, CA, DNA-TR-87-226-V2, Aug. 1987.

[41] R. Meckbach and P. Jacob, "Gamma Exposures due to Radionuclides Deposited in Urban Environments. Part II: Location Factors for Different Deposition Patterns," *Radiat. Prot. Dosimetry*, vol. 25, no. 3, pp. 181–190, 1988.

[42] R. Meckbach, P. Jacob, and H. G. Paretzke, "Gamma Exposures due to Radionuclides Deposited in Urban Environments. Part I: Kerma Rates from Contaminated Urban Surfaces," *Radiat. Prot. Dosimetry*, vol. 25, no. 3, pp. 167–179, 1988.

[43] C. F. Miller, "The Radiological Assessment and Recovery of Contaminated Areas," US Atomic Energy Commission, Washington DC, CEX-57.1, Sep. 1960.

[44] K. G. Andersson *et al.*, "Requirements for estimation of doses from contaminants dispersed by a 'dirty bomb' explosion in an urban area," *J. Environ. Radioact.*, vol. 100, no. 12, pp. 1005–1011, Dec. 2009.

[45] J. Velletri, R. Spring, J. Wagoner, and H. Gignilliat, "Experimental Analysis of Interior Partitions, Apertures, and Nonuniform Walls," Office of Civil Defense, TR-27, Dec. 1968.

[46] Z. Burson, D. Parry, and H. Borella, "Experimental Evaluation of the Fallout-Radiation Protection Afforded by a Southwestern Residence," US Atomic Energy Commission, Washington DC, CEX-60.5, Feb. 1962.

[47] T. D. Strickler and J. A. Auxier, "Experimental Evaluation of the Radiation Protection Afforded by Typical Oak Ridge Homes Against Distributed Sources," US Atomic Energy Commission, Washington DC, CEX-59.13, Apr. 1960.

[48] B. Shleien, *The Health Physics and Radiological Health Handbook*, Revised edition. Silver Spring, MD: Scinta Inc., 1992.

[49] P. H. Jensen, "Shielding Factors for Gamma Radiation from Activity Deposited on Structures and Ground Surfaces," Riso National Laboratory, Roskilde, Denmark, RISO-M-2270, Nov. 1982.

[50] T. Goorley *et al.*, "Initial MCNP6 Release Overview," *Nucl. Technol.*, vol. 180, no. 3, pp. 298–315, Dec. 2012.

[51] N. Matsuda, S. Mikami, T. Sato, and K. Saito, "Measurements of air dose rates in and around houses in the Fukushima Prefecture in Japan after the Fukushima accident," *J. Environ. Radioact.*, Mar. 2016.

[52] M. B. Dillon, D. S. Dennison, and P. P. Doshi, "Regional Shelter Analysis For Nuclear Fallout Planning - A Quick Start Guide (and Supplemental Material)," Lawrence Livermore National Laboratory, Livermore, CA, LLNL-SM-521751, Dec. 2011.

[53] E. L. Hill, W. K. Grogan, R. O. Lyday, H. G. Norment, and W. O. Doggett, "FINAL REPORT: Analysis of Survey Data," Office of Civil Defense/Research Triangle Institute, R-OU-81, Feb. 1964.

[54] S. Glasstone and P. J. Dolan, *The Effects of Nuclear Weapons*, 3rd ed. Washington DC: US Department of Defense and Energy Research and Development Administration, 1977.

[55] National Council on Radiation Protection and Measurements, "Radiation Protection Design Guidelines for 0.1 – 100 MeV Particle Accelerator Facilities," National Council on Radiation Protection and Measurements, NCRP Report 51, Mar. 1977.

[56] W. E. Selph, "Neutron and Gamma-Ray Albedos," Oak Ridge National Laboratory, Oak Ridge, TN, ORNL-RSIC-21; DASA-1892-2, Feb. 1968.

APPENDIX A: KEY FALLOUT SHELTER PHYSICS

FALLOUT RADIATION

After a nuclear explosion near the earth's surface, the resulting mushroom cloud rises high into the atmosphere and drifts downwind.[5] Over many hours, sand-sized radioactive fallout particles fall from the cloud, potentially contaminating a large area including many regions not otherwise directly affected by the nuclear explosion [1], [2].

Over the first week, the amount and energy of the radiation emitted by the fallout particles changes dramatically. Like hot metal cooling off, fallout particles emit less and less radiation with time as highly unstable (radioactive) materials rapidly decay into more stable materials.[6] Thus the hazard posed by deposited fallout particles decreases rapidly with time – with 55% of the potential radiation exposure occurring in the first hour and 80% in the first day. During the first week, the radiation energy, and hence the ability to penetrate buildings and affect indoor individuals, also changes. Over the first day, the radiation becomes "softer" – less penetrating – and so buildings become more effective at shielding their occupants.[7] Later (over the first week) the radiation "hardens" again – becoming more penetrating – and buildings become less effective at providing protection. While fallout particles emit a variety of different radiation energies, cobolt-60 (Co-60) and cesium-137 (Cs-137) emit radiation with roughly the same penetrating power as radiation emitted from 1 h and 1 d old fallout particles, respectively [9]. As a consequence, these radionuclides were often used in experimental studies of building protection. Unless otherwise noted, **we report protection factors valid 1 h post-detonation as the first few hours pose the greatest hazard** (this choice is consistent with most previous work).

[5] When the nuclear explosion occurs well-above the earth's surface, it is possible to NOT generate significant (local) fallout.

[6] At a practical level, this natural decrease in emission rates complicates the interpretation of measurements and predictions made at different times and locations. As a result, individual measurement and model results are often "corrected" back to radiation levels that would be observed 1 h after detonation. Note that such a "correction" does *not* imply that fallout particles were present at that location 1 h after the detonation.

[7] (1) Specifically, most of the energy in the fallout spectra shifts to lower frequencies. (2) Buildings provide approximately twice as much protection 1 d after detonation compared to 1 h, e.g., [19], [20].

EXTERNAL RADIATION DOSE

Individuals near fallout particles can be exposed to fallout radiation traveling both directly from the fallout particle and scattering off of environmental materials, including air, see *Figure A1*. Once exposed, the resulting (acute) health effects depend on the total amount of radiation energy absorbed by the individual (absorbed dose) – regardless of the direction or energy of the incoming radiation [4], [21], [22].[8]

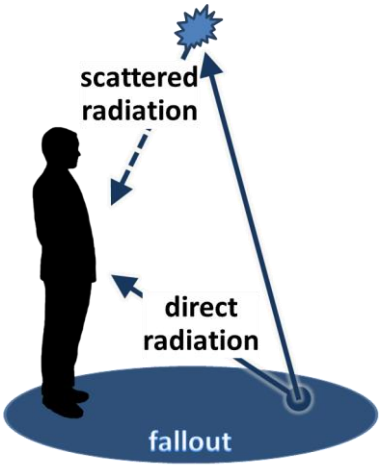

Figure A1. Illustration of direct and scattered radiation.

Dose conversion factors are commonly used to translate between environmental contamination and an individual absorbed dose. Standard tables of dose conversion factors are available [23]–[25]. The values in these tables assume that the exposed individual is standing on a flat, uniformly contaminated plane. Additional "modification" factors are used to scale these standard values for different source geometries (e.g., a roof radiation source; exclusion of deposited radiation by the building footprint) and changes to the incoming radiation caused by the environment (e.g., radiation energy changes as it scatters off of building materials). In the fallout literature, these modification factors are called *protection factors*[9] where the unsheltered (also called reference) dose is the dose 1 m above an infinite, flat, uniformly contaminated plane, see *Figure A2*.[10] US National Planning Guidance [1] has determined that **adequate protection (protection factor ≥ 10) is sufficient to protect against most acute radiation effects**.[11] Also, it should be noted that protection factors may vary with location within a building.

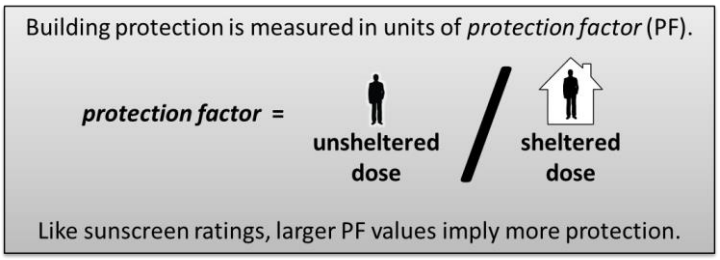

Figure A2. Protection factor definition.

[8] Radiation exposure increases the risk of cancer and may also increase risk of heritable disorders. While outside the scope of this report, buildings can also protect their occupants against these risks.

[9] In the nuclear power plant accident literature, some studies use the term protection factor to indicate other quantities.

[10] Protection factors are also valid for scaling whole body exposures as used in the RIPD model [22].

[11] This recommendation is based on single, relatively low yield (~10 KT) nuclear detonation. For multiple, larger detonation scenarios, larger protection factors (PF = 20 to 40) have been used, e.g., [9].

RADIATION SCATTERING

Fallout radiation interacts with the electrons present in air and building materials primarily through a process called *Compton scattering*, see *Figure A3*. The amount of Compton scattering depends on the number of electrons the fallout radiation encounters. For most building materials, the number of electrons per unit mass (electron density) is very similar, see *Table A1*, and so **the amount of scattering depends mostly on the amount (mass) of material the radiation passes through and not the material identity.**

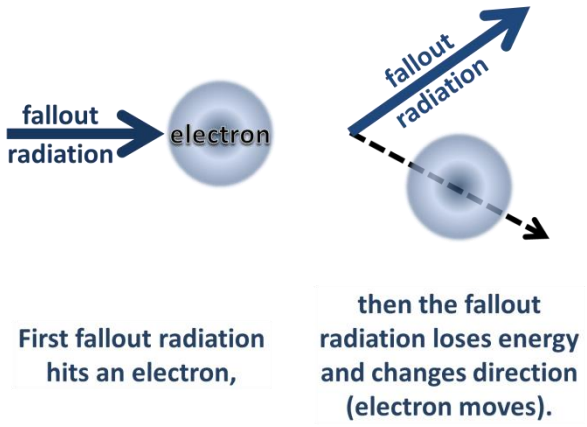

Figure A3. Illustration of Compton scattering.

Scattering affects fallout radiation dose in two ways, see *Figure A4*:

Attenuation Dose is *lower* when radiation is lost (scattered) while traveling in a direct path from the source to the detector (red dot).

Buildup Dose is *higher* when radiation that otherwise would not have reached a detector is scattered towards the detector (red dot).

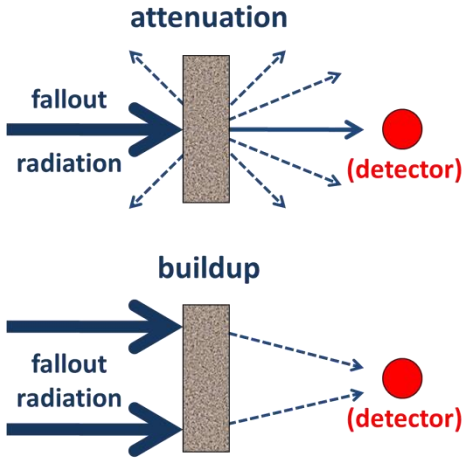

Figure A4. (top) Attenuation and (bottom) buildup.

Table A1. Electron density of (bottom) common materials and (right) elements [1]. Materials and elements have similar electron densities. Hydrogen has a high electron density but adds little to the building mass and so does not affect building protection for gamma radiation.

material	electron density (atomic number / atomic mass)
air	0.50
brick	0.50
concrete	0.50
steel	0.47
water	0.56
wood	0.53

common building material elements	electron density (atomic number / atomic mass)
Aluminum (Al)	0.48
Calcium (Ca)	0.50
Carbon (C)	0.50
Chlorine (Cl)	0.48
Copper (Cu)	0.46
Hydrogen (H)	0.99
Iron (Fe)	0.47
Magnesium (Mg)	0.49
Nitrogen (N)	0.50
Oxygen (O)	0.50
Phosphorus (P)	0.48
Potassium (K)	0.49
Silicon (Si)	0.50
Sodium (Na)	0.48

The PFscreen model uses *Figure A5* and *Equations A1 and A2* to account for scattering, see *Appendix D* for more details.

(Equation A1)

$$\frac{\left(\begin{matrix} outgoing\ radiation \\ reaching\ the\ detector \end{matrix}\right)}{incoming\ radiation} = A(FP) \times B(FP)$$

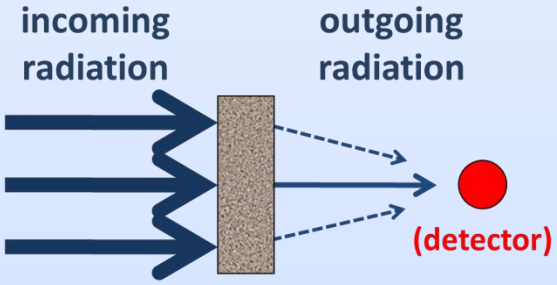

Figure A5. Combined attenuation and buildup.

(Equation A2)

$$FP = \mu \times \rho \times d$$

where

$A(FP)$	= attenuation (no units)
$B(FP)$	= buildup factor (no units)
FP	= number of mean free path lengths (no units) [12]
μ	= mass attenuation coefficient ($cm^2\ g^{-1}$)
ρ	= material density ($g\ cm^{-3}$)
d	= material thickness (cm)

The scattering effects are similar for air and common building materials for the radiation energies considered (0.5 to 3 MeV). PFscreen uses the concrete electron density as it is a common building material, see *Figure A6*.

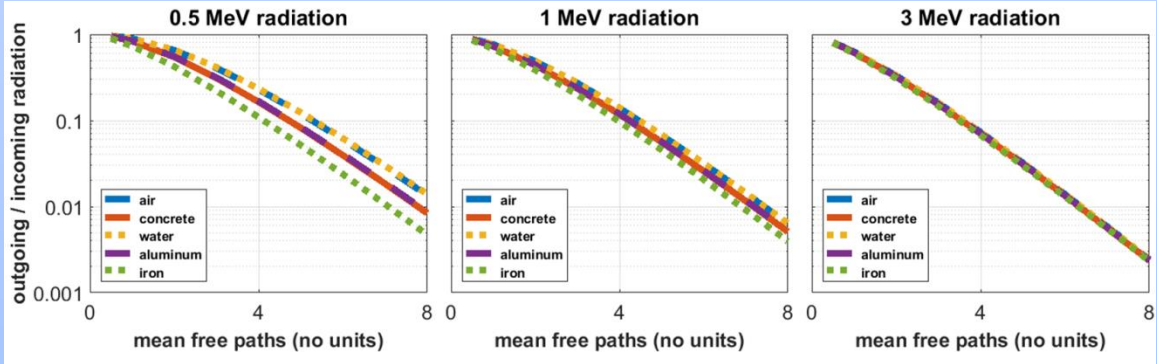

Figure A6. Scattering effects for 0.5, 1, 3 MeV radiation energy.

GROUND CONTAMINATION (INFINITE, FLAT PLANE)

An individual standing in a uniformly contaminated, flat plane is exposed to radiation that either (a) travels directly from the fallout particle or (b) scatters off of air. The amount of radiation reaching an individual varies significantly with height and the angle of the incoming radiation. **Near the ground, radiation doses are dominated by direct, horizontally traveling radiation**, *Figure A7* [9], [26]. Above 20 m, this effect is greatly diminished.

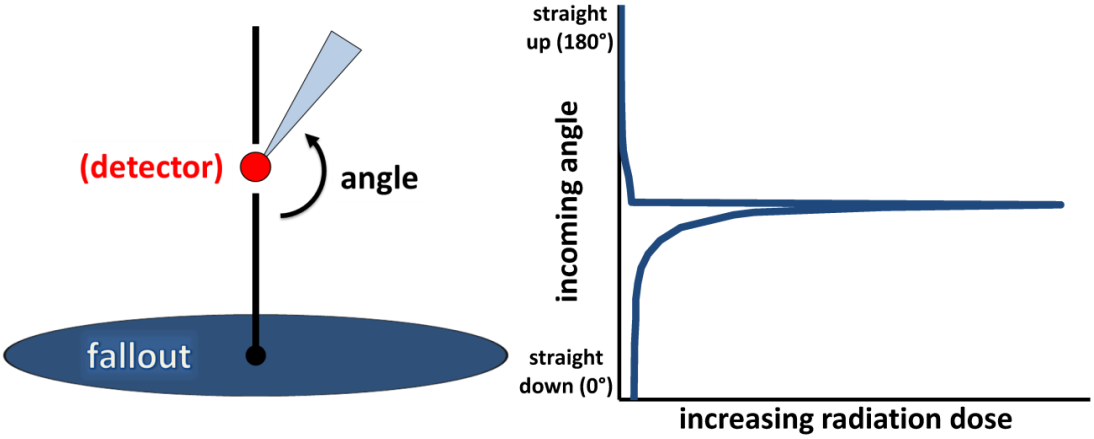

Figure A7. (left) Illustration of angle (light blue triangle) of incoming radiation to a detector (red dot). (right) Variation of radiation with incoming angle at 1 m above the ground.

Air reduces the amount of radiation reaching a detector from a distant source. Fallout radiation travels a few hundred meters through the air, on average, prior to scattering, and so **most of the radiation dose comes from sources within 300 m**, see *Figure A8*. Air scattering can result in increased protection (reduced dose) for people who are higher above the contaminated ground (e.g., on a building top), see *Figure A9*.[13] Similarly, standing in the middle of a fallout free zone will also reduce radiation doses, see *Figure A10*.[14] Adequate protection (PF ≥ 10) requires being ~150 m above the ground or being within a large, ~150 m radius, fallout free zone. The natural roughness of the ground or objects in the local environment can reduce this distance – see the following *Exterior Wall* subsection.

[13] In this (and following) figures, the term "protection factor" refers to the ratio of (a) the dose 1 m above an infinite, flat, uniformly contaminated plane to (b) the dose at the location of interest. This definition is consistent with the ratio of unsheltered to sheltered dose.

[14] In these figures, "PFscreen" = PFscreen model results (*Appendix B*); "NBS42" = [27]; "Theory" = *Appendix C*; "Zahringer 1998" = [28]; "Bursen 1970" = [29]; "Huddleston 1965" = [30]; "Bursen 1963" = [31]; "Breslin 1963" = [20]; "Schumchyk 1966" = [32]; "ARA 2016" = personal communication (Andy Li; Tyler Dant; Kevin Kramer); "Spring 1967" = [33].

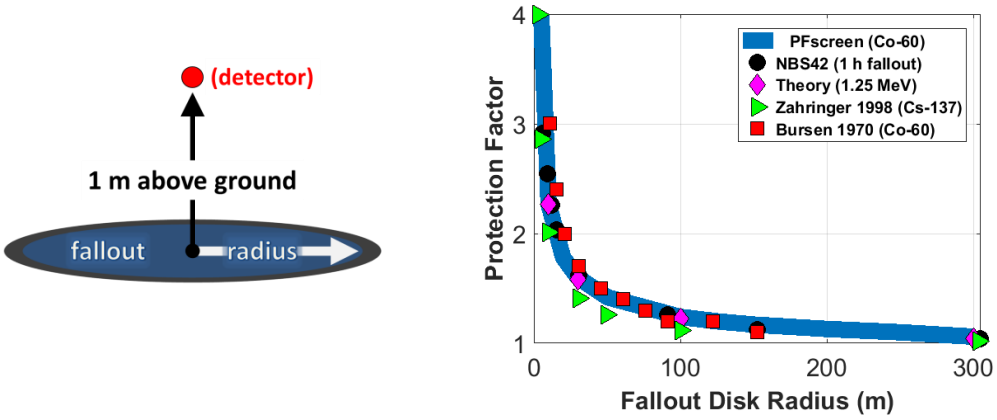

Figure A8. (left) Illustration of a detector 1 m above a flat, uniformly contaminated, finite sized fallout disk. (right) Change in protection factor with increasing disk size (radius).

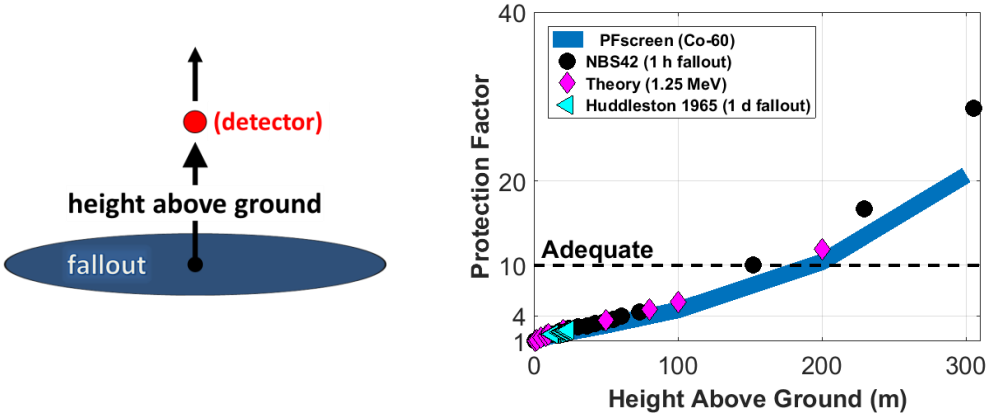

Figure A9. (left) Illustration of a detector at various heights above a uniformly contaminated, infinite plane. (right) Change in protection factor with height.

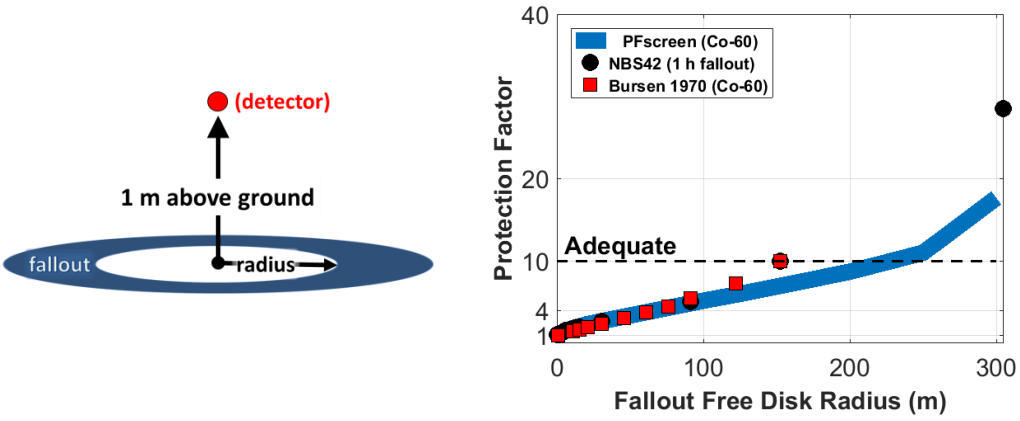

Figure A10. (left) Illustration of a detector above a fallout free zone within a uniformly contaminated, infinite plane. (right) Change in protection factor with the size (radius) of the fallout free zone.

The PFscreen model uses *Equation A3* to account for the angular dependence of incoming radiation on the incident angle (θ), height above ground level (h agl), and energy.

Spencer [27] calculated the relative radiation dose rate for 1.12 h old fission fallout as a function of incidence angle and height above the ground (agl), see *Figure A11*. Additional calculations on 28 h, 40 h and 131 h old fission fallout and individual radiation energies indicate that there is some, but limited change in the *relative* angular dose rate with time.[15] [26], [27], [30].

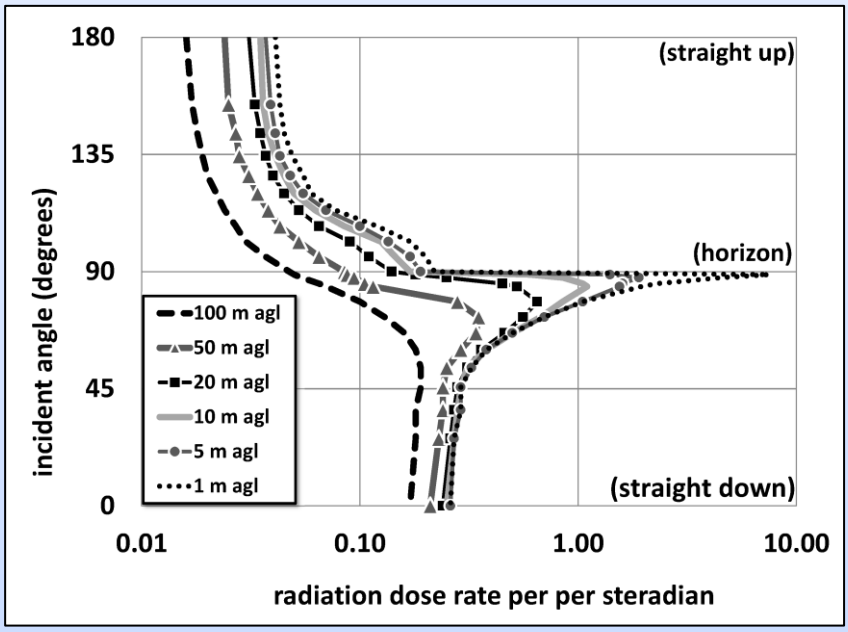

Figure A11. Relative dose rate angular distribution for select detector heights.

Spencer's predictions were later verified by experiments at the Department of Energy's Nevada Test Site [29], [30] with both (a) actual 1 d old fallout and (b) simulated fallout using sealed ^{60}Co sources[16] which were propelled at constant speed through tubing shaped in either a spiral or circular shape (or occasionally both) surrounding a collimated (0.03 steradian solid angle), 1.6 cm x 1.6 cm NaI(Tl) crystal spectrometer, see *Figure A12*.

Figure A12. Measurements of relative dose rate

[15] The absolute dose decreases greatly over this period.
[16] The penetration of ^{60}Co radiation is similar to that of 1 h old fallout [9].

The PFscreen model calculates the absolute dose rate by scaling the Spencer results.

(Equation A3)

$$Absolute\ Dose\ Rate(\theta, h, Radiation\ Energy) =$$

$$Relative\ Dose\ Rate(\theta, h)$$

$$\times\ {}^{60}Co\ Normalization\ Factor$$

$$\times \left(\frac{(Radiation\ Energy)}{({}^{60}Co\ Energy)} \right)$$

where

$Absolute\ Dose\ Rate(\theta, h, Radiation\ Energy)$
= absolute dose (rem s^{-1} sr^{-1})
(assumes the ground is contaminated with 1 Ci m^{-2} of radioactive material)

$Relative\ Dose\ Rate(\theta, h)$ = interpolated from *Figure A11* (rem m^2 Ci^{-1} s^{-1} sr^{-1})

${}^{60}Co\ Normalization\ Factor$ = 1.80 (Ci m^{-2})

= factor such that when all incoming radiation is considered, the mid-section bone marrow[17] dose rate at 1 m agl for 1 Ci m^{-2} of ^{60}Co contamination is 8.62×10^{-3} rem s^{-1} [24]

$Radiation\ Energy$ = effective photon energy (MeV)

${}^{60}Co\ Energy$ = 2.5 MeV = ^{60}Co radiation energy (1.17 MeV + 1.33 MeV)

[17] Bone marrow dose rate is used as PFscreen's index dose rate because when a person is exposed to fallout radiation, acute, life-threatening injury to the bone marrow occurs at a lower dose than that required to cause acute, life-threatening injuries to other critical organs.

EXTERIOR WALLS

Objects that block (scatter) direct, horizontally traveling radiation can reduce radiation exposure. These objects include exterior walls, free-standing concrete barriers, and the wall below a window sill.

Figure A13 illustrates this effect by adding a single story (3.66 m; 12 ft) concrete barrier around the edge of the fallout free zone shown in *Figure A10* (the barrier is open at the top). A wall density x thickness of 50 g cm^{-2} (~100 psf) roughly corresponds to adequate protection with respect to ground fallout.[18] This value corresponds to a 0.25 m (10 in) thick, 2 g cm^{-3} (125 pcf) concrete wall.

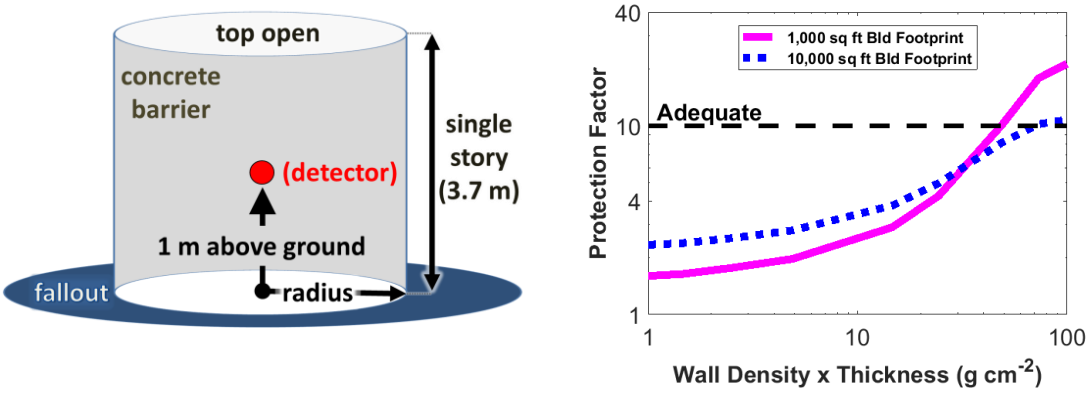

Figure A13. (left) Illustration of a detector above a fallout free zone enclosed within a single story, open top concrete barrier within a uniformly contaminated, infinite plane. (right) Change in protection factor with the wall density x thickness of the concrete barrier. For reference, the 1,000 sq ft and 10,000 sq ft building footprints have a corresponding fallout free disk radius of 5.44 m and 17.2 m, respectively, and are similar in size to a single family residence and small warehouse, respectively. The PFscreen analysis shown was modeled using a ^{60}Co radiation source.

Since they are often much lighter than the rest of the exterior wall, **windows and doors can provide portals through which outdoor radiation can penetrate an otherwise protective building shell (the wall below a window sill still provides radiation protection)**. Exposures that occur near (i.e., < 2 m from) the exterior wall can be dominated by radiation entering through these portals. For exposures farther away from the wall, these portals often become less

[18] (1) The specific value depends on other building properties such as the roof. (2) Significant radiation dose can occur if the area within the concrete barrier is contaminated (there is no fallout free zone).

important as direct radiation becomes blocked (scattered) by other parts of the building, e.g., [34].

While this report is focused on isolated buildings, it is worth noting that roughness in the earth's surface also provides protection – due in large part to the reduction of direct radiation [9], [30], [35]. The corresponding protection factors range from PF = 1.5 for natural, small-scale (≤ 0.125 m) roughness, PF = 3 at the centers of large 300 m (1,000 ft) hills and valleys, and potentially larger for congested urban areas

BASEMENT

Below ground individuals are similarly shielded from direct, horizontally traveling radiation. *Figure A14* illustrates this effect for a basement located within a lightweight, empty shed (6 m effective radius) [20], [31]. **Adequate protection is available immediately below ground.**

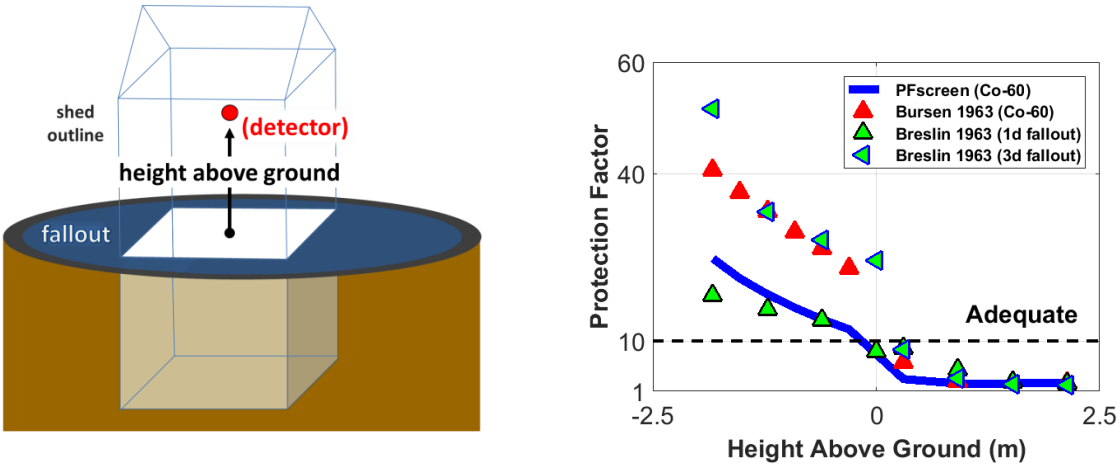

Figure A14. (left) Illustration of a detector in a lightweight, empty shed. (right) Change in protection factor with height above and depth below the ground.

Since below ground individuals are shielded from direct radiation, they are exposed only to scattered radiation. Two pathways exist – radiation scattering from the atmosphere (skyshine) and radiation scattering from the building itself.

For the skyshine pathway, **below ground radiation exposure depends on the amount (solid angle) of the sky that is visible**. Locations deeper below the ground level are more protective as less of the sky is visible, see *Figure A15*. Similarly, basement center locations are exposed to more skyshine, and hence are less protective, than locations near a wall. Corner locations are most protective. *Figure A16* illustrates these effects with an open air basement (2.4 m effective radius) [32].[19] For a given depth, the protection factor decreases with increasing basement size (not shown).

Radiation reflecting (scattering) from basement walls can increase the exposures.

[19] This basement does not have ground contamination within 0.762 m of the basement inner wall. If ground contamination is present at the basement wall edge, the basement protection can be reduced, see "lip effects" in [9].

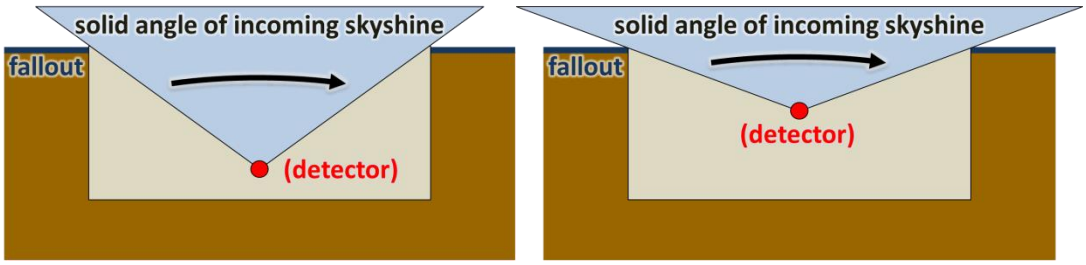

Figure A15. Basement walls constrain the amount (solid angle) of sky visible to below ground individuals. This reduces the amount of radiation scattered off of the atmosphere into the basement (skyshine). Less skyshine is present deeper in the basement (left panel) than closer to the surface (right panel).

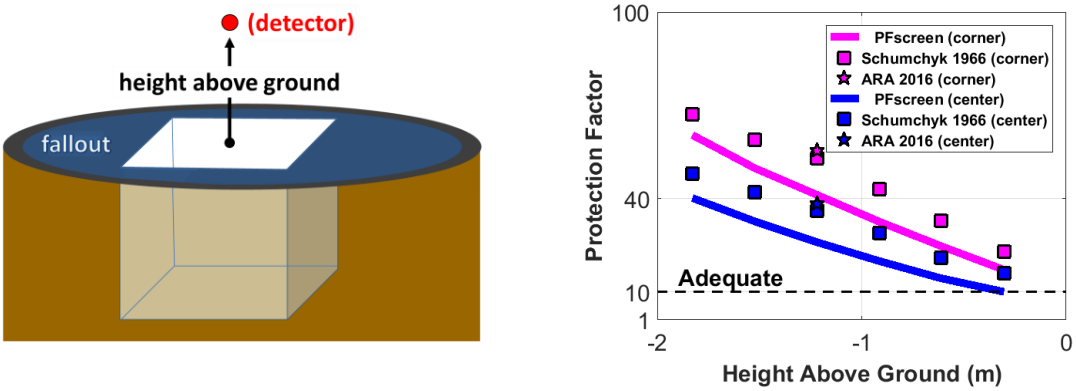

Figure A16. (left) Illustration of a detector above an open basement. (right) Change in the protection factor with depth below ground for center and corner locations. The PFscreen analysis shown was modeled using a ^{60}Co radiation source.

CEILINGS, FLOORS, AND ROOFS

Ceilings, floors, and roofs can both increase and decrease indoor radiation exposures. The net effect depends on the (a) detector location within the building and (b) building geometry, structural characteristics, and construction materials.

Radiation can be blocked (scattered) by ceilings, floors, and roofs and as with exterior walls, heavier ceilings, floors, and roofs provide more protection.

Heavy (e.g., concrete) ceilings, floors, and roofs protect individuals by limiting the amount (solid angle) of the ground and sky that is visible, see *Figure A17*. This effect is limited near the building edge, but becomes more important closer to the building center. For large footprint buildings, the difference between the building edge and center can become quite pronounced. For similar reasons, a person who is lying down may have a decreased radiation exposure. In the upper stories, building protection increases closer to the floor as more of the direct, ground source radiation is blocked (scattered). For example in an 80 m^2 footprint concrete building, measured exposures 0.3 m (1 ft) from the floor were ~ 40% less compared to the standard, ~1 m (3 ft), reference height [36].[20] This effect is less important for lightweight (e.g., wood) ceilings, floors, and roofs as such ceilings, floors, and roofs block (scatter) less of the radiation that passes through them.

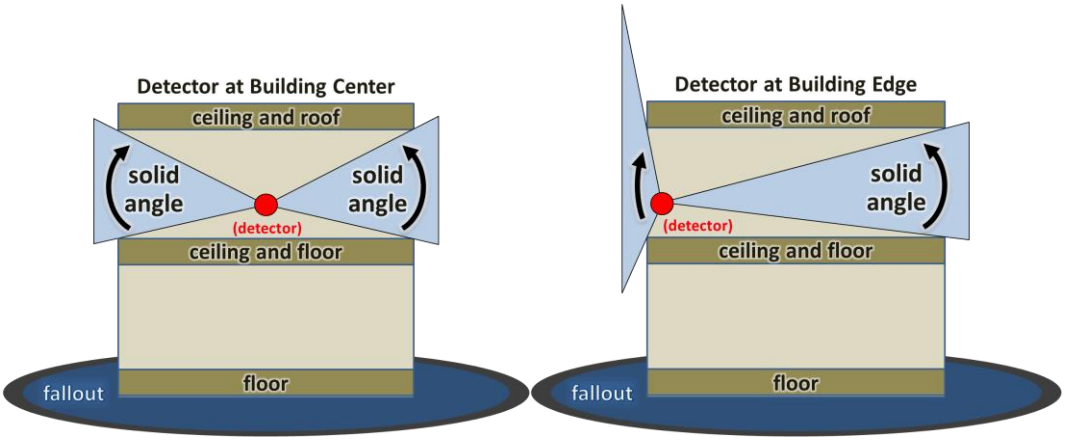

Figure A17. Heavy ceilings, floors, and roofs reduce the amount of contaminated ground and sky that is visible for indoor individuals. This effect is greater at the building center (left panel) than at the building edge (right panel).

[20] The change in protection depends on the individual's location within the building and the building construction.

Radiation reflecting (scattering) from ceilings, floors, and roofs can also increase exposures. This effect is particularly important for individuals just below a ceiling or floor that is illuminated by direct radiation emitted from the ground source. This effect can increase exposures in otherwise well protected locations, e.g., [9], [37]. For example, a basement in a lightweight house can provide *similar or less protection* (although still adequate) than an open air basement if the floor on the first story is above the ground, see *Figure A18*. The importance of reflected radiation to indoor exposures increases with (a) the ceilings, floors, and roof weight (increased material density increases scattering) and (b) degree to which ceilings, floors, and roofs limit the visible sky. Heavier exterior walls, and fewer windows, reduce this effect by blocking (scattering) the amount of radiation reaching the ceiling, floor, or roof.

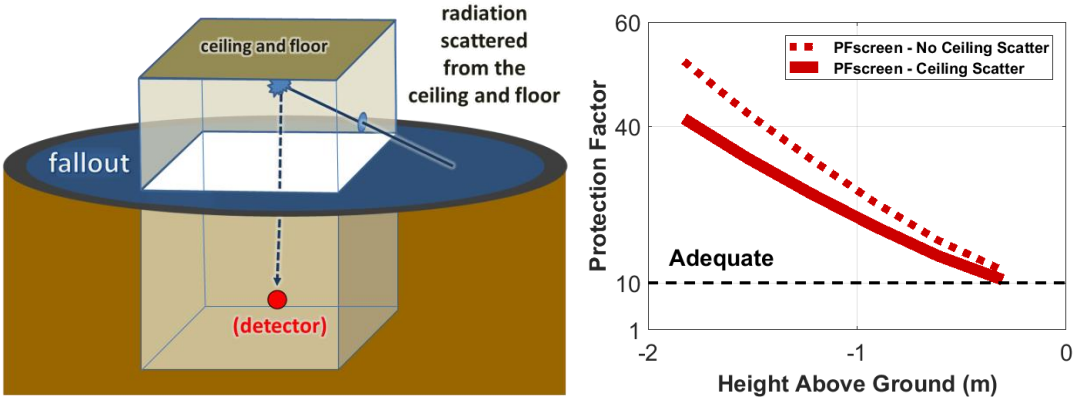

Figure A18. (left) Illustration of radiation scattering from a ceiling and floor into a basement. (right) PFscreen estimate of the protection factor in the center of the basement shown in *Figure A16* with and without the ceiling and floor scatter from a 0.064 m (2.5 in) concrete slab floating 0.91 m (3 ft) above the ground. For context, (1) the corresponding open basement case (no floating concrete slab, shown in *Figure A16*) is nearly identical to the ceiling scatter case (shown above), (2) the open basement and ceiling scatter cases provide less protection than the no ceiling scatter case (where the floating slab is present and blocks skyshine, but does not scatter groundshine), and (3) *Appendix B* contains a comparison between results from PFscreen and an independent Monte-Carlo model for this case. The PFscreen analysis shown was modeled using a ^{60}Co radiation source.

INTERIOR WALLS AND BUILDING CONTENTS

Material inside the building shell can block (scatter) radiation and so protect occupants. As with exterior walls, heavier interior materials provide more protection.

While interior walls are often lighter than exterior walls,[21] radiation may have to pass through many interior walls to reach interior portions of the building and so even relatively lightweight interior walls can provide significant protection.

In-use buildings can also contain contents. For some buildings – such as libraries, warehouses, and supermarkets – the mass of this material can exceed the mass of the roof or exterior walls.

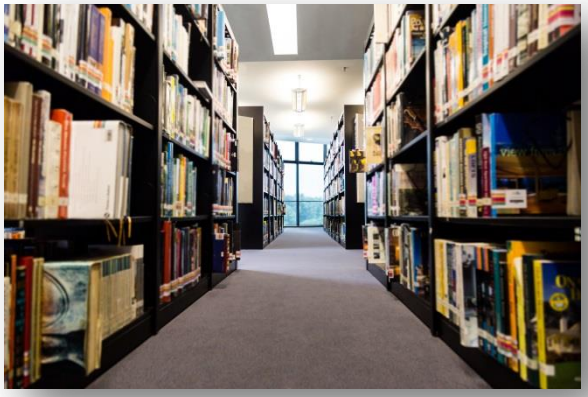

[21] For example, a typical drywall (sheetrock) wall has ~5% of the mass of foot-thick concrete (8 vs 125 psf).

ROOF CONTAMINATION

The sand-sized radioactive particles falling from the mushroom cloud can also settle on roofs and other horizontal building surfaces. **For some buildings, roof contamination contributes significantly to indoor radiation exposures**, e.g., [38], [39]. Limited modeling studies indicate that the radiation emitted from fallout deposited on other horizontal surfaces, including gutters and balconies, only significantly affects indoor exposures near the exterior wall [9], [40].[22]

Conceptually, **roof contamination is an elevated patch of ground contamination**. Like the ground contamination shown in *Figures A8* and *A9* and *Appendix C*, the dose an individual receives standing under a contaminated roof increases with the roof size and decreases with the distance from the roof. Radiation from roof contamination can likewise be blocked (scattered) by ceilings, floors, and the roof – with heavier structures providing more protection. *Figure A19* illustrates these effects with a roof source atop a multistory concrete structure with two different roof and floor thicknesses (5 m effective radius) [33].

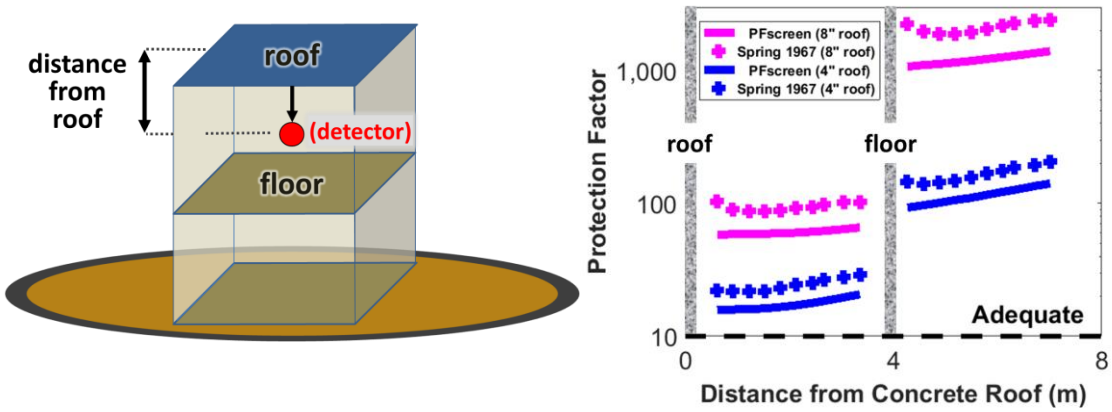

Figure A19. (left) Illustration of radiation scattering through a concrete roof and floor. (right) Change in protection factor with distance from a roof source. The concrete floor present at ~4 m has the same thickness as the roof. The PFscreen analysis shown was modeled using a ^{60}Co radiation source.

[22] Nearby, elevated contamination sources, including trees, can significantly affect indoor exposures, e.g., [9], [41], [42]. The impact of the surrounding environment is beyond the scope of this document.

The relative importance of ground and roof sources depends on the specific building construction and detector location within the building. Roof sources can dominate indoor radiation exposures for single-story, large footprint, commercial buildings with heavy (e.g., concrete) exterior walls, e.g., supermarkets, e.g., [38], [39].

The roof and ground may not be equally contaminated. While exposed, flat surfaces are expected to be contaminated to the same degree; many roofs are not flat and fallout particles can naturally slide off steep, smooth roofs. For example, roof contamination was measured to be 10% of ground contamination for a sloped plywood roof [20]. For comparison, fallout contamination was comparable on sloped, composition shingle and flat, concrete roofs and the nearby ground [43]. Fallout particles can also be washed off roofs – reducing the roof contamination and indoor dose. While the effects of natural rainfall have not been well studied,[23] in one study a fire hose washed 2/3 of fallout from a concrete roof [43] and rainfall is believed to contribute to the previously mentioned 90% difference in contamination between the ground and the sloped plywood roof [20].

[23] Natural rainfall is known to remove smaller radioactive particles, such as those emitted from nuclear power plant accidents, from building surfaces, see [44] and references within.

APPENDIX B: BUILDING ATTRIBUTE VERIFICATION

In this appendix, we assess the degree to which the identified physics and building attributes are capable of determining building protection. To perform this assessment, we developed the PFscreen model which calculates the distribution of building protection within an individual, isolated building on flat ground based on the key radiation physics and building attributes, see *Appendix D*.

These comparisons between (a) PFscreen and (b) independent experimental, theoretical, and modeled building protection results assess the degree to which the currently identified physics and building attributes are capable of determining building protection. Some such comparisons have already been shown in the main text. Here we provide additional, broader comparisons across a wide suite of buildings with available data. The comparisons performed to date represent much of the previously identified data listed in [3]. We note that there are several key building types for which no prior, independent study has been performed – leaving open the possibility that additional building attributes may be required for those buildings.

Two types of studies are discussed.[24] The first study type was performed for the explicit purpose of studying fallout building protection. The buildings and other related structures used in these studies are well characterized with respect to key building attributes. The second study type examined in-use buildings. These buildings studied lack precise characterization of one or more building attribute(s) and so we developed estimates using architectural drawings and descriptions. In most cases, we used a standard method to determine numerical values for key building attributes from architectural features [18]. Thus for the second building type, the comparison between PFscreen and prior study results provides a degree of verification for the method to convert architectural feature to fallout building attribute values.

In this appendix, we provide a brief description of the studied buildings and comparison results. Detailed building descriptions and model/measurement data are provided in supplemental spreadsheets and in the original study(ies) [12]. Standardized comparison graphs comparing PFscreen predicted results to actual building radiation protection factor data are presented with each comparison graph in this section formatted identically.

- The prior study protection factor is plotted on the horizontal (x) axis.
- The PFscreen model protection factor is plotted on the vertical (y) axis.
- Each symbol indicates a comparison between a PFscreen result and previously reported protection factor data at a single location and time within a building.
- For visualization purposes, we provide lines that indicate perfect agreement (1:1, black solid line), factor of 2 agreement (1:2 and 2:1, blue dashed lines), and factor of 10 agreement (1:10 and 10:1, magenta dotted lines).
- The number of comparison points (n) plotted is provided in the upper left corner.

[24] These types are distinct from the realistic and other structure categories discussed in [3].

OPEN BASEMENT

An empty, open basement (18.6 m^2 footprint) was studied using a Co-60 ground source, see *Figure B1* [32]. The PFscreen building model was developed using study reported attribute values. Measurements were made at 5 horizontal and 6 vertical positions (all locations were below the ground level). **All comparisons are within a factor of 2**, see *Figure B2*.

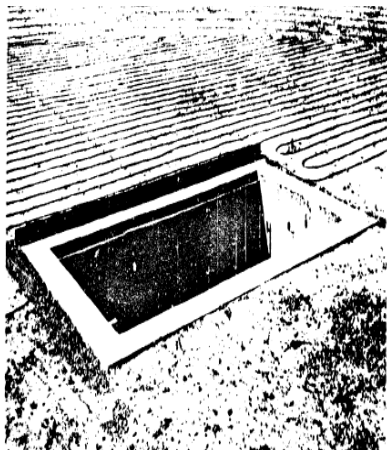

Figure B1. Open basement with tubing for Co-60 ground source.

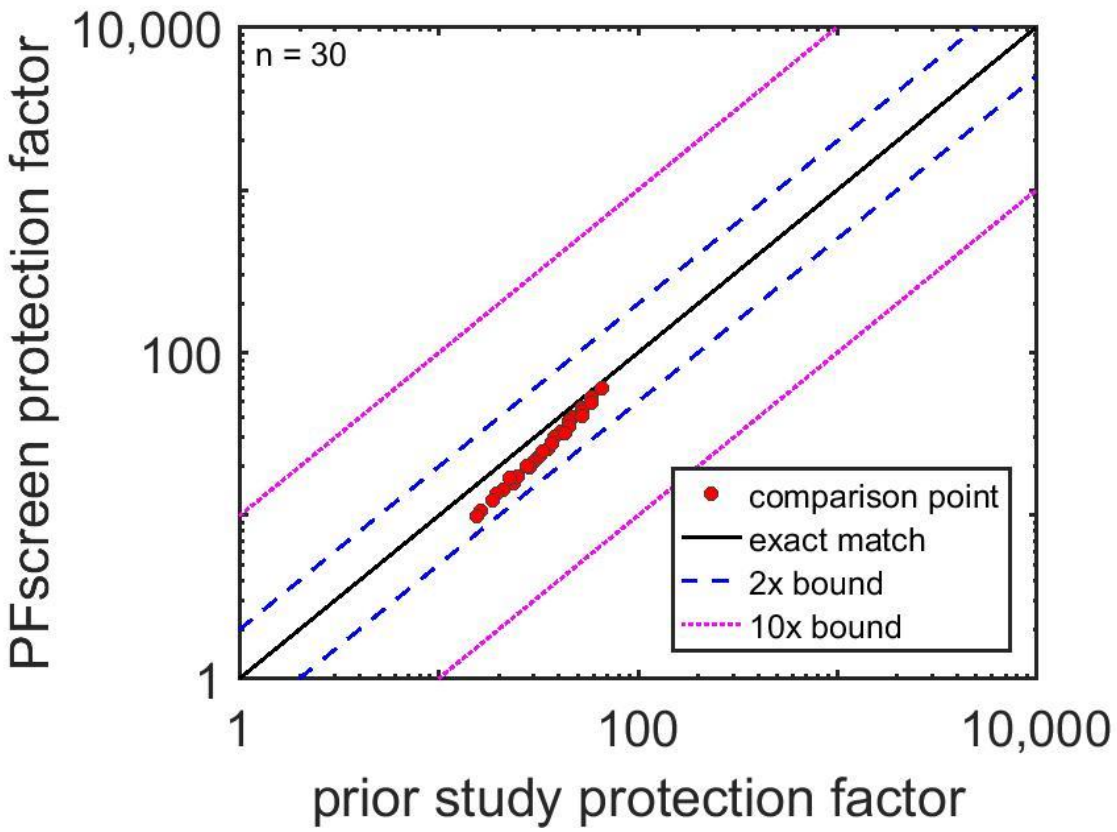

Figure B2. Comparison between PFscreen and prior study building protection estimates for an open basement. Each red dot indicates a comparison between PFscreen model and a prior study estimate for a single location.

OPEN BASEMENT WITH FLOATING CONCRETE SLAB

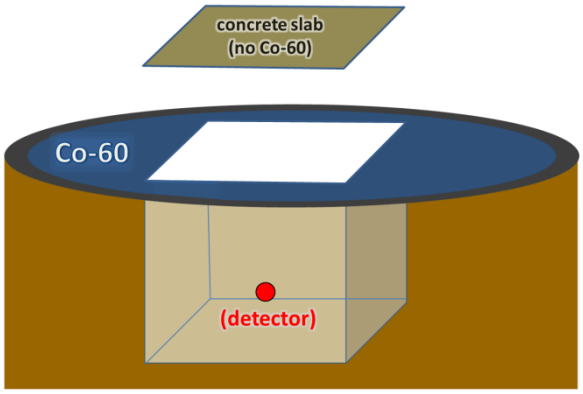

Figure B3. Open basement with floating concrete slab.

The open basement (18.6 m^2 footprint) with a slab of concrete floating 0.91 m (3 ft) above the ground was modeled with a Co-60 ground source using a high-fidelity Monte Carlo simulation, see *Figure B3*.[25] This comparison tests the absolute and relative importance of (a) skyshine and (b) radiation scattered from a floor. The modeled concrete slab thicknesses ranged from 0 (no slab) to 64 cm. Comparisons were made at 5 horizontal positions 0.91 m (3 ft) from the basement floor. **All comparisons are within a factor of 2**, see *Figure B4*.

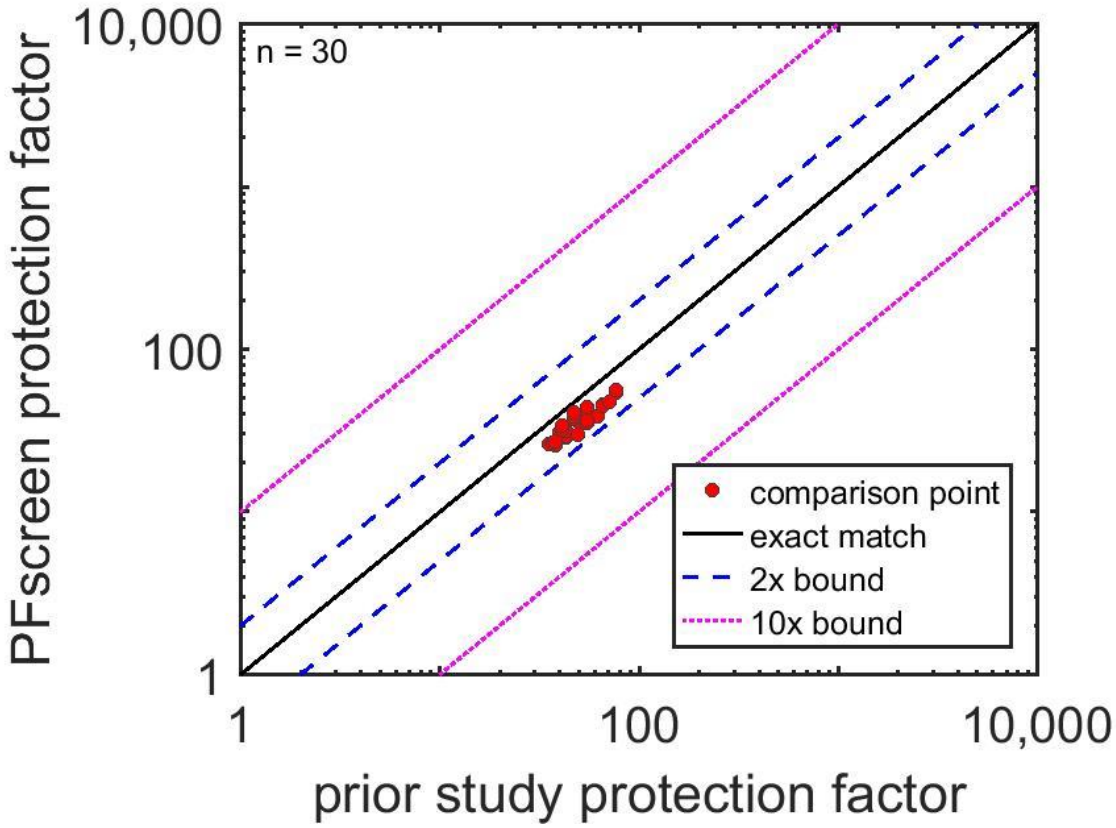

Figure B4. Comparison between PFscreen and prior Monte Carlo study building protection estimates for an open basement with a concrete slab floating 0.91 m above the ground. Each red dot indicates a comparison between PFscreen model and a prior study estimate for a single location.

[25] personal communication (Andy Li; Tyler Dant; Kevin Kramer)

TEST BUILDING

A 3-story experimental test building (80 m^2 footprint) was studied using Co-60 roof and ground sources, see *Figure B5* [33], [36], [45]. The PFscreen building models were developed using reported building attribute values for 17 different configurations. These configurations spanned a wide range of exterior and interior wall densities (including non-uniform walls), floor densities, roof densities, and apertures. This comparison uses measurements made on a variety of heights above the floor of each story. **Almost all comparisons are within a factor of 2**, see *Figure B6*.

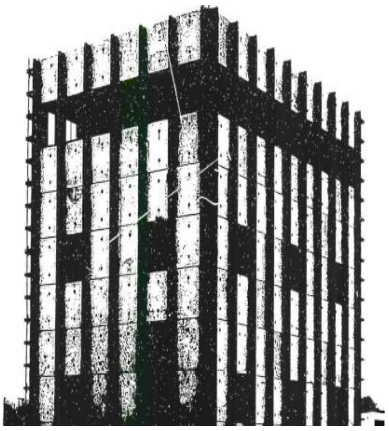

Figure B5. Test building with apertures.

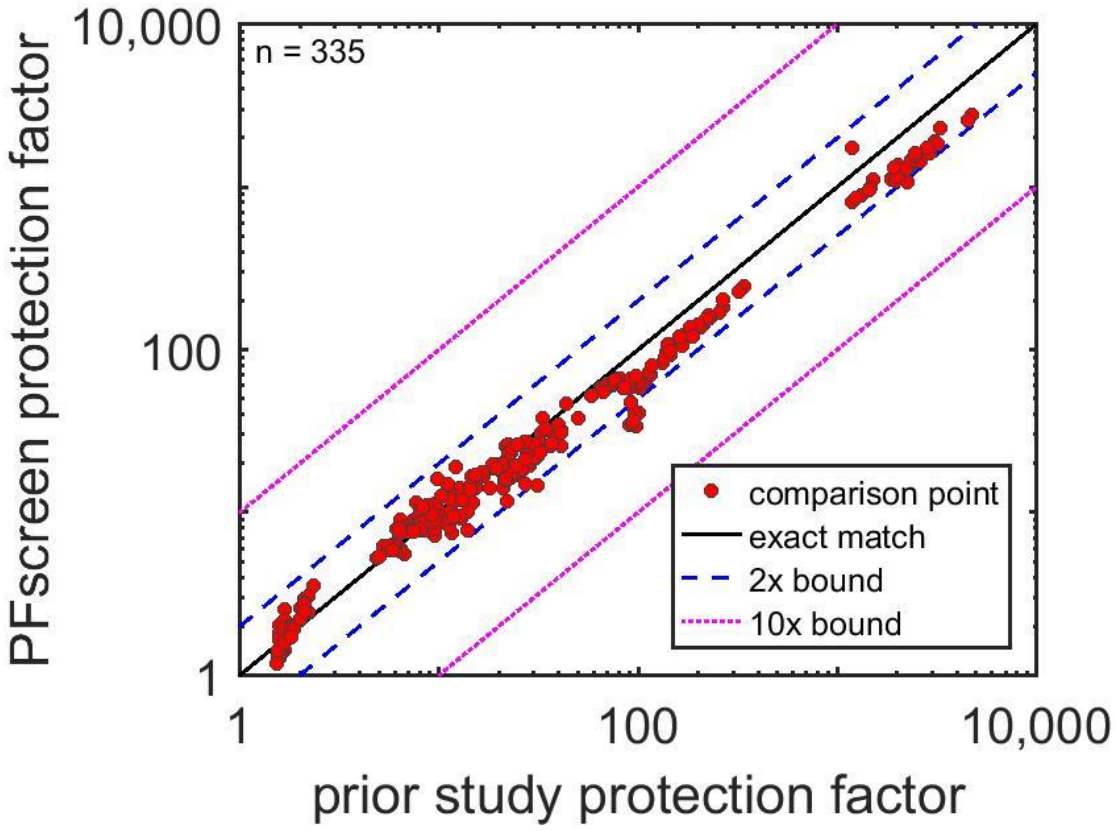

Figure B6. Comparison between PFscreen and prior study building protection estimates for 17 test building configurations. Each red dot indicates a comparison between PFscreen model and a prior study estimate for a single location.

BUTLER BUILDING

Figure B7. Butler building.

An empty Butler building (120 m^2 footprint metal shed) was studied with a Co-60 source and 1 h, 1d, and 3 d old fallout,[26] see *Figure B7* [20], [31]. The PFscreen building models were developed using reported building attribute values. Measurements were made at 37 horizontal and 10 vertical positions above and below the ground level. The instrument used for the below ground 1 h and 3 d data was known to have overestimated the protection factor by 1/3 or more [20].[27]

Almost all Co-60 comparisons are within a factor of 2, see top panels in *Figures B8* and *B9*.

The fallout comparisons have a wider spread but are within a factor of 10, see the bottom panels in *Figures B8* and *B9*. **The above ground fallout comparisons (PF ~ 2) generally agree to within a factor of 2**.[28] PFscreen underestimates the below ground protection for the ground and roof case (*Figure B9*) due to the roof contamination being 10% of the ground contamination. PFscreen normally assumes an equally contaminated roof and ground. As *Figure B9* shows, in normal usage PFscreen underestimates, on average, the 1 d fallout below ground measurements by about a factor of 2 and the 1 h and 3 d fallout below ground measurements by a bit more. **When configured to match the measured roof contamination, most of the below ground fallout comparisons agree to within a factor of 2 (data shown in main text).** When only ground fallout is considered (*Figure B8*), PFscreen agrees with the below ground 1 d fallout measurements within a factor of 2. PFscreen underestimates, on average, the below ground 3 d fallout measurements by a bit more than a factor of 2 – consistent with the known instrument bias in this study.

[26] PFscreen analyses assume the 1 d and 3 d fallout spectra was similar to Cs-137 and Co-60, respectively.

[27] The instrument used is less sensitive at low, e.g., 0.4 MeV, radiation energies present in the basement.

[28] In In the 1 h to 3 d fallout source panel, the cluster of comparisons at PFscreen PF ~ 4 (1 d fallout PF ~ 10; 3 d fallout PF ~ 20) are ground-level (~0 m agl) measurements. PFscreen assumes these measurements are above the ground and so exposed to direct radiation. Based on the protection factor values, it is likely that these measurements were only partially (or not at all) exposed to direct radiation, potentially due to a short (0.1 m high) concrete foundation that extends above the ground. These measurements are included for completeness, but provide a less reliable verification of the PFscreen model results.

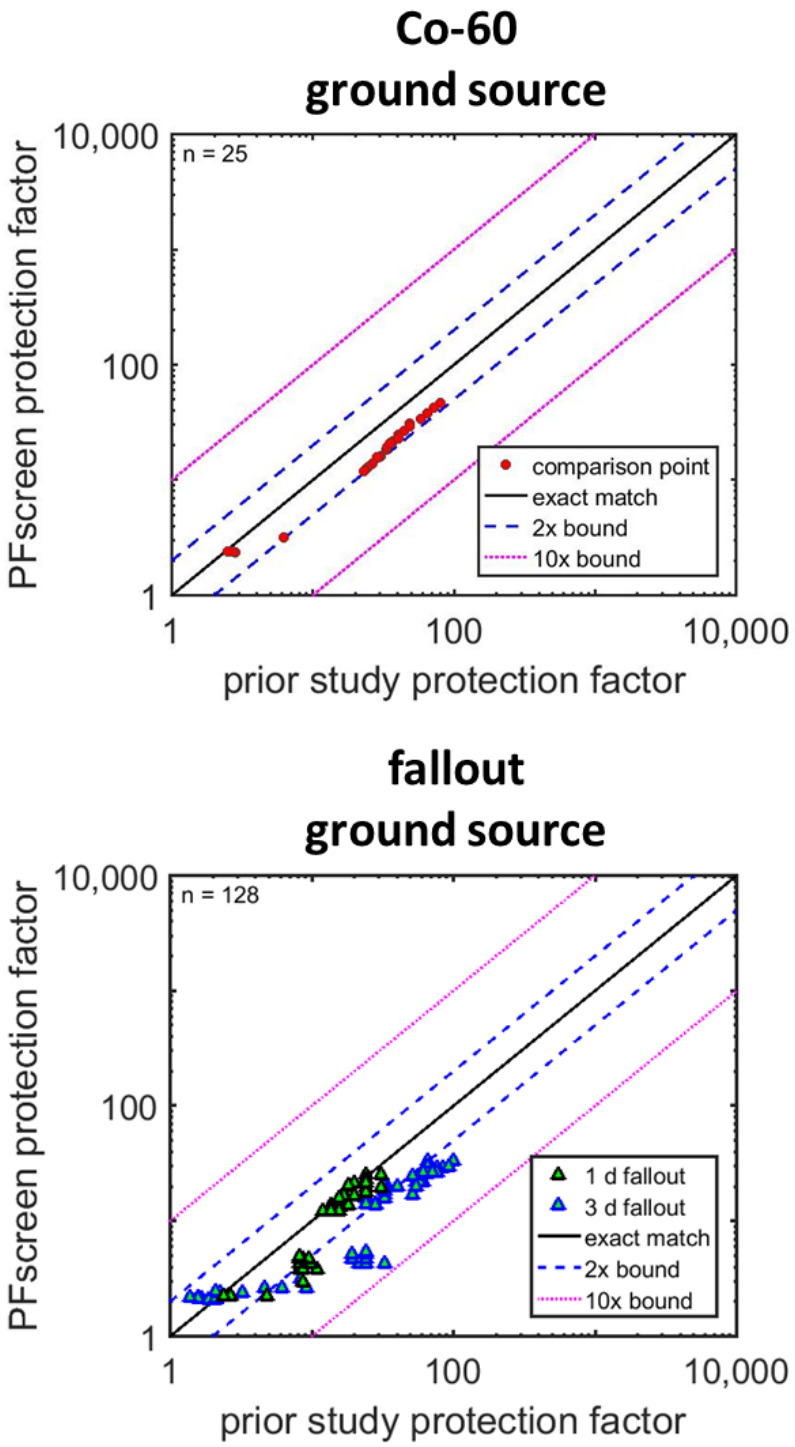

Figure B8. Comparison between PFscreen and prior study building protection estimates for the Butler building ground source comparisons. Each symbol indicates a comparison between PFscreen model and a prior study estimate for a single location.

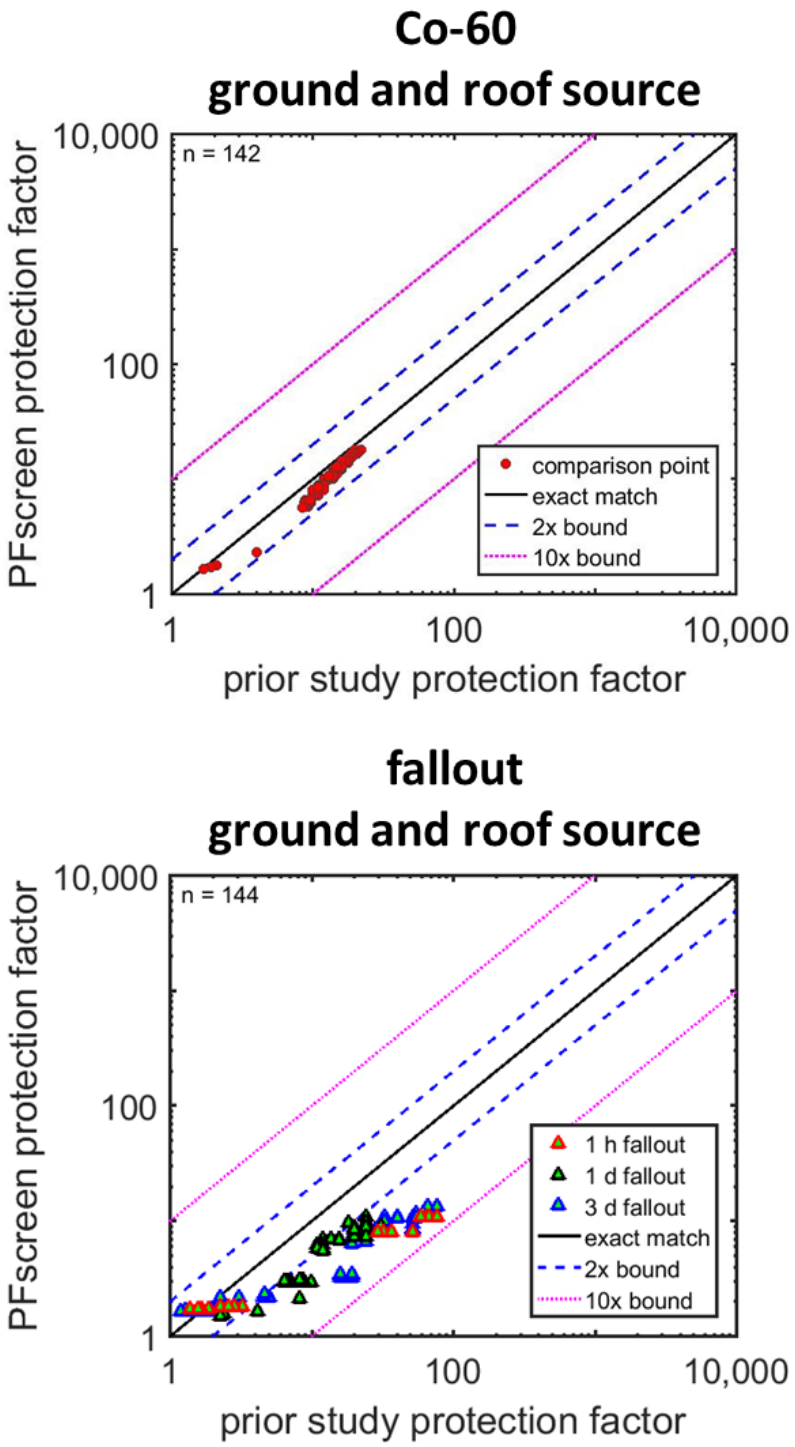

Figure B9. Comparison between PFscreen and prior study building protection estimates for the Butler building ground and roof source comparisons. For the fallout measurements (bottom panel), the roof contamination was measured to be 10% of the ground contamination (PFscreen assumes equal levels of contamination). Each symbol indicates a comparison between PFscreen model and a prior study estimate for a single location.

SINGLE FAMILY RESIDENCES

Figure B10. Cemesto house.

A collection of lightweight, in-use, single family residences (80 to 250 m^2 footprint) were studied using Co-60 roof and ground sources [46], [47]. The exterior wall material ranged from wood siding, Cemesto panels (*Figure B10*), stucco, and concrete block. These houses were on flat and sloping ground as well as in a valley. The PFscreen building models were developed using (a) architectural drawings and descriptions and (b) a mapping to building attributes values. We use measurements made ~1 m above the floor of each story. **Almost all comparisons are within a factor of 2**, see *Figure B11*.

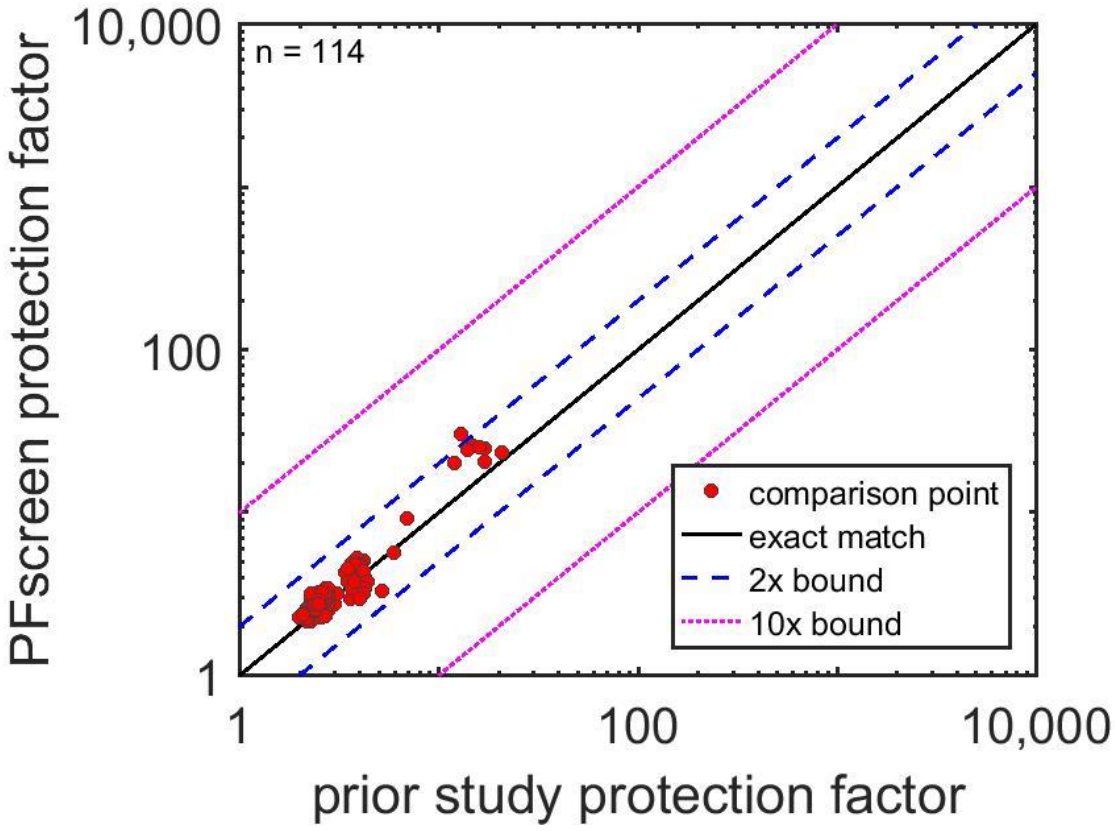

Figure B11. Comparison between PFscreen and prior study building protection estimates for 12 lightweight single family residences. Each red dot indicates a comparison between PFscreen model and a prior study estimate for a single location.

LARGE FOOTPRINT CONCRETE STRUCTURE

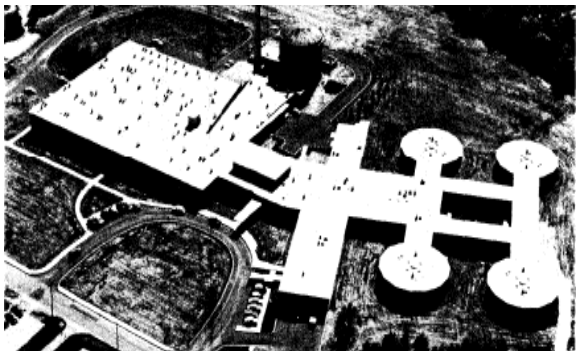

Figure B12. Brookhaven Medical Laboratory. Study area is square portion on the left.

A portion of the Brookhaven Medical Laboratory (505 m^2 footprint) was studied using Co-60 roof and ground sources, see *Figure B12* [38]. The ground level varied and so the basement depth ranged from 0 m (ground level) to 3.3 m (buried) - PFscreen assumed a 2.7 m depth. The PFscreen building models were developed using (a) architectural drawings and descriptions and (b) a mapping to building attributes values. Measurements were made ~1 m above the floor of each story. **Almost all above ground comparisons (the cluster of comparisons with PF near 20) are within a factor of 2**, see *Figure B13*. **In the basement (the cluster of comparisons with PF near 300), the average agreement is also good**, but ~25% of the comparisons differ by more than a factor of 2.

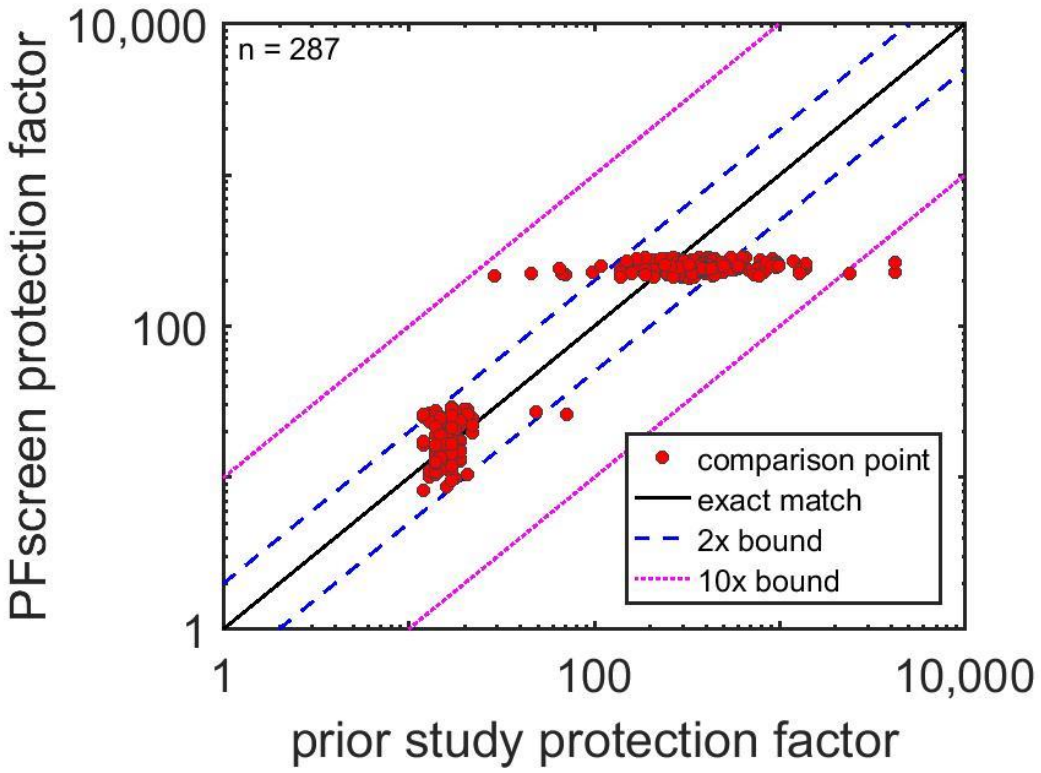

Figure B13. Comparison between PFscreen and prior study building protection estimates for the Brookhaven Medical Laboratory. Each red dot indicates a comparison between PFscreen model and a prior study estimate for a single location.

LOW-RISE CONCRETE STRUCTURES

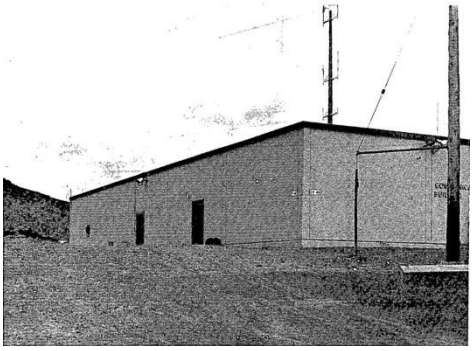

Figure B14. Control Point Building 40.

A collection of low-rise (1 and 2 story) concrete buildings (~800 m^2 footprint) with few doors and windows were studied using Co-60 and Cs-137 roof and ground sources, see *Figure B14* [19]. The ground level varied and so the basement depth ranged from 0 m (ground level) to 3.6 m (buried) - PFscreen assumed a 2.7 m depth. The PFscreen building models were developed using (a) using reported building attribute values, (b) architectural drawings and descriptions and (c) a mapping to building attributes values. Measurements were made ~1 m above the floor of each story. **Almost all above ground comparisons (cluster of comparisons with PF near 70) are within a factor of 2**, see *Figure B15*. **In the basement (PFscreen PF ~ 250), the average agreement is also good**, but half of the comparisons differ by more than a factor of 2.

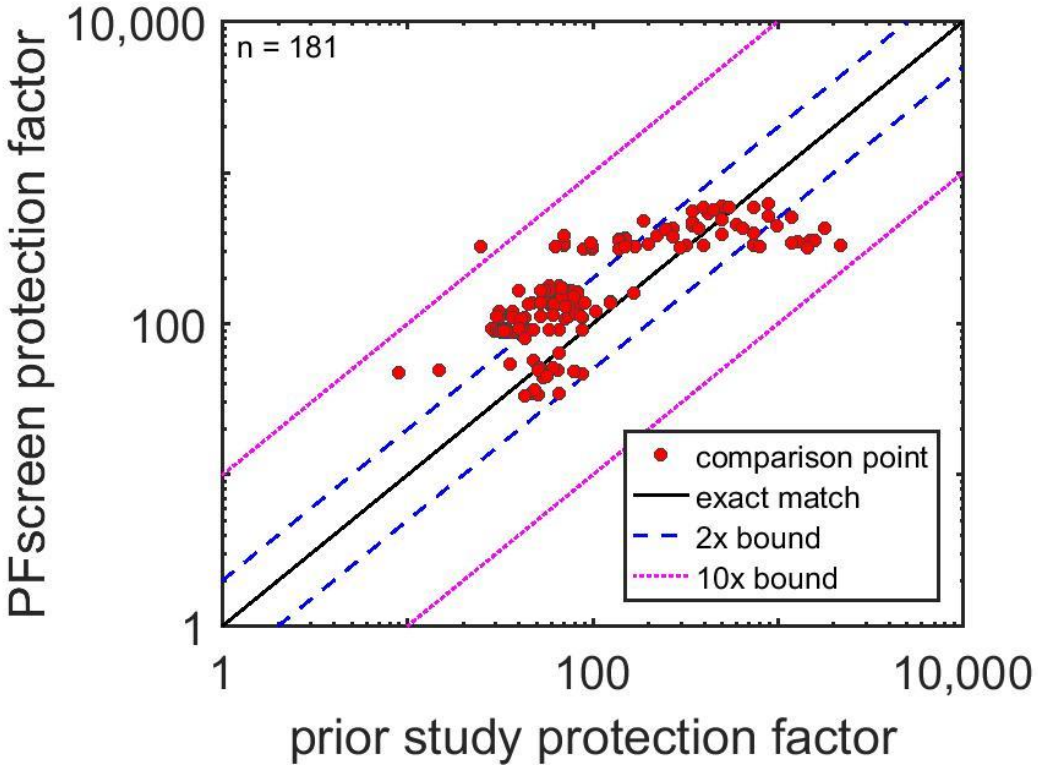

Figure B15. Comparison between PFscreen and prior study building protection estimates for 2 low-rise concrete buildings. Each red dot indicates a comparison between PFscreen model and a prior study estimate for a single location.

APPENDIX C: THEORETICAL CALCULATION OF UNSHIELDED DOSE RATE WITH HEIGHT

In this appendix, we derive the radiation dose rate at a point above an infinite, uniformly contaminated, flat plane as function of radiation energy and height.

First we consider a dose contributed by point A, a location on a finite-sized disk of fallout radiation, to a point, P centered above the fallout disk, see *Figure C1*. Based on the scattering considerations discussed in *Scattering* section (*Appendix A*), *Equations C1 to C3* provides the contribution of dose rate at point P due to the contamination at point A.[29]

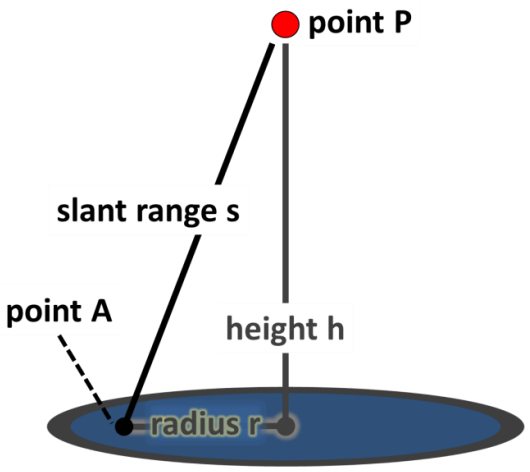

Figure C1. Geometry for calculation of the contribution of the photon flux from point A to the dose rate at point P.

(*Equation C1*)

$$DR = \frac{\Psi \times SC \times B(FP) \times e^{(-FP)}}{4\pi \times s^2} dA$$

(*Equation C2*)

$$FP(s) = \mu \times \rho \times s$$

(*Equation C3*)

$$s = \sqrt{h^2 + r^2}$$

where

DR	= dose rate at point P (rad s^{-1})
Ψ	= conversion from photon flux to dose rate (rad $photon^{-1}$ cm^2)
SC	= surface contamination (photon cm^{-2} s^{-1})
B(FP)	= buildup factor (dimensionless)
FP	= number of mean free path lengths (dimensionless) [30]
dA	= (infinitely small) area of point A (cm^2)
s	= distance from points A to P, also called the slant range (cm)
h	= height of point P (cm)
r	= distance from the center of fallout disk to point A (cm)
μ	= mass attenuation coefficient (cm^2 g^{-1})
ρ	= air density (g cm^{-3})

[29] The dose rate scales with s^2 since it depends on the surface area of an expanding sphere.

[30] The mean free path is the average distance radiation will travel in a straight line. For the radiation energies considered here (0.5 to 3 MeV), this corresponds to a distance of ~100 to ~250 m in air.

Table C1. Buildup factors, B(FP), for common materials assuming a point radiation source (adapted from Table 6.4.1 in [48])

		photon energy (MeV)											
		0.5	**1**	**2**	**3**	**0.5**	**1**	**2**	**3**	**0.5**	**1**	**2**	**3**
		water				**aluminum**				**concrete**			
mean free paths	**0.5**	1.60	1.47	1.38	1.34	1.57	1.45	1.37	1.33	1.57	1.45	1.37	1.33
	1	2.44	2.08	1.83	1.71	2.28	1.99	1.78	1.68	2.27	1.98	1.77	1.67
	2	4.88	3.62	2.81	2.46	4.07	3.26	2.66	2.38	4.03	3.24	2.65	2.38
	3	8.35	5.50	3.87	3.23	6.35	4.76	3.62	3.11	6.26	4.72	3.60	3.09
	4	12.80	7.68	4.98	4.00	9.14	6.48	4.64	3.86	8.97	6.42	4.61	3.84
	5	18.40	10.10	6.15	4.80	12.40	8.41	5.72	4.64	12.20	8.33	5.68	4.61
	6	25.00	12.80	7.38	5.61	16.30	10.50	6.86	5.44	15.90	10.40	6.80	5.40
	7	32.70	15.80	8.65	6.43	20.70	12.90	8.05	6.26	20.20	12.70	7.97	6.20
	8	41.50	19.00	9.97	7.27	25.70	15.40	9.28	7.10	25.00	15.20	9.18	7.03
		air				**iron**							
mean free paths	**0.5**	1.60	1.47	1.38	1.34	1.48	1.41	1.35	1.32				
	1	2.44	2.08	1.83	1.71	1.99	1.85	1.71	1.64				
	2	4.84	3.60	2.81	2.46	3.12	2.85	2.49	2.28				
	3	8.21	5.46	3.86	3.22	4.44	4.00	3.34	2.96				
	4	12.60	7.60	4.96	4.00	5.96	5.30	4.25	3.68				
	5	17.90	10.00	6.13	4.79	7.68	6.74	5.22	4.45				
	6	24.20	12.70	7.35	5.60	9.58	8.31	6.25	5.25				
	7	31.60	15.60	8.61	6.43	11.70	10.00	7.33	6.09				
	8	40.10	18.80	9.92	7.26	14.00	11.80	8.45	6.96				

Table C2. Mass attenuation coefficients, μ, for common materials in $cm^2\ g^{-1}$ (adapted from Table 5.1 in [48])

	photon energy (MeV)			
	0.5	**1**	**2**	**3**
water	0.0966	0.0707	0.0494	0.0397
air	0.0869	0.0635	0.0445	0.0358
concrete	0.0872	0.0637	0.0448	0.0365
aluminum	0.0839	0.0613	0.0432	0.0354
iron	0.0824	0.0595	0.0425	0.0362

Table C3. Air kerma (kinetic energy released per unit mass) dose rate conversion factors ($Gy\ s^{-1}\ Bq^{-1}\ m^2$)

	height (m)	photon energy (MeV)		
		0.5	**1**	**2.25**
Beck 1968 [26]	**1 (m)**	6.32E-16	1.18E-15	2.21E-15
	10 (m)	3.65E-16	6.80E-16	1.27E-15
	100 (m)	1.00E-16	1.98E-16	4.13E-16
theory (this study)	**1 (m)**	7.88E-16	1.27E-15	2.65E-15
	10 (m)	4.35E-16	7.02e-16	1.53e-15
	100 (m)	1.1e-16	2.12e-16	5.28e-16

Table C1 provides the buildup factors for common elements and materials.[31] A buildup factor is the fraction of the radiation that is scattered at least once prior to reaching Point P. For a given number of mean free paths (distance) and photon energy, we interpolate the *Table C1* values. For this appendix, we use the air values (the PFscreen model uses the concrete values) and assume that the air density is constant between points A and P.

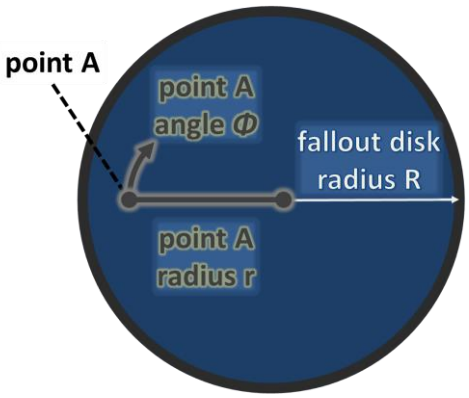

Figure C2. Disk integration geometry

Table C2 provides the mass attenuation coefficients for common elements and materials. For a given photon energy, we interpolate the *Table C2* values. For this appendix, we use the air values (PFscreen calculations use the concrete values).

Integrating *Equation C1* over a disk of radius R yields the contribution of the disk to the dose rate at point P, see *Equation C4* and *Figure C2*. *Equation C5* provides the corresponding protection factor.

We evaluated *Equations C4* and *C5* numerically for a 1 km radius disk.

(*Equation C4*)

$$DR(h,R) = \frac{\Psi \times SC}{4\pi} \int_{\Phi=0}^{2\pi} \int_{r=0}^{R} \frac{B\left(\mu \times \rho \times \sqrt{h^2+r^2}\right) \times e^{\left(-\mu \times \rho \times \sqrt{h^2+r^2}\right)}}{h^2+r^2} r\, dr d\theta$$

(*Equation C5*)

$$PF(h,R) = \frac{DR(1,R)}{DR(h,R)} = \frac{\int_{r=0}^{R} \left(\left(B\left(\mu \times \rho \times \sqrt{1+r^2}\right) \times e^{\left(-\mu \times \rho \times \sqrt{1+r^2}\right)}\right)/(1+r^2)\right) r dr}{\int_{r=0}^{R} \left(\left(B\left(\mu \times \rho \times \sqrt{h^2+r^2}\right) \times e^{\left(-\mu \times \rho \times \sqrt{h^2+r^2}\right)}\right)/(h^2+r^2)\right) r dr}$$

where

R	= radius of the fallout disk (cm)
PF(h,R)	= protection factor (dimensionless)[32]

Within 100 m of the ground, the protection factors have limited dependence on photon energy over the energy range of interest (varies less than 2x).[33] These theoretical prediction of dose rate and protection factors are consistent with prior estimates, see *Figure C3* and *Table C3*.[34]

[31] 8 mean free path lengths correspond to a slant range of ~1,250 m, e.g., ~800 m above a disk of 1 km radius, for 1 h old fallout radiation.

[32] Protection factor = the ratio of the dose rate at height 1 m to the dose rate at height h.

[33] There is minimal (< 10%) variation of protection factor with energy at a location 1 m above the ground for a disk radius ranging from 3 to 300 m.

[34] In this figure, "NBS42" = [27]; "Theory" = *Appendix C* results; "Huddleston 1965" = [30].

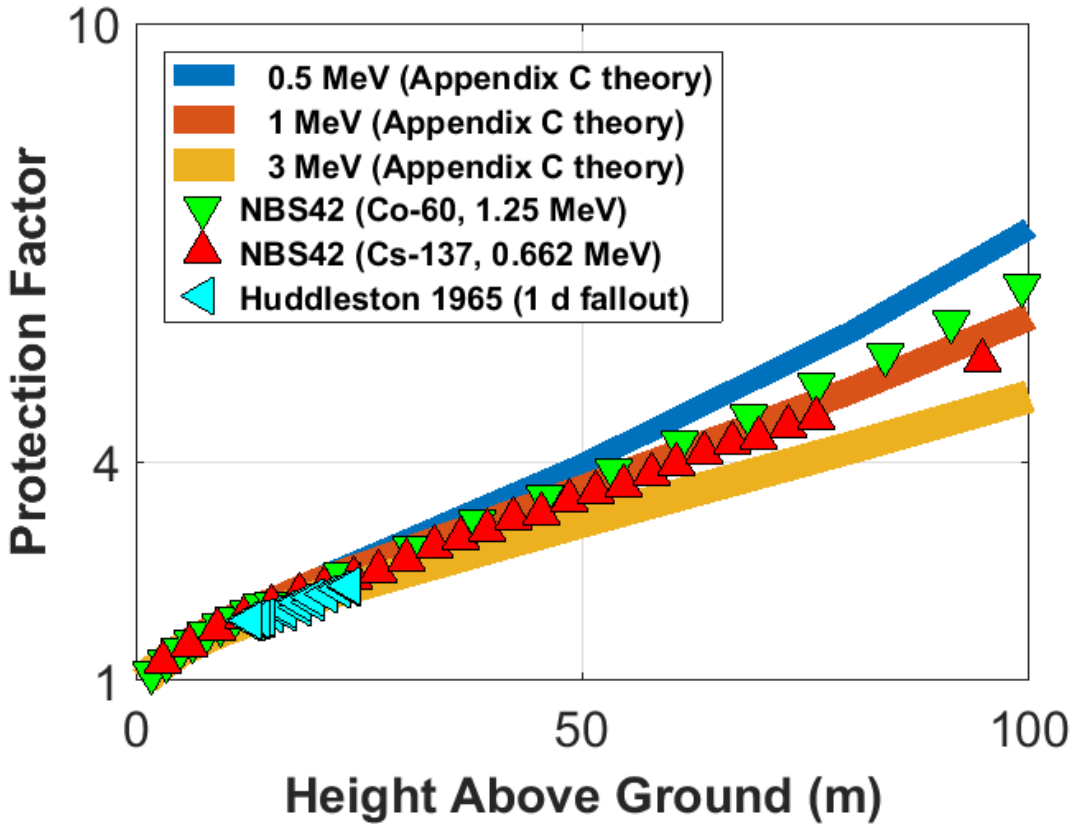

Figure C3. Protection factor over a uniformly contaminated radiation disk 1 km in radius

APPENDIX D: PFSCREEN MODEL DESCRIPTION

The PFscreen model estimates the distribution of protection that buildings provide their occupants against external radiation exposure. This appendix describes the PFscreen algorithms and their fast running (few minutes per building) PC computer code implementation. It is intended to facilitate interpretation of the PFscreen model results and provide a deeper understanding of both the model capabilities and limitations as well as the key physics involved in building protection.

INTRODUCTION

Building protection against external gamma radiation exposure has been studied for decades within the context of (a) nuclear fallout protection and (b) the remediation of nuclear power plant accidents, see [3] and refs therein. During this period, a variety of techniques have been developed for assessing building protection including (a) the "engineering method," a manual method developed in the 1960s by the US Office of Civil Defense to characterize civilian shelter protection [9]; (b) "point-kernel" methods, computerized methods used in the 1980s [49]; and (c) Monte-Carlo radiation transport computer codes which can now provide high accuracy and resolution estimates [40], [50]. Capability development has historically focused on increased prediction accuracy for arbitrary, complex buildings. As a consequence, modern state-of-the-art capabilities, while accurate and flexible, require significant time, expertise, and computational resources to initialize, compute, and quality assure – reducing their utility in assessing the protection provided by the wide variety of buildings present in the world.

Limited attention has been paid to identifying a small set of building properties required for a "reasonable" estimate of building protection. For example, prior authors have reported that the following properties can be important: mass (areal density) of external walls, roof, and floors; the presence of a basement; the number of stories; the internal building structure; location within the building; the presence of apertures (e.g., windows, doors); radiation spectra; and the surrounding environment, e.g., [9], [41], [42], [51]. Furthermore for some buildings such as libraries and warehouses, building contents contain more mass than the building construction materials, e.g. [52], and there is some evidence that even in office and residential structures, building contents (and interior walls) may significantly alter protection estimates [53].

To help address this knowledge gap, we developed the PFscreen model to provide building protection estimates based on a simplified description of the building and radiation transport physics, see *Figure D1*.[35] From a historical point of view, the PFscreen model represents a hybrid between, and builds upon, the previously referenced engineering and point-kernel methods. The degree to which the PFscreen model reproduces previously reported building protection

[35] As a screening tool, PFscreen is neither intended for high accuracy estimates nor for unusually shaped buildings. When such estimates are required, we recommend using modern Monte-Carlo radiation transport codes, such as the Los Alamos Monte Carlo N-particle (MCNP) transport code, the Oak Ridge Discrete Ordinates Radiation Transport Codes (DENOVO), and/or the Lawrence Livermore National Laboratory MERCURY code.

estimates (see the main text) reflects our confidence in the degree to which the set of building properties we describe here and in the main report is capable of determining the building protection for similar buildings (the suite of comparison buildings available do not cover the full range of reasonable input parameter values). We note that the prior estimates of building protection were available – and reviewed – during the model development process. As such, the comparison between PFscreen predictions and prior work represents verification, not validation, of the PFscreen algorithms.[36] We note that all "correction terms" used are physically based, i.e., the PFscreen model does not contain arbitrary "fudge factors." Note that we use the term "building component" in this appendix to denote a building attribute shown in *Figure D1*, such as a roof or exterior wall, which can scatter radiation.

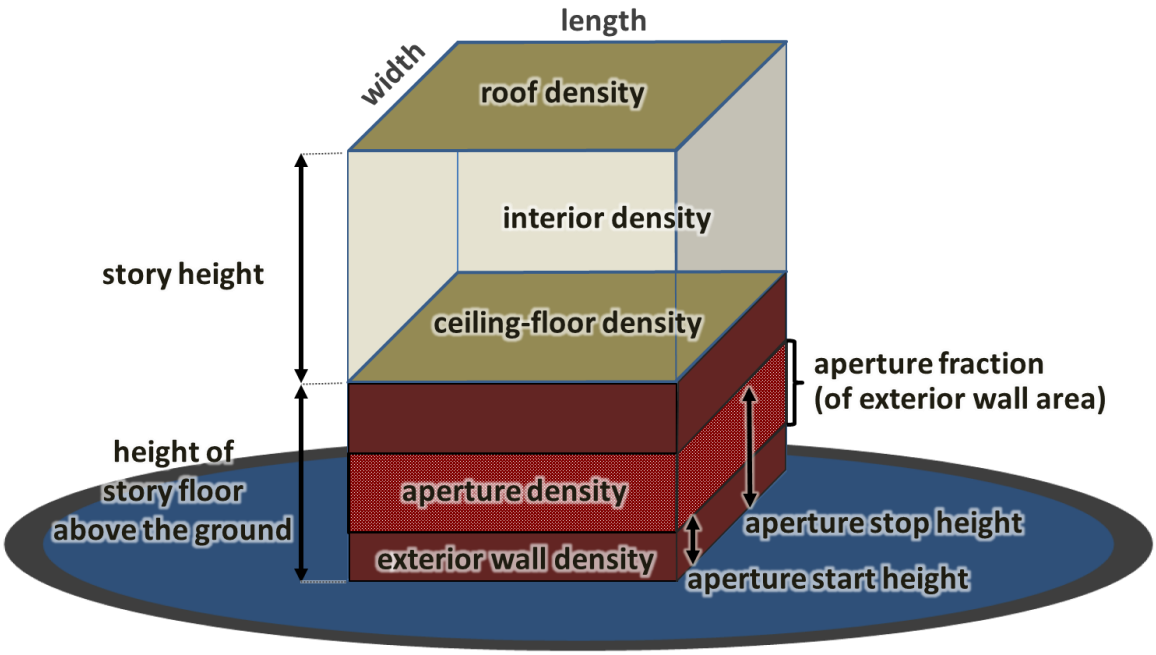

Figure D1. Illustration of a PFscreen model building, which can include multiple floors (including basements, not included in the figure) and apertures. Each PFscreen building is isolated and rectangular with (a) general building attributes (length, width, number of stories) and (b) story specific attributes (height of story above the ground; individual story height; mass of the exterior wall, ceiling, floor, roof, and interior (interior walls and contents); and aperture(s) location and amount). Interior mass is assumed to be uniformly distributed within each story. The thickness of the exterior walls, roof, and ceiling-floor is not required as inputs (PFscreen uses areal density). Specification of radiation source attributes (location and energy/spectra) is also required.

[36] (1) "Verification" refers to the degree to which the PFscreen algorithms are able to recreate previously known results ;(2) "Validation" refers to the degree to which the PFscreen algorithms are able to predict previously unknown results, e.g., new experimental and/or modeling data.

THEORY

PROTECTION FACTOR DEFINITION

For each building location analyzed, the PFscreen model estimates building protection in units of protection factor (PF) – which is defined as the ratio of the unsheltered to sheltered exposure, see *Equation D1*.[37] Like sunscreen and respirator ratings, higher protection factor values indicate increased protection. For our application, the radiation exposure ratio is equal to the radiation dose ratio. Thus unsheltered exposure refers to the reference dose rate measured 1 m above an infinite, flat plane uniformly contaminated with radioactive material, see the top panel of *Figure D2*. Similarly, sheltered exposure refers to the indoor dose rate at location (x, y, h) when the surrounding ground and/or building is contaminated with radioactive material, see the bottom panel of *Figure D2*. By convention, protection factor values are referenced to the energy of the initially emitted radiation, $h\upsilon$, and account for the effects of changing radiation energy as the radiation interacts with matter.

(*Equation D1*)

$$Protection\ Factor(x, y, h; h\upsilon) \equiv \frac{unsheltered\ exposure}{sheltered\ exposure} = \frac{DR_{reference}(h\upsilon)}{DR_{analysis\ location}(x, y, h; h\upsilon)}$$

where

x = distance along the building length axis that corresponds to the x-axis coordinate for the analysis location. By convention, length is the long axis. (m)

y = distance along the building width axis that corresponds to the y-axis coordinate for the analysis location. (m)

h = height of the analysis location above the ground. (m)

$h\upsilon$ = radiation (photon) energy. (MeV)

$Protection\ Factor(x, y, h; h\upsilon)$ = protection factor at location (x, y, h) for radiation energy $h\upsilon$. (dimensionless)

$DR_{reference}(h\upsilon)$ = mid-section bone marrow dose rate 1 m above an infinite, flat plane uniformly contaminated with 1 Bq m^{-2} of radioactive material that emits photons of energy $h\upsilon$, see *Appendix C*. (Sv s^{-1})

$DR_{analysis\ location}(x, y, h; h\upsilon)$ = mid-section bone marrow dose rate at location (x, y, h) assuming that the surrounding ground and building roof are uniformly contaminated with 1 Bq m^{-2} of radioactive material that emits photons of energy $h\upsilon$. (Sv s^{-1})

[37] In the nuclear power plant accident literature, some studies use the term protection factor to indicate other quantities.

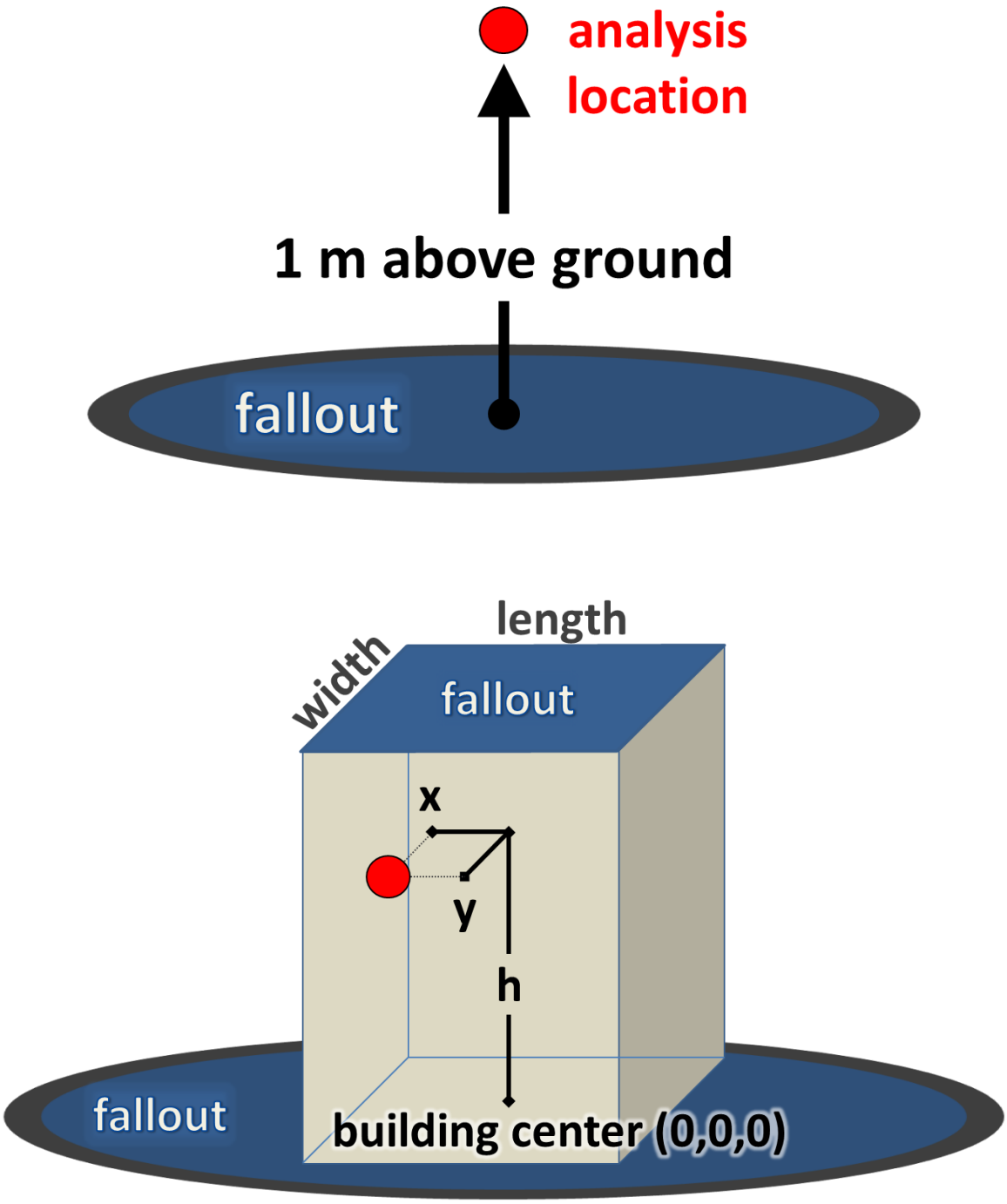

Figure D2. Illustration of the (top) reference, unsheltered, and (bottom) analysis, sheltered, locations. In both figures, the red dot represents the analysis location.

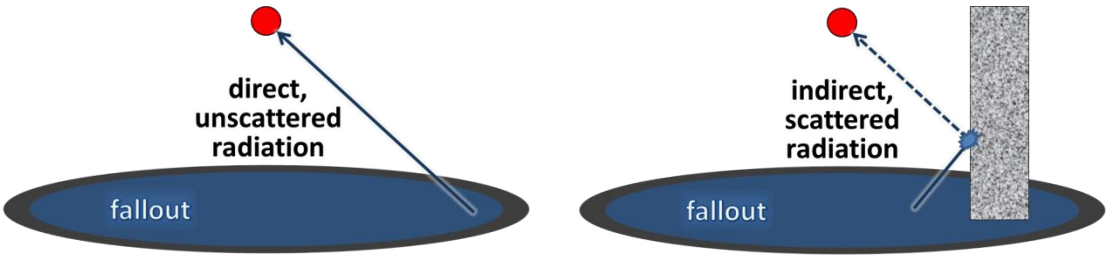

Figure D3. Illustration of the (left) direct, unscattered radiation and (right) indirect, scattered radiation from the ground source. In both panels, the red dot indicates the analysis location. Radiation can scatter from any material, including air. In this illustration, the radiation scatters from a wall.

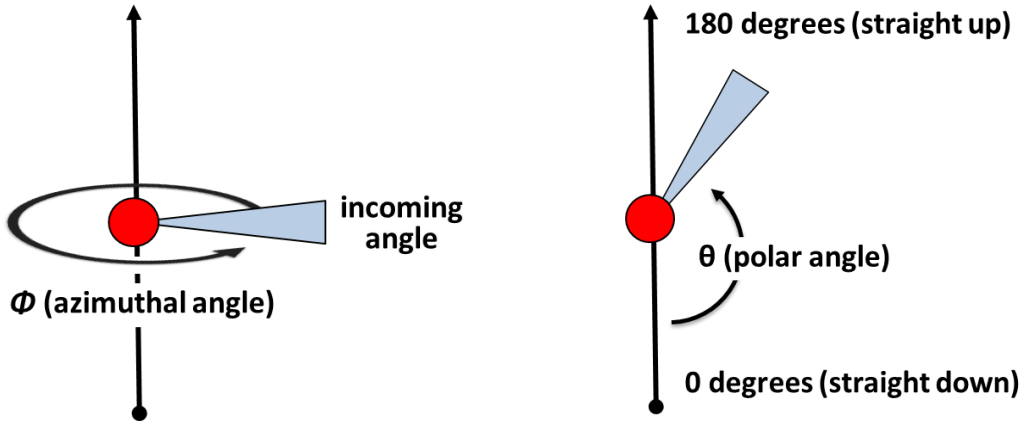

Figure D4. Illustration of the spherical coordinate convention used by the PFscreen model. In both panels, the red dot indicates the analysis location and the blue triangle indicates the incoming angle defined by the combination of the (left) azimuthal, $\emptyset$, and (right) polar, θ, angles.

ANALYSIS OF LOCATION SPECIFIC DOSE RATES

The PFscreen model uses *Equation D2* to estimate the radiation dose rate at a specific analysis location, $DR_{analysis\ location}(x, y, h; h\upsilon)$, based on unscattered radiation from ground and roof sources as well as radiation scattered from the atmosphere, building walls, floors, ceilings, and interior contents, see *Figure D3*.[38] PFscreen follows the spherical coordinate convention in defining the incoming angle $(\theta, \emptyset)$, see *Figure D4*.

(*Equation D2*)

$$DR_{analysis\ location}(x, y, h; h\upsilon) = Surface\ Contamination \cdot \left(\int_{\theta=0}^{180^\circ} \int_{\emptyset=0}^{360^\circ} \left(DR_{ground}(\theta, \emptyset; x, y, h; h\upsilon) + DR_{roof}(\theta, \emptyset; x, y, h; h\upsilon) \right) d\emptyset d\theta + DR_{ceiling-floor}(x, y, h; h\upsilon) + DR_{basement\ wall}(x, y, h; h\upsilon) \right)$$

where

$Surface\ Contamination$ = assumed to be 1. (Bq m^{-2})

θ = the polar angle. (degrees)

$\emptyset$ = the azimuthal angle. (degrees)

$DR_{ground}(\theta, \emptyset; x, y, h; h\upsilon)$ = mid-section bone marrow dose rate due to radiation whose original energy is $h\upsilon$ arriving at the analysis location (x, y, h) along the incoming angle $(\theta, \emptyset)$ that originates from the ground source and includes some of the radiation scattered from building interior and exterior walls, floors, ceilings, and interior contents. (Sv m^2 Bq^{-1} s^{-1} sr^{-1})

$DR_{roof}(\theta, \emptyset; x, y, h; h\upsilon)$ = mid-section bone marrow dose rate due to radiation whose original energy is $h\upsilon$ arriving at the analysis location (x, y, h) along the incoming angle $(\theta, \emptyset)$ that originates from the roof source and includes some of the radiation scattered from building interior walls, floors, ceilings, and interior contents. (Sv m^2 Bq^{-1} s^{-1} sr^{-1})

$DR_{ceiling-floor}(x, y, h; h\upsilon)$ = mid-section bone marrow dose rate term that accounts for some of the ground source radiation whose original energy is $h\upsilon$ that arrives at the analysis location (x, y, h) after scattering off of a ceiling, roof, or floor. (Sv m^2 Bq^{-1} s^{-1})

$DR_{basement\ wall}(x, y, h; h\upsilon)$ = mid-section bone marrow dose rate correction term that accounts for some of the ground source radiation whose original energy is $h\upsilon$ that arrives at the analysis location (x, y, h) after scattering off of a basement wall. (Sv m^2 Bq^{-1} s^{-1})

[38] For discussion purposes, *Equation D2* is shown here as an integral. The PFscreen model uses a Riemann sum with a polar and azimuthal angle resolution ≤ 4.9×10^{-3} steradian.

GROUND SOURCE

When no building is present, the PFscreen model calculates the mid-section bone marrow dose rate, $Absolute\ Dose\ Rate_{ground,no\ building}(\theta, h; h\upsilon)$, above an infinite, flat plane uniformly contaminated with radioactive material by scaling published estimates of the relative angular dose rate to account for desired radiation energy, see *Equations D3* and *D4*. These equations include both unscattered radiation and radiation scattered in the atmosphere.

(*Equation D3*)

$$Absolute\ Dose\ Rate_{ground,no\ building}(\theta, h; h\upsilon) = \begin{pmatrix} Relative\ Dose\ Rate_{ground,no\ building}(\theta, h) \\ \cdot\ Normalization\ Factor_{ground}(h\upsilon) \end{pmatrix}$$

(*Equation D4*)

$$Normalization\ Factor_{ground}(h\upsilon) = {}^{60}Co\ Normalization\ Factor_{ground} \cdot \frac{h\upsilon}{h\upsilon_{60Co}}$$

where

$Absolute\ Dose\ Rate_{ground,no\ building}(\theta, h; h\upsilon)$ = mid-section bone marrow dose rate per unit surface contamination due to radiation whose original energy is $h\upsilon$ arriving at a location h above the ground along the incoming angle θ assuming a uniformly contaminated ground. (Sv m^2 Bq^{-1} s^{-1} sr^{-1})

$Relative\ Dose\ Rate_{ground,no\ building}(\theta, h)$ = mid-section bone marrow dose rate for 1 h old fallout as interpolated from *Table D1* values[39] (Sv m^2 Bq^{-1} s^{-1} sr^{-1})

[39] *Spencer* [27] calculated the dose rate above an infinite, flat, uniformly contaminated plane of 1.12 hr old fission fallout as a function of incidence angle and height. Additional calculations on 28 h, 40 h, and 131 h old fission fallout indicate that there is some, but limited change in the *relative* angular dose rate – which is neglected in the PFscreen calculation [26], [27], [30]. After deposition, the absolute dose rate due to fallout radiation decreases rapidly, $t^{-1.2}$ [54]. While a detailed study has yet to be performed, the angular dose rate calculations are estimated to be accurate to within 20% [9].

Spencer's predictions were later verified by experiments at the Department of Energy's Nevada Test Site with both (a) actual 1 d old fallout and (b) simulated fallout using sealed ^{60}Co sources (^{60}Co emits radiation that penetrates buildings similar to 1 h old fallout) [29], [30]. The ^{60}Co sources were propelled at constant speed through tubing shaped in either a spiral or circular shape (or occasionally both) surrounding a collimated (0.03 steradian), 1.6 cm x 1.6 cm NaI(Tl) crystal spectrometer.

Spencer reports relative dose rate values without specifying units in [27]. However as these values agree closely with the experimental data, we assume Spencer's units match the experimental data units of R hr^{-1} ft^2 Ci^{-1} as integrated over 0.03 sr [29].

$Normalization\ Factor_{ground}(h\upsilon)$ = radiation energy, $h\upsilon$, dependent scaling factor chosen such that the mid-section bone marrow dose rate at 1 m above an infinite, flat plane contaminated with 1 Bq m^{-2} fallout matches prior estimates. (dimensionless)

$^{60}Co\ Normalization\ Factor_{ground}$ = 1.80 = scaling factor chosen such that when all incoming radiation is considered by the PFscreen model, the mid-section bone marrow dose rate at 1 m above an infinite, flat plane contaminated with 1 Bq m^{-2} of ^{60}Co contamination is 2.33×10^{-15} Sv s^{-1} [24]. PFscreen neglects the small (< 10%) change in the ^{60}Co normalization factor with height. (dimensionless)

$h\upsilon_{60Co}$ = 2.5 MeV = total energy of the most commonly emitted ^{60}Co gamma rays (1.17 MeV and 1.33 MeV). (MeV)

Table D1. Angular distribution of the dose rate for an infinite plane uniformly contaminated with 1.12 h old fallout as reported in Figure 26.1 in [27] and multiplied by 2.325×10^{-16} Sv rem^{-1} Ci Bq^{-1} m^2 ft^{-2} h s^{-1} sr^{-1} to normalize to Sv m^2 s^{-1} Bq^{-1} sr^{-1}.

Incident Angle (degrees)	Height (m above ground level)								
	1	2	5	10	20	50	100	200	366
180	9.53E-18	9.30E-18	8.60E-18	8.14E-18	7.21E-18	5.58E-18	3.72E-18	1.86E-18	6.28E-19
154	1.00E-17	9.53E-18	9.07E-18	8.37E-18	7.67E-18	5.81E-18	3.95E-18	1.98E-18	6.51E-19
143	1.05E-17	9.88E-18	9.53E-18	8.83E-18	8.14E-18	6.28E-18	4.18E-18	2.09E-18	6.74E-19
134	1.14E-17	1.05E-17	1.00E-17	9.53E-18	8.60E-18	6.51E-18	4.42E-18	2.21E-18	7.21E-19
127	1.28E-17	1.22E-17	1.12E-17	1.05E-17	9.30E-18	7.21E-18	4.65E-18	2.32E-18	7.44E-19
120	1.39E-17	1.35E-17	1.28E-17	1.16E-17	1.05E-17	7.90E-18	5.11E-18	2.56E-18	8.14E-19
114	1.80E-17	1.74E-17	1.63E-17	1.45E-17	1.22E-17	8.83E-18	5.58E-18	2.79E-18	8.72E-19
107	2.79E-17	2.56E-17	2.32E-17	1.98E-17	1.51E-17	1.00E-17	6.28E-18	2.91E-18	9.30E-19
102	3.95E-17	3.60E-17	3.14E-17	2.91E-17	2.09E-17	1.22E-17	6.97E-18	3.25E-18	1.02E-18
95.7	4.65E-17	4.42E-17	3.95E-17	3.37E-17	2.56E-17	1.51E-17	8.60E-18	3.60E-18	1.10E-18
90.0	5.11E-17	4.88E-17	4.42E-17	3.95E-17	3.25E-17	1.98E-17	1.10E-17	4.18E-18	1.28E-18
88.9	1.74E-15	9.30E-16	3.25E-16	1.39E-16	4.18E-17	2.03E-17	1.16E-17	4.30E-18	1.30E-18
87.7	1.05E-15	6.97E-16	4.42E-16	1.98E-16	5.81E-17	2.19E-17	1.26E-17	4.42E-18	1.31E-18
85.4	5.35E-16	4.88E-16	3.72E-16	2.44E-16	1.05E-16	2.44E-17	1.51E-17	5.00E-18	1.39E-18
84.3	4.53E-16	4.53E-16	3.60E-16	2.56E-16	1.22E-16	2.67E-17	1.63E-17	5.23E-18	1.46E-18
78.5	2.44E-16	2.44E-16	2.44E-16	1.98E-16	1.51E-16	6.51E-17	2.32E-17	7.44E-18	1.80E-18
72.5	1.63E-16	1.63E-16	1.63E-16	1.57E-16	1.30E-16	8.14E-17	3.02E-17	1.02E-17	2.32E-18
66.4	1.16E-16	1.16E-16	1.16E-16	1.16E-16	1.07E-16	7.90E-17	3.72E-17	1.34E-17	3.25E-18
60.0	8.83E-17	8.83E-17	8.83E-17	8.83E-17	8.37E-17	6.74E-17	4.18E-17	1.69E-17	4.30E-18
53.1	7.56E-17	7.56E-17	7.56E-17	7.21E-17	7.21E-17	5.81E-17	4.42E-17	1.98E-17	5.58E-18
45.6	6.74E-17	6.74E-17	6.74E-17	6.74E-17	6.51E-17	5.58E-17	4.42E-17	2.09E-17	6.97E-18
36.9	6.74E-17	6.74E-17	6.74E-17	6.51E-17	6.28E-17	5.58E-17	4.18E-17	2.21E-17	8.14E-18
25.8	6.28E-17	6.28E-17	6.28E-17	6.28E-17	6.04E-17	5.35E-17	4.18E-17	2.32E-17	9.30E-18
0.00	6.04E-17	6.04E-17	6.04E-17	5.81E-17	5.58E-17	4.88E-17	3.95E-17	2.32E-17	1.02E-17

To account for the presence of the building, the PFscreen model adjusts the $Absolute\ Dose\ Rate_{ground,no\ building}(\theta, h; h\upsilon)$ by accounting for (a) the amount of attenuation and scattering that occurs as the radiation travels through the building mass and (b) the exclusion of fallout from the building footprint,[40] see *Equations D5 to D17*.

(*Equation D5*)

$$DR_{ground}(\theta, \emptyset; x, y, h; h\upsilon) = \begin{pmatrix} Absolute\ Dose\ Rate_{ground,no\ building}(\theta, h; h\upsilon) \\ \cdot\ Building\ Mass\ Adjustment_{ground}\left(\theta, \emptyset; x, y, h; h\upsilon_{ground}(\theta; h\upsilon)\right) \\ \cdot\ Building\ Footprint\ Correction(\theta; x, y, h; h\upsilon) \end{pmatrix}$$

(*Equation D6*)

$$Building\ Mass\ Adjustment_{ground}(\theta, \emptyset; x, y, h; h\upsilon) = Attenuation\big(FP_{slant}(\theta, \emptyset; x, y, h; h\upsilon; all\ building\ components\ except\ air)\big) \cdot \begin{pmatrix} Buildup(FP_{normal}(\theta, \emptyset; x, y, h; h\upsilon; exterior\ wall); h\upsilon)\ \cdot Finite\ Wall\ Correction(\emptyset; x, y, h) \\ + Buildup(FP_{slant}(\theta, \emptyset; x, y, h; h\upsilon; all\ building\ components\ except\ the\ exterior\ wall\ and\ air); h\upsilon) \end{pmatrix}$$

(*Equation D7*)

$$Finite\ Wall\ Correction(\emptyset; x, y, h) = Wall\ Angle(\emptyset; x, y, h)/180°$$

(*Equation D8*)

$$FP_{slant}(\theta, \emptyset; x, y, h; h\upsilon; building\ components) = Mass\ Attenuation\ Coefficient(h\upsilon) \cdot \sum_{i\ \in\ building\ components} \begin{pmatrix} Areal\ Density_{slant}(\theta, \emptyset; x, y, h; i) \\ \cdot\ Building\ Component\ Hit(\theta, \emptyset; x, y, h; i) \end{pmatrix}$$

(*Equation D9*)

$$FP_{normal}(\theta, \emptyset; x, y, h; h\upsilon; building\ components) = Mass\ Attenuation\ Coefficient(h\upsilon) \cdot \sum_{i\ \in\ building\ components} \begin{pmatrix} Areal\ Density_{normal}(i) \\ \cdot\ Building\ Component\ Hit(\theta, \emptyset; x, y, h; i) \end{pmatrix}$$

[40] The contribution of fallout on the roof is handled separately.

(*Equation D10*)

$$Mass\ Attenuation\ Coefficient(h\upsilon) = \begin{cases} 0.057, & where\ h\upsilon = {}^{60}Co \\ 0.077, & where\ h\upsilon = {}^{137}Cs \\ 0.063 \cdot h\upsilon^{-0.489}, & where\ 0.5 \le h\upsilon \le 3 \end{cases}$$

(*Equation D11*)

$$Areal\ Density_{slant}(\theta, \emptyset; x, y, h; i) = \begin{cases} Density(i) \cdot Slant\ Range(\theta, \emptyset; x, y, h; i), & where\ i \in interior\ wall, contents, and\ air \\ \dfrac{Areal\ Density_{normal}(i)}{Slant\ Range\ Adjustment(\theta, \emptyset; x, y, h; i)}, & where\ i \in roof, exterior\ wall, ceiling - floor \end{cases}$$

(*Equation D12*)

$$Areal\ Density_{normal}(i) = \begin{cases} Areal\ Density_{user}(i), & where\ i \in roof\ or\ ceiling - floor \\ Areal\ Density_{building\ exterior}(i) & where\ i \in exterior\ wall \end{cases}$$

(*Equation D13*)

$$Areal\ Density_{building\ exterior}(i) = \begin{cases} Areal\ Density_{user}(\ exterior\ wall\ i), & where\ the\ incoming\ angle\ intersects\ exterior\ wall\ above\ or\ below\ aperature \\ \begin{cases} Areal\ Density_{user}\binom{exterior}{wall\ i}, & Random\ Number > Aperature\ Fraction \\ Areal\ Density_{user}(aperature), & Random\ Number \le Aperature\ Fraction \end{cases}, & where\ the\ incoming\ angle\ intersects\ exterior\ wall\ where\ aperatures\ are\ present \end{cases}$$

(*Equation D14*)

$$Building\ Footprint\ Correction(\theta; x, y, h; h\upsilon) = \begin{cases} 0, & where\ \theta \le 90°\ and\ the\ incoming\ angle\ originates\ within\ the\ building\ footprint \\ 1 - \dfrac{Effective\ Building\ Radius}{Air\ Scatter\ Radius(h\upsilon)}, & where\ \theta > 90° \end{cases}$$

(*Equation D15*)

$$Effective\ Building\ Radius = \sqrt{Building\ Length \cdot Building\ Width \cdot \pi^{-1}}$$

(*Equation D16*)

$$Air\ Scatter\ Radius(hv) = \frac{-ln(0.05)}{Mass\ Attenuation\ Coefficient(hv)\ \cdot\ Density(air)}$$

(*Equation D17*)

$$hv_{ground}(\theta; hv) = \begin{cases} hv, & where\ \theta \leq 90° \\ 0.5, & where\ \theta > 90° \end{cases}$$

where

$Building\ Mass\ Adjustment_{ground}(\theta, \emptyset; x, y, h; hv)$ = radiation energy, hv, specific scaling factor that accounts for the effects of building mass present along the incoming angle $(\theta, \emptyset)$ between the analysis location (x, y, h) and the building exterior. (dimensionless)

$Building\ Footprint\ Correction(\theta; x, y, h; hv)$ = correction factor for the mid-section bone marrow dose rate at the analysis location (x, y, h) along the incoming angle (θ) that accounts for the displacement (removal) of ground fallout by the building footprint. (dimensionless)

$Attenuation(FP) = e^{-FP}$ = loss of incoming radiation through interaction with matter. (dimensionless)

$Buildup(FP; hv)$ = fraction of the radiation emitted that is scattered at least once by building materials prior to reaching the analysis location, also called a buildup factor. (dimensionless)

The buildup values used are determined by a piecewise, 3rd order polynomial interpolation of concrete values reported in Table 6.4.1 in reference [48]. The buildup values are limited to the range of 1 to 200 (inclusive).

$$Buildup(FP, hv) = Y_1(FP) + \left(Y_2(FP) - Y_1(FP)\right) \cdot \frac{hv - X_1}{X_2 - X_1}$$

$$X_1 = \begin{cases} 0.5, & where\ 0.5 \leq hv < 1 \\ 1, & where\ 1 \leq hv < 2 \\ 2, & where\ 2 \leq hv < 3 \end{cases}$$

$$X_2 = \begin{cases} 1, & where\ 0.5 \leq hv < 1 \\ 2, & where\ 1 \leq hv < 2 \\ 3, & where\ 2 \leq hv < 3 \end{cases}$$

$$Y_1(FP) = \begin{cases} 0.00124 \cdot FP^3 + 0.2541 \cdot FP^2 + 0.8984 \cdot FP + 1.109, & where\ 0.5 \le hv < 1 \\ -0.0006385 \cdot FP^3 + 0.1018 \cdot FP^2 + 1.03 \cdot FP + 0.8299, & where\ 1 \le hv < 2 \\ -0.0001886 \cdot FP^3 + 0.02238 \cdot FP^2 + 0.8799 \cdot FP + 0.8475, & where\ 2 \le hv < 3 \end{cases}$$

$$Y_2(FP) = \begin{cases} -0.0006385 \cdot FP^3 + 0.1018 \cdot FP^2 + 1.03 \cdot FP + 0.8299, & where\ 0.5 \le hv < 1 \\ -0.0001886 \cdot FP^3 + 0.02238 \cdot FP^2 + 0.8799 \cdot FP + 0.8475, & where\ 1 \le hv < 2 \\ -0.00008372 \cdot FP^3 + 0.008765 \cdot FP^2 + 0.6942 \cdot FP + 0.9634, & where\ 2 \le hv < 3 \end{cases}$$

$Finite\ Wall\ Correction(\theta, \emptyset; x, y, h)$ = correction factor that accounts for the finite size of the building wall (the buildup values used assume an infinite wall). (dimensionless)

$Wall\ Angle(\emptyset; x, y, h)$ = angle subtended from the analysis location (x, y, h) and the horizontal edges of the exterior wall intersected by a ray traveling along $(\emptyset)$, see *Figure D5*. (°)

$FP_{normal}(\theta, \emptyset; x, y, h; hv; building\ components)$ = number of mean free path lengths at radiation energy hv assuming the radiation travels a path normal to each building component considered, see *Figure D5*. For context, a mean free path is the average distance that radiation travels prior to being scattered. (dimensionless)

$FP_{slant}(\theta, \emptyset; x, y, h; hv; building\ components)$ = number of mean free path lengths at radiation energy hv along the slant range defined by the analysis location (x, y, h), building exterior, and incoming angle $(\theta, \emptyset)$, see *Figure D5*. (dimensionless)

$Mass\ Attenuation\ Coefficient(hv)$ = mass attenuation coefficient for radiation energy, hv, interpolated from the concrete values provided in Table 5.1 in reference [48]. ($cm^2\ g^{-1}$)

$Areal\ Density_{slant}(\theta, \emptyset; x, y, h; i)$ = areal density due to the mass of building component i per unit area when radiation travels between the analysis location (x, y, h) and the building exterior along the incoming angle $(\theta, \emptyset)$. ($g\ cm^{-2}$)

$Areal\ Density_{normal}(i)$ = areal density due to the mass of building component i per unit area along a path normal to the building component. ($g\ cm^{-2}$)

$Areal\ Density_{building\ exterior}(i)$ = areal density due to the mass of the building exterior per unit area associated with the exterior wall i. ($g\ cm^{-2}$)

$Areal\ Density_{user}(i)$ = areal density of building component i as supplied by the user in the PFscreen input file. ($g\ cm^{-2}$)

i = index indicating a specific building component, such as an exterior wall, roof, ceiling/floor, interior building mass (interior wall or contents), or interior air. (dimensionless)

$Density(i)$ = density of the building component i, supplied by the user, or air, which is assumed to be 0.001293. ($g\ cm^{-3}$)

$Slant\ Range(\theta, \emptyset; x, y, h; i)$ = distance (slant range) within building component i of a ray originating at the analysis location (x, y, h) and traveling at angle $(\theta, \emptyset)$ to the building exterior, see *Figure D5*. (cm)

$Slant\ Range\ Adjustment(\theta, \emptyset; x, y, h; i) = cos(\omega)$ = scaling factor that accounts for the difference in distance within an exterior wall, roof, or ceiling-floor that the radiation actually travels relative to a path normal to the building component. This factor equals the cosine of the intersection angle (ω), see *Figure D5*. (dimensionless)

$Effective\ Building\ Radius$ = radius of a circle equal in area to the building footprint. (m)

$Air\ Scatter\ Radius(hv)$ = distance at which direct, unscattered radiation of energy hv will be attenuated to 5% of its original value in the atmosphere. For computational convenience, the mass attenuation coefficient for concrete is used rather than air (air and concrete mass attenuation coefficients are very similar for the radiation energies of interest, see *Appendix C*). (m)

$Building\ Component\ Hit(\theta, \emptyset; x, y, h; i)$ = binary value equal to 1 if the ray leaving the analysis location (x, y, h) along angle $(\theta, \emptyset)$ intersects building component i, otherwise equals 0. Value always equals to 0 when i = air and the FP is being determined for ground sources. (dimensionless) (Air scatter is already included in the $Absolute\ Dose\ Rate_{ground,no\ building}(\theta, h; hv)$ term).

$Random\ Number$ = random number selected from a uniformly distribution between 0 and 1. (dimensionless)

$Aperature\ Fraction$ = fraction of building story exterior, between a defined aperture start and stop heights. Supplied by the user. (dimensionless)

$hv_{ground}(\theta; hv)$ = adjusts the spectra of incoming, ground source radiation to 0.5 MeV to account for spectral shift of scattered radiation [55]. (MeV)

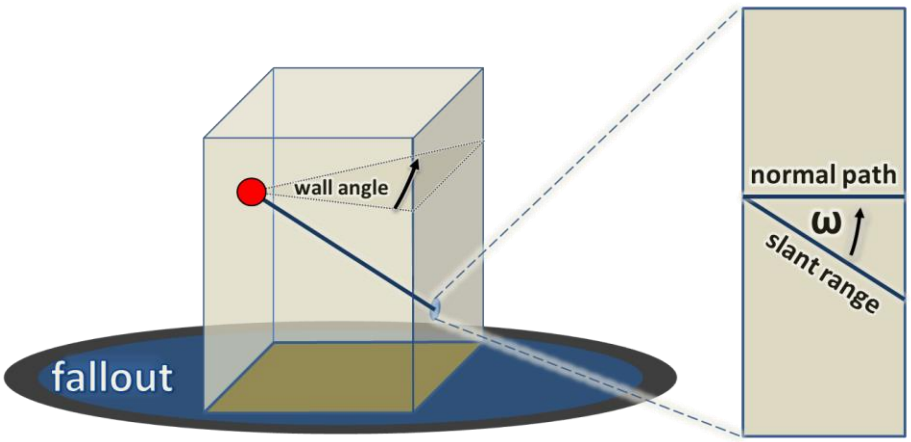

Figure D5. Illustration of (left) the wall angle, the solid angle subtended by the analysis location (red dot) and an exterior wall; and (right) the normal path, slant range, and intersection angle (ω) for an exterior wall.

ROOF SOURCE

The PFscreen model calculates the roof source contribution to the total dose rate along a given incoming angle $(\theta, \emptyset)$ by assuming that (a) the roof is a flat plane uniformly contaminated with radioactive material, (b) the roof source can be approximated by a collection of small area sources, and (c) the building mass is uniformly distributed between the analysis location and the roof source, see *Equations D18 to D23*. Appendix C discusses a very similar, but not identical, case in more detail.

(*Equation D18*)

$$DR_{roof}(\theta, \emptyset; x, y, h; h\upsilon) = \begin{pmatrix} Absolute\ Dose\ Rate_{roof,no\ building}\ (\theta, \emptyset; x, y, h; h\upsilon) \\ \cdot\ Building\ Mass\ Adjustment_{roof}(\theta, \emptyset; x, y, h; h\upsilon) \end{pmatrix}$$

(*Equation D19*)

$$Absolute\ Dose\ Rate_{roof,no\ building}\ (\theta, \emptyset; x, y, h; h\upsilon) = \begin{pmatrix} Dose\ Rate\ 1m\ From\ a\ Point\ Source_{no\ building}\ (h\upsilon) \\ \cdot\ Distance\ Adjustment\ Factor_{roof}(\theta; h) \\ \cdot\ Source\ Area(\theta, \emptyset; x, y, h) \end{pmatrix}$$

(*Equation D20*)

$$Dose\ Rate\ 1m\ From\ a\ Point\ Source_{no\ building}\ (h\upsilon) = \begin{cases} 1.03\ x\ 10^{-16}, & where\ h\upsilon = {}^{60}Co \\ 2.87\ x\ 10^{-17}, & where\ h\upsilon = {}^{137}Cs \\ 2.21\ x\ 10^{-11}\ \cdot\ exp\begin{pmatrix} -13.113 \\ +0.72008\ \cdot\ ln(h\upsilon) \\ -0.033603\ \cdot (ln(h\upsilon))^2 \end{pmatrix}, & where\ 0.5 \le h\upsilon \le 3 \end{cases}$$

(*Equation D21*)

$$Distance\ Adjustment\ Factor_{roof}(\theta; h)\ = 1\ m^2\ /\ max\begin{pmatrix} 0.5^2, \\ s_{roof}(\theta; h)^2 \end{pmatrix}$$

(*Equation D22*)

$$s_{roof}(\theta; h) = \frac{Building\ Roof\ Height\ -\ h}{\cos(180° - \theta)}$$

(*Equation D23*)

$$Building\ Mass\ Adjustment_{roof}(\theta, \emptyset; x, y, h; h\upsilon) = \begin{pmatrix} Attenuation\big(FP_{slant}(\theta, \emptyset; x, y, h; h\upsilon; all\ building\ components)\big) \\ \cdot\ Buildup\big(FP_{slant}(180°, 0°; x, y, h; h\upsilon; all\ building\ components)\big) \end{pmatrix}$$

where

$Absolute\ Dose\ Rate_{roof,no\ building}(\theta, \emptyset; x, y, h; h\upsilon)$ = mid-section bone marrow dose rate per unit roof contamination due to radiation whose original energy is $h\upsilon$ that arrives at the analysis location (x, y, h) along the incoming angle $(\theta, \emptyset)$ assuming a uniformly contaminated roof. (Sv m^2 Bq^{-1} s^{-1} sr^{-1})

$Building\ Mass\ Adjustment_{roof}(\theta, \emptyset; x, y, h; h\upsilon)$ = radiation energy, $h\upsilon$, specific scaling factor that accounts for the effects of building mass present along the incoming angle $(\theta, \emptyset)$ between the analysis location (x, y, h) and the building roof. This term accounts for both the attenuation of the direct, unscattered radiation and the contribution of indirect, scattered radiation (illustrated in *Figure D6*). (dimensionless)

$Dose\ Rate\ 1m\ From\ a\ Point\ Source_{no\ building}(h\upsilon)$ = radiation energy, $h\upsilon$, dependent mid-section bone marrow dose rate at 1 m from a 1 Bq point source. (Sv Bq^{-1} s^{-1})

The ^{60}Co and ^{137}Cs values are from Table 6.1.2 in [48]. The general radiation energy equation is from Table 6.1.1 in [48] and is valid for 0.5 to 5.0 MeV. The following unit conversion factor translates from the reported (rem h^{-1} cm^2 s) to (Sv s^{-1}) for an arbitrary radiation energy, $h\upsilon$.

$$2.21\ x\ 10^{-11} = \frac{1\ Bq}{4\pi\ \cdot\ 10^4\ cm^2} \cdot \frac{1\ photon}{1\ Bq} \cdot \frac{1\ Sv}{100\ rem} \cdot \frac{1\ h}{3600\ s}$$

$Distance\ Adjustment\ Factor_{roof}(\theta; h)$ = reduction in mid-section bone marrow dose rate due to the distance between the analysis location (h) and the portion of the roof contamination being considered along the incoming angle (θ) relative to a 1m reference distance. For numerical reasons, the distance is limited ≥ 0.5 m. (dimensionless)

$s_{roof}(\theta; h)$ = distance from the analysis location height (h) to the roof along the polar angle (θ). Also called slant range, see *Figure D7*. (m)

$Building\ Roof\ Height$ = height of the building roof above the ground (assumes roof thickness is negligible). (m)

$Source\ Area(\theta, \emptyset; x, y, h)$ = area of the roof source portion being considered. This area depends upon the solid angle being considered. (m^2 sr^{-1})

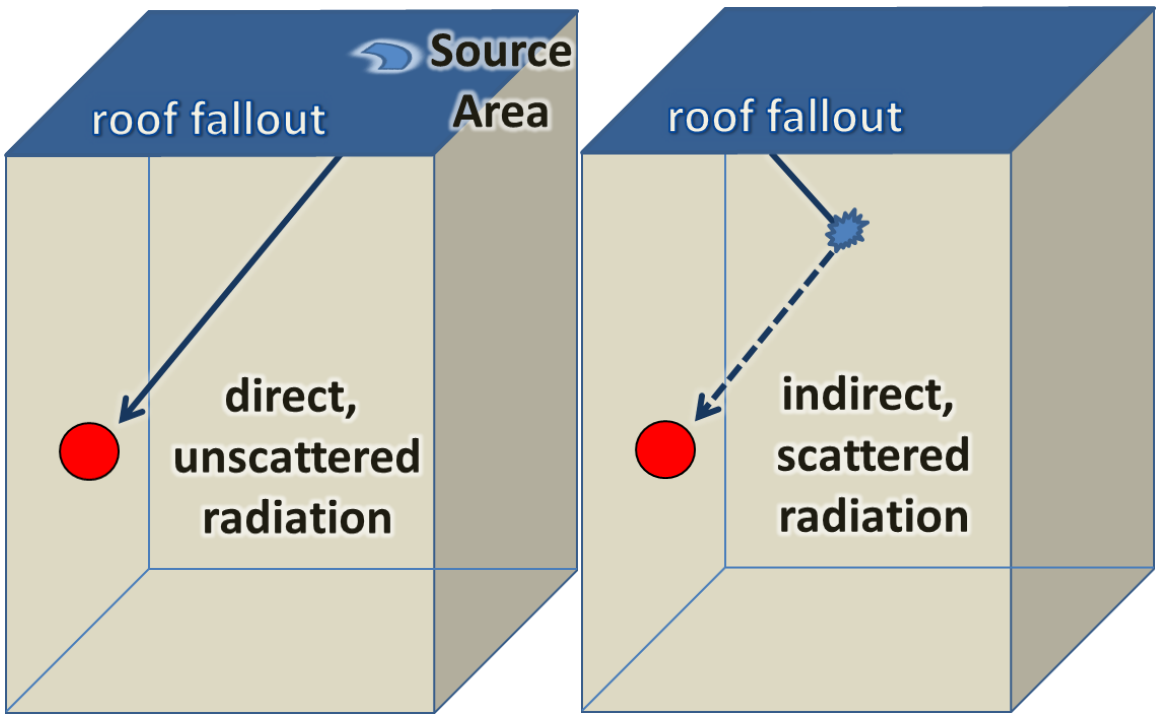

Figure D6. Illustration of the (left) direct, unscattered and (right) indirect, scattered radiation from the roof source. The red dot indicates the analysis location. Light blue area labeled "Source Area" in the left panel indicates the area of the roof area being considered for a given analysis location and incoming angle

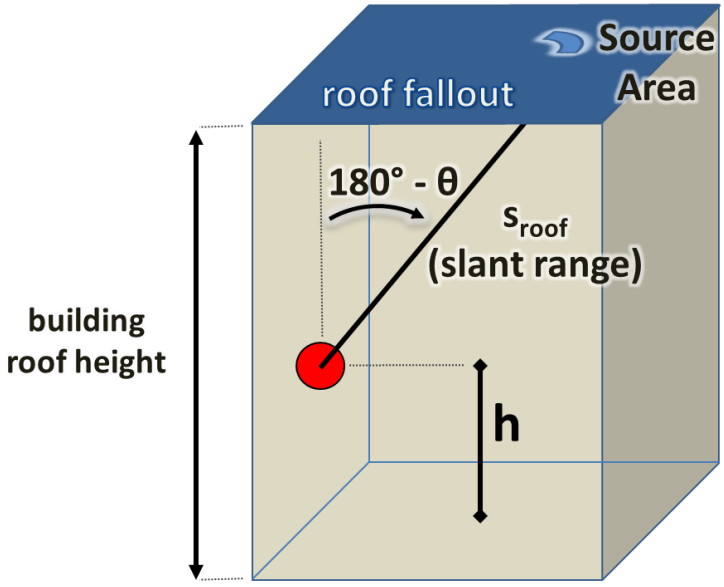

Figure D7. Illustration of the s_{roof} (slant range) calculation. The red dot indicates the analysis location.

CORRECTION FACTORS

CEILING-FLOOR CORRECTION FACTOR

Due to their mass, roofs, ceilings, and floors can scatter a significant amount of the incoming radiation. This scattering is only partially captured by the $Buildup$ term used in the ground and roof source contributions previously discussed (DR_{ground} and DR_{roof}, respectively). The PFscreen model therefore includes a ceiling-floor (and roof) correction factor to account for some of the ground source radiation not previously considered, see *Equation D24 to D32*.

The accomplish this, the PFscreen model first creates an array of virtual, point sources (one array for each roof or ceiling-floor) within the building that accounts for the amount of radiation that will be scattered downward at each roof or ceiling-floor, see the top panel of *Figure D8*. Then the PFscreen model calculates the within-building exposures to the analysis locations on the same story as these virtual sources, see the bottom panel of *Figure D8*. Attenuation of the dose rate from the within-building sources considers the effects of air and mass within the building and assumes the radiation from the virtual sources is 0.5 MeV [55].

(*Equation D24*)

$$DR_{ceiling-floor}(x,y,h;hv) = \sum_{i \in \binom{roof,}{ceiling-floor}} \sum_{x_v(i)} \sum_{y_v(i)} \sum_{h_v(i)} \begin{pmatrix} DR_{virtual\ source}(x_v(i),y_v(i),h_v(i);hv) \\ \cdot\ Dose\ Rate\ at\ 1m\ Adjustment_{virtual\ source}(x_v(i),y_v(i),h_v(i);hv;i) \\ \cdot\ Distance\ Adjustment\ Factor_{virtual\ source}(x,y,h;\ x_v(i),y_v(i),h_v(i)) \\ \cdot\ Building\ Mass\ Adjustment_{virtual\ source}(x,y,h;\ x_v(i),y_v(i),h_v(i);0.5) \end{pmatrix}$$

(*Equation D25*)

$$DR_{virtual\ source}(x_v,y_v,h_v;hv) = \int_{\theta=0}^{180} \int_{\emptyset=0}^{360} DR_{ground}(\theta,\emptyset;x_v,y_v,h_v;hv) d\emptyset d\theta$$

(*Equation D26*)

$$Dose\ Rate\ at\ 1m\ Adjustment_{virtual\ source}(x_v,y_v,h_v;hv;i) = \begin{pmatrix} Scatter\ Coefficient(hv;i)\ \cdot\ dA\ sr \\ \cdot\ Areal\ Density\ Adjustment\left(FP_{normal}(180{,}0;x_v,y_v,h_v;hv;i)\right) \\ \cdot\ Area_{virutal\ source}(x_v,y_v,h_v)\ \cdot\ dA^{-1}\ m^2 \end{pmatrix}$$

(*Equation D27*)

$$Scatter\ Coefficient(hv;i) = \begin{cases} 0.006 \cdot hv^{-0.791}, & where\ i \in \binom{roof,}{ceiling-floor} \\ 0.0104 \cdot hv^{-1.01}, & where\ i \in basement\ wall \end{cases}$$

(*Equation D28*)

$$Areal\ Density\ Adjustment(FP) = \begin{cases} FP, & where\ FP\ \leq 1 \\ 1, & where\ FP\ > 1 \end{cases}$$

(*Equation D29*)

$$Distance\ Adjustment\ Factor_{virtual\ source}(x, y, h;\ x_v, y_v, h_v) = 1\ m^2\ /\ max\begin{pmatrix} 0.25\ m^2, \\ s(x, y, h;\ x_v, y_v, h_v)^2 \end{pmatrix}$$

(*Equation D30*)

$$s(x_1, y_1, h_1;\ x_2, y_2, h_2) = \sqrt{(x_1 - x_2)^2 + (y_1 - y_2)^2 + (h_1 - h_2)^2}$$

(*Equation D31*)

$$Building\ Mass\ Adjustment_{virtual\ source}(x, y, h;\ x_v, y_v, h_v; hv) = \begin{pmatrix} Attenuation\big(FP_{virtual\ source}(x, y, h;\ x_v, y_v, h_v; hv; interior\ mass\ and\ air)\big) \\ \cdot\ Buildup\big(FP_{virtual\ source}(x, y, h;\ x_v, y_v, h_v; hv; interior\ mass\ and\ air)\big) \end{pmatrix}$$

(*Equation D32*)

$$FP_{virtual\ source}(x, y, h;\ x_v, y_v, h_v; hv; building\ components) = Mass\ Attenuation\ Coefficient(hv) \cdot \sum_{i\ \in\ building\ components} \begin{pmatrix} Areal\ Density_{slant}(\theta, \emptyset; x, y, h; i) \\ \cdot\ Building\ Component\ Hit_{virtual\ source}(x, y, h; x_v, y_v, h_v; i) \end{pmatrix}$$

where

$\big(x_v(i), y_v(i), h_v(i)\big)$ = location of a single virtual point source associated with building component i. For the roof or ceiling-floor virtual point sources, each set of $\big(x_v(i), y_v(i)\big)$ locations is a regularly spaced array that parallels roof or ceiling-floor i, but is 1 cm lower in height, see *Figure D8*. (m, m, m)

$DR_{virtual\ source}(x_v, y_v, h_v; hv)$= mid-section bone marrow dose rate at the virtual point source location (x_v, y_v, h_v) resulting from ground contamination that emits radiation of energy hv. (Sv m^2 Bq^{-1} s^{-1})

$Dose\ Rate\ at\ 1m\ Adjustment_{virtual\ source}(x_v, y_v, h_v; hv; i)$ = factor that scales (a) the mid-section bone marrow dose rate at the virtual source location (x_v, y_v, h_v) due to incoming, ground source radiation to (b) the mid-section bone marrow dose rate 1 m from the virtual source due to radiation scattered from the area of building component i associated with the specified virtual source. (dimensionless)

The dA m^2 constant reflects the nominal target area implicit in the definition of $DR_{virtual\ source}$, i.e., the virtual source dose rate (radiation flux) due to incoming, ground source radiation. This value, when combined with $Area_{virutal\ source}$, the area of the building component associated with a virtual source, is used to estimate the total amount of incoming, ground source radiation being scattered at the specified virtual source.

The dA sr constant reflects the solid angle associated with the nominal dA m^2 target located 1 m from a point source. The target area was chosen such that $Dose\ Rate\ at\ 1m\ Adjustment$ scales the incoming dose to the outgoing dose at 1 m.

$Scatter\ Coefficient(hv; i)$ = fraction of the incoming radiation that is scattered from a point on a flat concrete slab. While the scattering coefficient is known to depend on the angle of incoming and outgoing of the radiation, we use nominal (central) values associated with the energy hv (this choice implicitly assumes the incoming radiation was not previously scattered). For example, we assume a ceiling-floor scatter coefficient of ~ 5x10^{-3} for 1 MeV radiation while the actual values range from ~ 10^{-3} to ~ 10^{-2}, see Figures 4.33 and 4.34 in [56]. The scatter coefficient assumes the building component is infinitely thick. ([outgoing dose rate in Sv s^{-1}] [incoming dose rate in Sv s^{-1}]$^{-1}$ sr^{-1})

The energy dependent scatter coefficient for the (a) ceiling-floor and (b) basement wall was calculated separately due to differences in the incoming and outgoing angles. For the ceiling-floor, the incident radiation angle is relatively shallow and we fit to nominal values of 0.009, 0.005, 0.0035, and 0.002 associated with 0.6, 1.25, 2, and 4 MeV, respectively (see θ ~ 15° in Figure 4.33 in [56]). For the basement wall, the incident angle is relative acute and we fit to nominal values of 0.018, 0.01, 0.005, and 0.0026 associated with 0.6, 1, 2, and 4 MeV, respectively (see θ ~ 30° in Figure 4.25 in [56]).

$Areal\ Density\ Adjustment(FP_i)$ = scattering factor correction term that accounts for finite thickness of the roof or ceiling-floor i as measured in units of mean free path (the scatter coefficient assumes an infinitely thick roof or ceiling-floor). See Table 4.13 and associated discussion in [56] for more details. (dimensionless)

$Area_{virutal\ source}(x_v, y_v, h_v)$ = area of the building component i (e.g., ceiling-floor) associated with the virtual source location (x_v, y_v, h_v) (m^2)

$Distance\ Adjustment\ Factor_{virtual\ source}(x, y, h;\ x_v, y_v, h_v)$ = reduction in mid-section bone marrow dose rate due to the distance between the virtual point source at (x_v, y_v, h_v) and the analysis location (x, y, h). For numerical reasons, the distance is limited to ≥ 0.5 m. (dimensionless)

$s(x_1, y_1, h_1;\ x_2, y_2, h_2)$ = distance between the virtual point source (x_v, y_v, h_v) and the analysis location (x, y, h), also called slant range. Value limited to 0.5 m for numerical considerations. (m)

$FP_{virtual\ source}(x, y, h;\ x_v, y_v, h_v; hv; i)$ = number of mean free path lengths at radiation energy hv along the path between the analysis location (x, y, h) and the virtual source (x_v, y_v, h_v) considering building components i, see *Figure D5*. (dimensionless)

$Building\ Component\ Hit_{virtual\ source}(x, y, h;\ x_v, y_v, h_v; i)$ = binary value equal to 1 if building component i is between the analysis location (x, y, h) and the virtual source (x_v, y_v, h_v) (equals 0 otherwise). Value always equals to 0 when the analysis location and the virtual source are on different building stories. (dimensionless)

$Building\ Mass\ Adjustment_{virtual\ source}(x, y, h;\ x_v, y_v, h_v; hv)$ = radiation energy, hv, specific scaling factor that accounts for the effects of building mass present between the analysis location (x, y, h) and the virtual source (x_v, y_v, h_v). This term accounts for both the attenuation of the direct, unscattered radiation and the contribution of indirect, scattered radiation. (dimensionless)

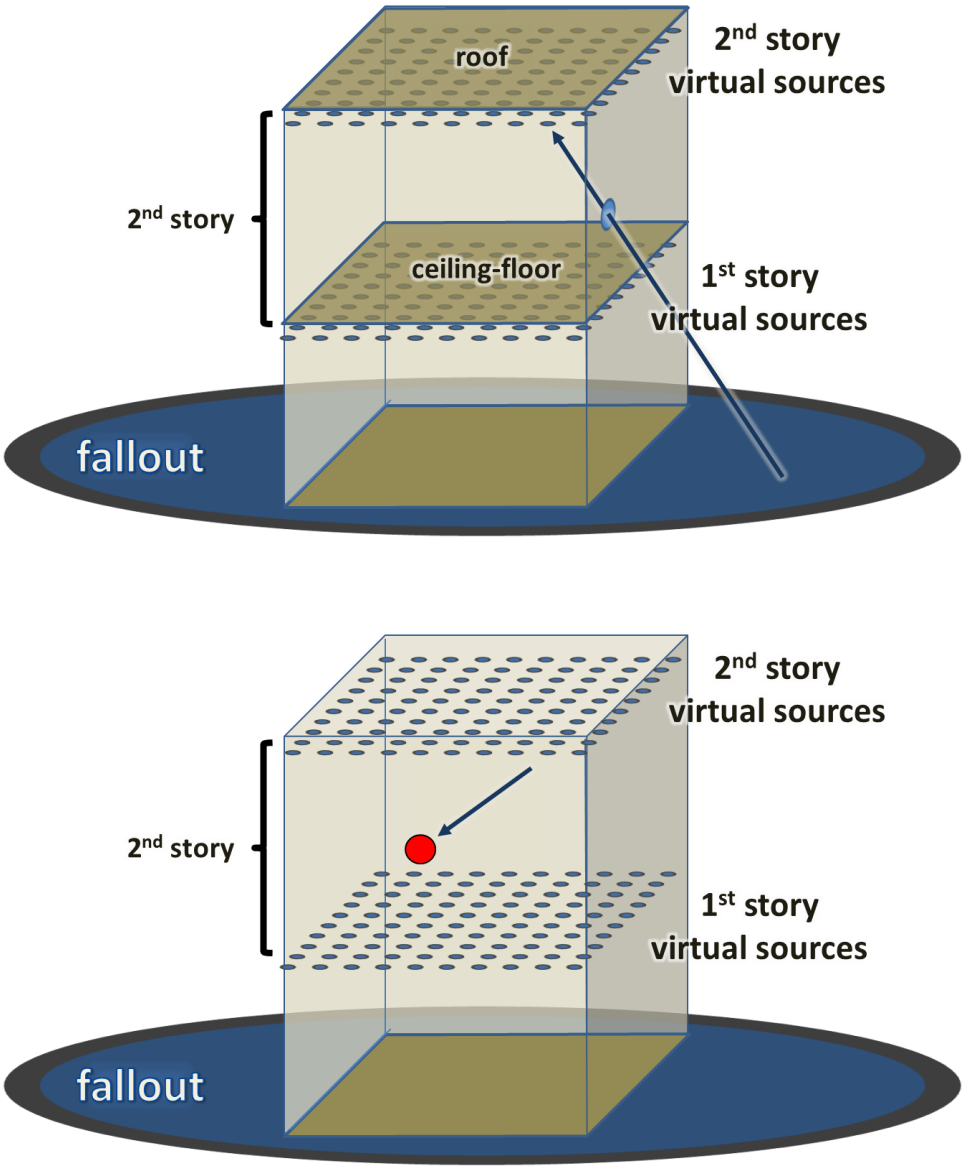

Figure D8. Illustration of the ceiling-floor (and roof) correction factor calculation for an analysis location (red dot) on the 2nd story. The top panel shows the creation of an array of virtual point sources just below each ceiling-floor (and roof) based on radiation emitted from the ground contamination. The bottom panel shows the subsequent contribution of one virtual source to the analysis location (red dot). The 1st story virtual sources do not contribute to 2nd story analysis locations as upward scatter is accounted for in the buildup term used in the DR_{ground} term.

BASEMENT WALL CORRECTION FACTOR

Basement walls can scatter a significant amount of the incoming radiation. This scattering is not captured by the $Buildup$ term used in the ground and roof source contributions previously discussed. The PFscreen model includes a basement wall correction factor to account for some of the ground source radiation that was not previously considered, see *Equation D33*.

The PFscreen model first creates four arrays of virtual, point sources (one array per basement wall) within the building that accounts for the amount of radiation that will be scattered at each basement wall, see top panel of *Figure D9*. The PFscreen model then calculates the within-basement exposures to these virtual sources, see bottom panel of *Figure D9*. In contrast to the ceiling-floor correction factor, the PFscreen model assumes that the basement virtual sources are created solely with radiation that has passed through the building prior to scattering from the basement wall (the *Buildup* term accounts for radiation scattering from the basement wall that has not passed through the building). Attenuation of the dose rate from these within-building sources considers the effects of air and mass within the building.

(*Equation D33*)

$$DR_{basement\ wall}(x,y,h;hv) = \sum_{i\ \in\ basement\ wall} \sum_{x_v(i)} \sum_{y_v(i)} \sum_{h_v(i)} \left(\begin{array}{c} DR_{virtual\ source}(x_v(i),y_v(i),h_v(i);hv) \\ \cdot\ Dose\ Rate\ at\ 1m\ Adjustment_{virtual\ source}(x_v(i),y_v(i),h_v(i);hv;i) \\ \cdot\ Distance\ Adjustment\ Factor_{virtual\ source}(x,y,h;\ x,y,h;\ x_v(i),y_v(i),h_v(i)) \\ \cdot\ Building\ Mass\ Adjustment_{virtual\ source}(x,y,h;\ x_v(i),y_v(i),h_v(i);0.5) \end{array} \right)$$

where

$(x_v(i), y_v(i), h_v(i))$ = location of a single virtual point source associated with building component i. For the basement wall virtual point sources, each set of $(x_v(i), y_v(i), h_v(i))$ locations is a regularly spaced array that parallels basement wall i, but is offset 10 cm. (m, m, m)

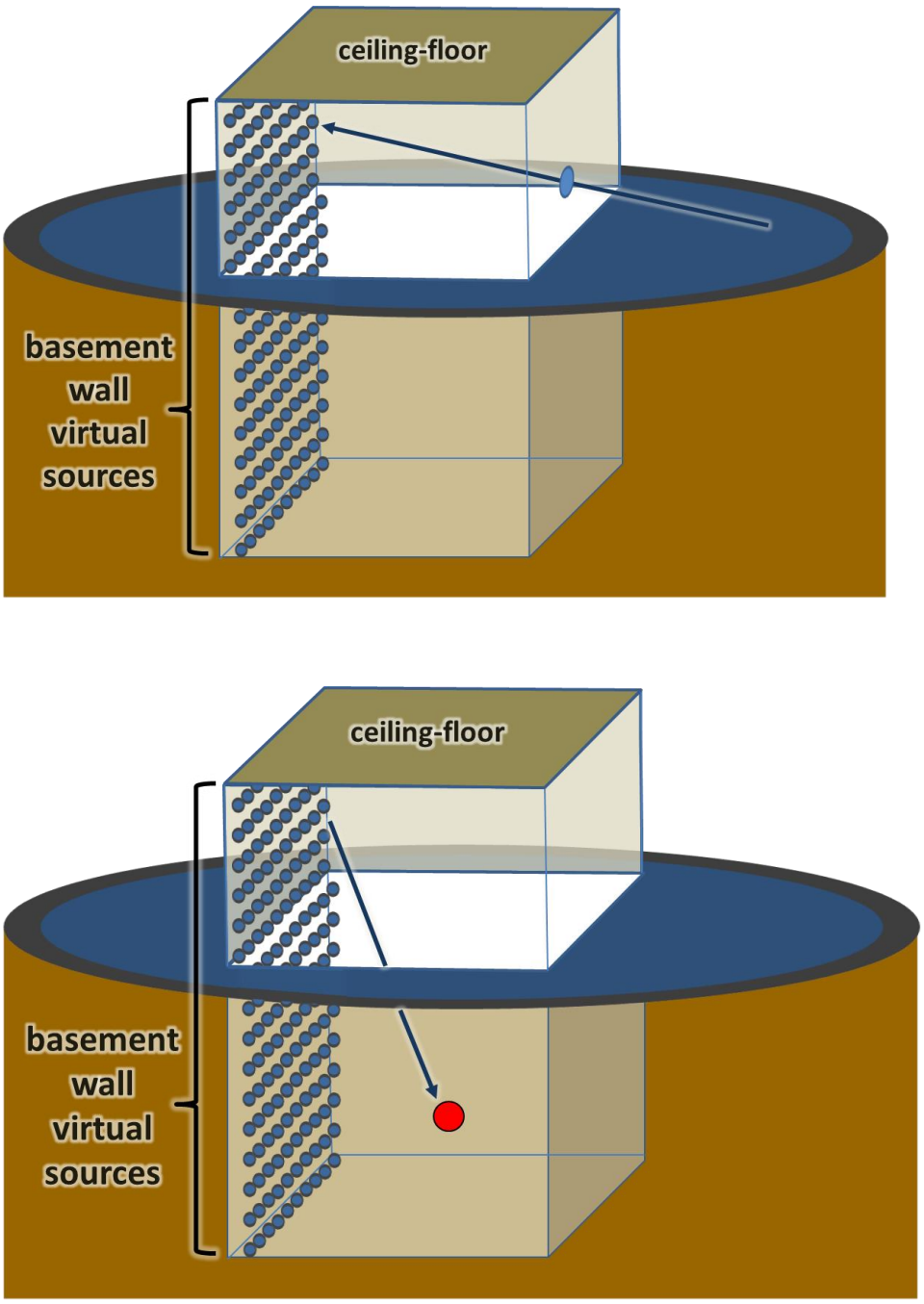

Figure D9. Illustration of the basement wall correction factor calculation. The top panel shows the creation of an array of virtual point sources next to each basement wall (which in this case extends above the ground) based on the radiation emitted from the ground contamination. For visual clarity, only one of four wall arrays is shown. The bottom panel shows the subsequent contribution a virtual source to an analysis location (red dot).

IMPLEMENTATION

The PFscreen model estimates the distribution of protection factors within a given building in the following manner. First the analysis points within the building are identified - four hundred regularly spaced points (x,y) are selected within a quarter of each building story, see the array of light red dots in *Figure D10*.[41] Then, the PFscreen model evaluates *Equation D1* for each analysis location (dark red sphere) where the analysis location height, (h), is determined by the (a) floor height and the (b) detector height above the floor.

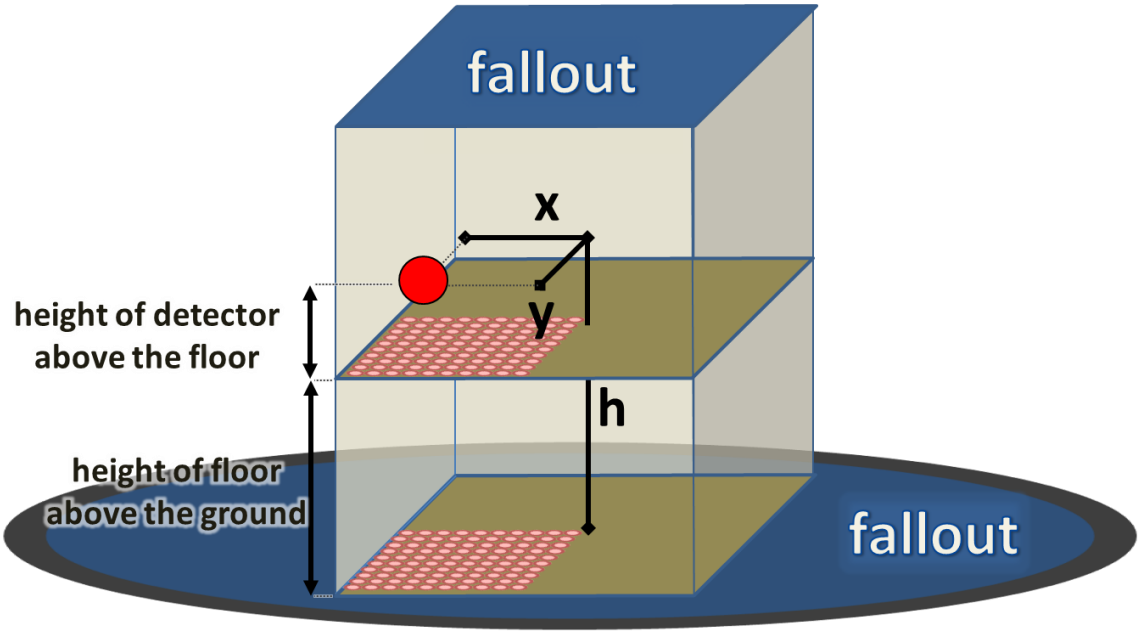

Figure D10. Illustration of building locations analyzed by the PFscreen model.

[41] By symmetry, the protection factor estimates are identical in all four building quadrants.

INPUT

For each building, the PFscreen computer code requires a user-supplied ASCII text file that describes the building and radiation source(s) attributes depicted in *Figure D1*.[42] This input file contains (a) 5 general parameters that must be specified for each building analysis, (b) 9 additional story-specific parameters that must be specified for each building story, and (c) the word "Complete" at the end of the building specification. We note that the PFscreen input variables are related, but not identical, to the key building attributes discussed in the main text (see *Building Attributes* section in the main text which describes the mapping between architectural building attributes and PFscreen input values). *Figure D11* shows an example input file with each section labeled.

Unlike a standard "namelist" input file in which parameter values are assigned based on user provided parameter names, the PFscreen code assigns parameter values based on the order each parameter value is specified in the file. As a consequence, the variable "names" to the left of the equals sign ("=") are intended to assist the user and do not affect the code operation. For example, the first parameter value specified is the building width and the second is the building length.

The PFscreen computer code has limited error reporting on the input file specification. When incorrect or inconsistent information is provided, the PFscreen model typically does not execute or produces an empty output file (i.e., no error codes are provided).

General

Building.Width (m) is the width of the building footprint (y-axis).

Building.Length (m) is the length of the building footprint. By convention, length is the long axis (x-axis).

Building.Detector.Height (m) is the height of the analysis location above the building floor. Typically, this parameter is set to 1 meter,[43] but can be varied to account for sitting or lying individuals.

Building.RadiationSource specifies the effective penetration energy of the external gamma radiation. This parameter can be set to any value between "0.5 MeV" and "3 MeV". Alternately, it can be set to reflect "Co-60" (with an effective energy of 1.25 MeV) and "Cs-137" (0.66 MeV). Prior work demonstrated that Co-60 is a reasonable surrogate for 1 h old nuclear fallout while Cs-137 is a reasonable surrogate for 1 d old nuclear fallout [9].

[42] A batch mode, in which multiple input files are evaluated in sequence, is also available.

[43] The approximate femur height of a person standing, sitting in a chair, or lying on a bed. Radiation damage to bone marrow, resulting in the loss of ability to generate new red blood cells, is the most sensitive, potentially life-threatening acute radiation injury pathway.

Building.RadiationSourceLocation specifies the location of the external radiation sources. This parameter can be set to “Ground”, “Roof”, or “Ground Roof” which considers (a) an infinite, flat plane of ground level radiation source, (b) roof radiation source, or (c) both, respectively. The ground and roof sources are assumed to have the same, uniform levels of contamination.

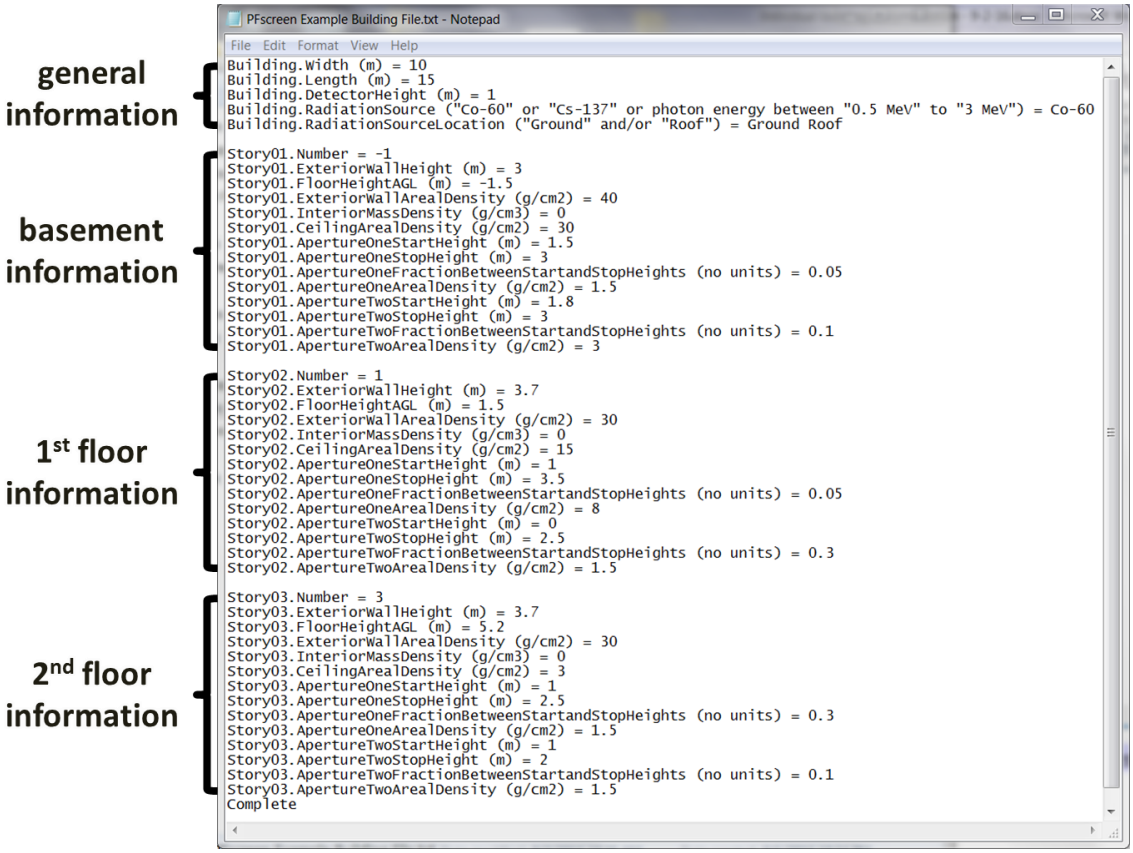

Figure D11. Example PFscreen input file for a hypothetical two story building with a basement.

Story-Specific

The following parameters are specified for each building story. In the following description, "[XX]" indicates a building story which starts at "01" and increases with each story specified. PFscreen allows the user to specify two types of apertures – allowing for separate treatment of windows and doors.

Story[XX].Number is the building story being specified. A negative number indicates a below ground story, i.e., a basement. Positive numbers indicate an above ground story (the ground story is 01). There is no "zero" story.

Story[XX].ExteriorWallHeight (m) is the distance between the story floor and ceiling.

Story[XX].FloorHeightAGL (m) is the distance between the story floor and the ground.

Story[XX].ExteriorWallArealDensity (g/cm2) is the mass of the exterior wall per unit wall area (areal density). The exterior wall areal density should consider structural columns, diagonal braces, etc., along the building perimeter; but should exclude (a) structural beams, braces, etc. within the floor or ceiling and (b) wall apertures (low density regions) such as windows and doors as these are modeled separately.

Story[XX].InteriorMassDensity (g/cm3) is the mass of the building story interior per unit volume. The building interior mass should include both structural elements (e.g., interior walls, columns, and beams) as well as non-structural elements (e.g., furniture, books, and machinery). This parameter does not include external wall, floor, or ceiling materials. The specified density is assumed to be constant throughout the building story interior.

Story[XX].CeilingArealDensity (g/cm2) is the mass of the building story ceiling per unit ceiling area (areal density). The specified ceiling areal density should include (a) ceiling covering materials such as stucco, tiles, and drywall; (b) structural elements such as joists, beams, and braces; and (c) material immediately above the structural elements. The latter includes both flooring material such as carpet and hardwood planks as well roofing materials such as rafters and asphalt shingles (top story only).

Story[XX].ApertureOneStartHeight (m) is the distance between the bottom of aperture one and the story floor.

Story[XX].ApertureOneStopHeight (m) is the distance between the top of aperture one and the story floor.

Story[XX].ApertureOneFractionBetweenStartandStopHeights (no units) is the ratio of the area of aperture one to the total exterior wall area between the aperture one start and stop heights.

Story[XX].ApertureOneArealDensity (g/cm2) is the mass of aperture one per unit aperture area (areal density).

Story[XX].ApertureTwoStartHeight (m) is the distance between the bottom of aperture two and the story floor.

Story[XX].ApertureTwoStopHeight (m) is the distance between the top of aperture two and the story floor.

Story[XX].ApertureTwoFractionBetweenStartandStopHeights (no units) is the ratio of the area of aperture two to the total exterior wall area between the aperture two start and stop heights.

Story[XX].ApertureTwoArealDensity (g/cm2) is the mass of aperture two per unit aperture area (areal density).

OUTPUT

For each building, the PFscreen computer code generates a coma separated text file with the same name as the corresponding input file, but with a "csv" extension. For example, an input file named "OriginalFileName.txt" results in an output file named "OriginalFileName.txt.csv". Each output file contains (a) 3 lines that summarize the analysis performed and (b) columns of analysis results. *Figure D12* shows a portion of an example output file.

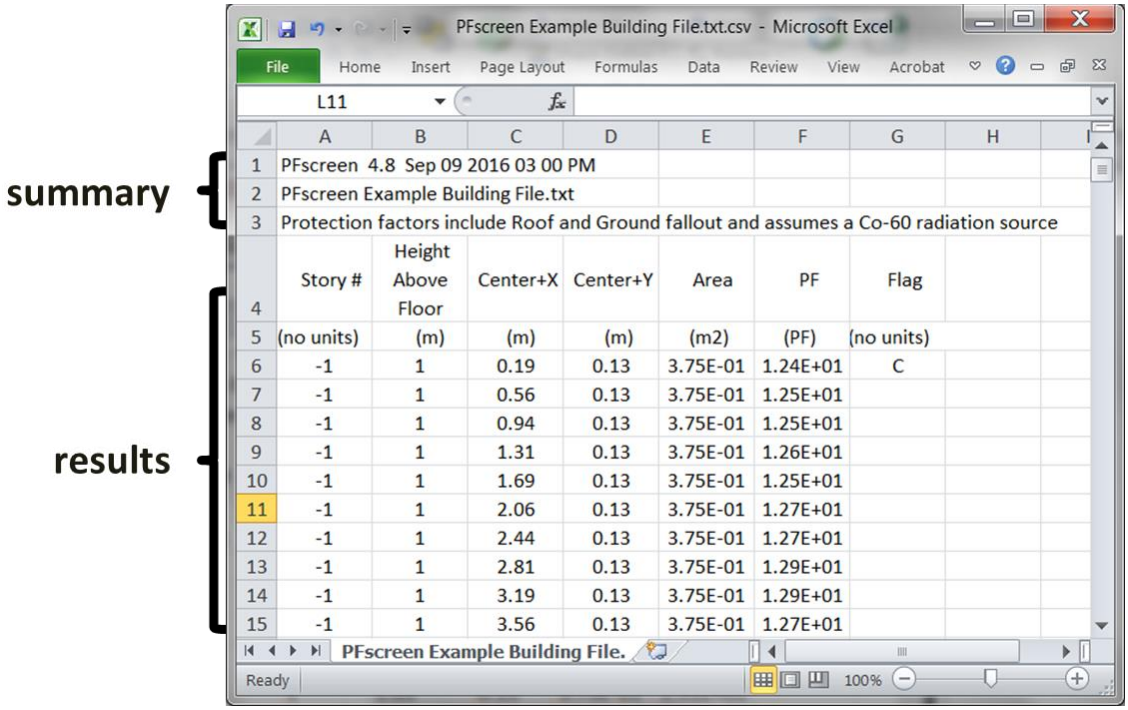

Figure D12. Portion of an example PFscreen output file.

Summary

1st line specifies the PFscreen version and the date/time the analysis was performed.

2nd line specifies the name of the input file analyzed.

3rd line specifies the radiation source geometry and energy.

Results

This section records the results for every analysis location evaluated by the PFscreen model. Each row corresponds to a different location in the building. The columns are:

Story # (no units) is the building story of the analysis location. Negative numbers indicate a below ground story(ies), i.e., basement(s). Positive numbers indicate an above ground story (the ground story is 1). There is no "zero" story.

Height Above Floor (m) is the distance between the analysis location and the story floor.

Center+X (m) is the distance from the building center to the analysis location along the building length axis. By convention, length is the long axis.

Center+Y (m) is the distance from the building center to the analysis location along the building width axis.

Area (m2) is the square footage of portion of the building corresponding to the analysis location.

Building Protection (PF) is the protection factor at the analysis location.

Flag (no units) is a code indicating if the analysis location is in the center of the building ("C"), along an outer wall ("W"), or neither (blank).